

Deep learning approximations for non-local nonlinear PDEs with Neumann boundary conditions

Victor Boussange^{1,2}, Sebastian Becker³, Arnulf Jentzen^{4,5},
Benno Kuckuck⁶, and Loïc Pellissier^{7,8}

¹ Unit of Land Change Science, Swiss Federal Research Institute
for Forest, Snow and Landscape (WSL), Switzerland

² Landscape Ecology, Institute of Terrestrial Ecosystems,
Department of Environmental Systems Science, ETH Zürich,
Switzerland, e-mail: bvictor@ethz.ch

³ Risklab, Department of Mathematics, ETH Zürich,
Switzerland, e-mail: sebastian.becker@math.ethz.ch

⁴ School of Data Science and Shenzhen Research Institute of Big Data,
The Chinese University of Hong Kong, Shenzhen, China,
e-mail: ajentzen@cuhk.edu.cn

⁵ Applied Mathematics: Institute for Analysis and Numerics,
Faculty of Mathematics and Computer Science, University of Münster,
Germany, e-mail: ajentzen@uni-muenster.de

⁶ Applied Mathematics: Institute for Analysis and Numerics,
Faculty of Mathematics and Computer Science, University of Münster,
Germany, e-mail: bkuckuck@uni-muenster.de

⁷ Unit of Land Change Science, Swiss Federal Research Institute
for Forest, Snow and Landscape (WSL), Switzerland

⁸ Landscape Ecology, Institute of Terrestrial Ecosystems,
Department of Environmental System Science, ETH Zürich,
Switzerland, e-mail: loic.pellissier@usys.ethz.ch

May 10, 2022

Abstract

Nonlinear partial differential equations (PDEs) are used to model dynamical processes in a large number of scientific fields, ranging from finance to biology. In many applications standard local models are not sufficient to accurately account for certain non-local phenomena such as, e.g., interactions at a distance. In order to properly capture these phenomena non-local nonlinear PDE models are frequently employed in the literature. In this article we propose two numerical methods based on machine learning and on Picard iterations, respectively, to approximately solve non-local nonlinear PDEs. The proposed machine learning-based method is an extended variant of a deep learning-based splitting-up type approximation method previously introduced in the literature and utilizes neural networks to provide approximate solutions on a subset of the spatial domain of the solution. The Picard iterations-based method is an extended variant of the so-called *full history recursive multilevel Picard* approximation scheme previously introduced in the literature and provides an approximate solution for a single point of the domain. Both methods are mesh-free and allow non-local nonlinear PDEs with Neumann boundary conditions to be solved in high dimensions. In the two methods, the numerical difficulties arising due to the dimensionality of the PDEs are avoided by (i) using the correspondence between the expected trajectory of reflected stochastic processes and the solution of PDEs (given by the Feynman–Kac formula) and by (ii) using a plain vanilla Monte Carlo integration to handle the non-local term. We evaluate the performance of the two methods on five different PDEs arising in physics and biology. In all cases, the methods yield good results in up to 10 dimensions with short run times. Our work extends recently developed methods to overcome the curse of dimensionality in solving PDEs.

Contents

1	Introduction	4
2	Machine learning-based approximation method in a special case	6
2.1	Partial differential equations (PDEs) under consideration	7
2.2	Reflection principle for the simulation of time discrete reflected processes	7
2.3	Description of the proposed approximation method in a special case	8
3	Machine learning-based approximation method in the general case	11
3.1	PDEs under consideration	11
3.2	Description of the proposed approximation method in the general case	11
4	Multilevel Picard approximation method for non-local PDEs	14
4.1	Description of the proposed approximation method	14
4.2	Examples for the approximation method	15
5	Numerical simulations	18
5.1	Fisher–KPP PDEs with Neumann boundary conditions	20
5.2	Non-local competition PDEs	21
5.3	Non-local sine-Gordon type PDEs	22
5.4	Replicator-mutator PDEs	23
5.5	Allen–Cahn PDEs with conservation of mass	32
6	JULIA source codes	33
6.1	General package for high-dimensional PDE approximations	33
6.2	Implementation of the machine learning-based approximation method	37
6.3	Implementation of the multilevel Picard approximation method	40
6.4	JULIA source codes associated to Subsection 5.1	43
6.5	JULIA source codes associated to Subsection 5.2	45
6.6	JULIA source codes associated to Subsection 5.3	46
6.7	JULIA source codes associated to Subsection 5.4	47
6.8	JULIA source codes associated to Subsection 5.5	49

1 Introduction

In this article, we derive numerical schemes to approximately solve high-dimensional non-local nonlinear partial differential equations (PDEs) with Neumann boundary conditions. Such PDEs have been used to describe a variety of processes in physics, engineering, finance, and biology, but can generally not be solved analytically, requiring numerical methods to provide approximate solutions. However, traditional numerical methods are for the most part computationally infeasible for high-dimensional problems, calling for the development of novel approximation methods.

The need for solving non-local nonlinear PDEs has been expressed in various fields as they provide a more general description of the dynamical systems than their local counterparts [63, 29, 90]. In physics and engineering, non-local nonlinear PDEs are found, e.g., in models of Ohmic heating production [66], in the investigation of the fully turbulent behavior of real flows [20], in phase field models allowing non-local interactions [7, 41, 25, 49], or in phase transition models with conservation of mass [86, 88]; see [63] for further references. In finance, non-local PDEs are used, e.g., in jump-diffusion models for the pricing of derivatives where the dynamics of stock prices are described by stochastic processes experiencing large jumps [74, 22, 65, 1, 15, 90, 28, 26]. Penalty methods for pricing American put options such as in Kou's jump-diffusion model [58, 42], considering large investors where the agent policy affects the assets prices [5, 1], or considering default risks [83, 55] can further introduce nonlinear terms in non-local PDEs. In economics, non-local nonlinear PDEs appear, e.g., in evolutionary game theory with the so-called replicator-mutator equation capturing continuous strategy spaces [79, 62, 50, 3, 4] or in growth models where consumption is non-local [6]. In biology, non-local nonlinear PDEs are used, e.g., to model processes determining the interaction and evolution of organisms. Examples include models of morphogenesis and cancer evolution [71, 24, 91], models of gene regulatory networks [80], population genetics models with the non-local Fisher–Kolmogorov–Petrovsky–Piskunov (Fisher–KPP) equations [38, 51, 18, 82, 17, 57, 92], and quantitative genetics models where populations are structured on a phenotypic and/or a geographical space [19, 43, 16, 78, 77, 85, 30, 76]. In such models, Neumann boundary conditions are used, e.g., to model the effect of the borders of the geographical domain on the movement of the organisms.

Real world systems such as those just mentioned may be of considerable complexity and accurately capturing the dynamics of these systems may require models of high dimensionality [30], leading to complications in obtaining numerical approximations. For example, the number of dimensions of the PDEs may correspond in finance to the number of financial assets (such as stocks, commodities, exchange rates, and interest rates) in the involved portfolio; in evolutionary dynamics, to the dimension of the strategy space; and in biology, to the number of genes modelled [80] or to the dimension of the geographical or the phenotypic space over which the organisms are structured. Standard approximation methods for PDEs such as finite difference approximation methods, finite element methods, spectral Galerkin approximation methods, and sparse grid approximation methods all

suffer from the so called *curse of dimensionality* [14], meaning that their computational costs increase exponentially in the number of dimensions of the PDE under consideration.

Numerical methods exploiting stochastic representations of the solutions of PDEs can in some cases overcome the curse of dimensionality. Specifically, simple Monte Carlo averages of the associated stochastic processes have been proposed a long time ago to solve high-dimensional linear PDEs, such as, e.g., Black–Scholes and Kolmogorov PDEs [75, 8]. Recently, two novel classes of methods have proved successful in dealing with high-dimensional nonlinear PDEs, namely deep learning-based and full history recursive multilevel Picard approximation methods (in the following we will abbreviate *full history recursive multilevel Picard* by MLP). The explosive success of deep learning in recent years across a wide range of applications [69] has inspired a variety of neural network-based approximation methods for high-dimensional PDEs; see [12] for an overview. One class of such methods is based on reformulating the PDE as a stochastic learning problem through the Feynman–Kac formula [32, 52, 10]. In particular, the *deep splitting* scheme introduced in [9] relies on splitting the differential operator into a linear and a nonlinear part and in that sense belongs to the class of splitting-up methods [27, 48, 56]. The PDE approximation problem is then decomposed along the time axis into a sequence of separate learning problems. The deep splitting approximation scheme has proved capable of computing reasonable approximations to the solutions of nonlinear PDEs in up to 10000 dimensions. On the other hand, the MLP approximation method, introduced in [34, 60, 36], utilizes the Feynman–Kac formula to reformulate the PDE problem as a fixed point equation. It further reduces the complexity of the numerical approximation of the time integral through a multilevel Monte Carlo approach. However, neither the deep splitting nor the MLP method can, until now, account for non-localness and Neumann boundary conditions.

The goal of this article is to overcome these limitations and thus we generalize the deep splitting method and the MLP approximation method to approximately solve non-local nonlinear PDEs with Neumann boundary conditions. We handle the non-local term by a plain vanilla Monte Carlo integration and address Neumann boundary conditions by constructing reflected stochastic processes. While the MLP method can, in one run, only provide an approximate solution at a single point $x \in D$ of the spatial domain $D \subseteq \mathbb{R}^d$ where $d \in \mathbb{N} = \{1, 2, \dots\}$, the machine learning-based method can in principle provide an approximate solution on a full subset of the spatial domain D (however, cf., e.g., [53, 54, 46] for results on limitations on the performance of such approximation schemes). We use both methods to solve five non-local nonlinear PDEs arising in models from biology and physics and cross-validate the results of the simulations. We manage to solve the non-local nonlinear PDEs with reasonable accuracy in up to 10 dimensions.

For an account of classical numerical methods for solving non-local PDEs, such as finite differences, finite elements, and spectral methods, we refer the reader to the recent survey [29]. Several machine-learning based schemes for solving non-local PDEs can also be found in the literature. In particular, the *physics-informed neural network* and *deep*

Galerkin approaches [84, 87], based on representing an approximation of the whole solution of the PDE as a neural network and using automatic differentiation to do a least-squares minimization of the residual of the PDE, have been extended to fractional PDEs and other non-local PDEs [81, 72, 47, 2, 94]. While some of these approaches use classical methods susceptible to the curse of dimensionality for the non-local part [81, 72], mesh-free methods suitable for high-dimensional problems have also been investigated [47, 2, 94].

The literature also contains approaches that are more closely related to the machine learning-based algorithm presented here. Frey & Köck [39, 40] propose an approximation method for non-local semilinear parabolic PDEs with Dirichlet boundary conditions based on and extending the deep splitting method in [9] and carry out numerical simulations for example PDEs in up to 4 dimensions. Castro [21] proposes a numerical scheme for approximately solving non-local nonlinear PDEs based on [59] and proves convergence results for this scheme. Finally, Gonon & Schwab [45] provide theoretical results showing that neural networks with ReLU activation functions have sufficient expressive power to approximate solutions of certain high-dimensional non-local linear PDEs without the curse of dimensionality.

There is a more extensive literature on machine learning-based methods for approximately solving standard PDEs without non-local terms but with various boundary conditions, going back to early works by Lagaris et al. [68, 67] (see also [73]), which employed a grid-based method based on least-squares minimization of the residual and shallow neural networks to solve low-dimensional ODEs and PDEs with Dirichlet, Neumann, and mixed boundary conditions. More recently, approximation methods for PDEs with Neumann (and other) boundary conditions have been proposed using, e.g., physics-informed neural networks [72, 89, 93], the *deep Ritz* method (based on a variational formulation of certain elliptic PDEs) [37, 70, 23], or adversarial networks [95].

The remainder of this article is organized as follows. Section 2 discusses a special case of the proposed machine learning-based method, in order to provide a readily comprehensible exposition of the key ideas of the method. Section 3 discusses the general case, which is flexible enough to cover a larger class of PDEs and to allow more sophisticated optimization methods. Section 4 presents our extension of the MLP approximation method to non-local nonlinear PDEs, which we use to obtain reference solutions in Section 5. Section 5 provides numerical simulations for five concrete examples of (non-local) nonlinear PDEs. Section 6 provides the source codes used for the computations in Section 5.

2 Machine learning-based approximation method in a special case

In this section, we present in Framework 2.2 in Subsection 2.3 below a simplified version of our general machine learning-based algorithm for approximating solutions of non-local

nonlinear PDEs with Neumann boundary conditions proposed in Section 3 below. This simplified version applies to a smaller class of non-local heat PDEs, specified in Subsection 2.1 below. In Subsection 2.2 we introduce some notation related to the reflection of straight lines on the boundaries of a suitable subset $D \subseteq \mathbb{R}^d$ where $d \in \mathbb{N}$, which will be used to describe time-discrete reflected stochastic processes that are employed in our approximations throughout the rest of the article. The simplified algorithm described in Subsection 2.3 below is limited to using neural networks of a particular architecture that are trained using plain vanilla stochastic gradient descent, whereas the full version proposed in Framework 3.1 in Subsection 3.2 below is formulated in such a way that it encompasses a wide array of neural network architectures and more sophisticated training methods, in particular Adam optimization, minibatches, and batch normalization. Stripping away some of these more intricate aspects of the full algorithm is intended to exhibit more acutely the central ideas in the proposed approximation method.

The simplified algorithm described in this section as well as the more general version proposed in Framework 3.1 in Subsection 3.2 below are based on the deep splitting method introduced in Beck et al. [9], which combines operator splitting with a previous deep learning-based approximation method for Kolmogorov PDEs [10]; see also Beck et al. [12, Sections 2 and 3] for an exposition of these methods.

2.1 Partial differential equations (PDEs) under consideration

Let $T \in (0, \infty)$, $d \in \mathbb{N}$, let $D \subseteq \mathbb{R}^d$ be a closed set with sufficiently smooth boundary ∂_D , let $\mathbf{n}: \partial_D \rightarrow \mathbb{R}^d$ be an outer unit normal vector field associated to D , let $g \in C(D, \mathbb{R})$, let $\nu_x: \mathcal{B}(D) \rightarrow [0, 1]$, $x \in D$, be probability measures, let $f: \mathbb{R} \times \mathbb{R} \rightarrow \mathbb{R}$ be measurable, let $u = (u(t, x))_{(t,x) \in [0,T] \times D} \in C^{1,2}([0, T] \times D, \mathbb{R})$ have at most polynomially growing partial derivatives, assume¹ for every $t \in (0, T]$, $x \in \partial_D$ that $\langle \mathbf{n}(x), (\nabla_x u)(t, x) \rangle = 0$, and assume for every $t \in [0, T]$, $x \in D$ that $u(0, x) = g(x)$, $\int_D |f(u(t, x), u(t, \mathbf{x}))| \nu_x(d\mathbf{x}) < \infty$, and

$$\left(\frac{\partial}{\partial t} u\right)(t, x) = (\Delta_x u)(t, x) + \int_D f(u(t, x), u(t, \mathbf{x})) \nu_x(d\mathbf{x}). \quad (1)$$

Our goal in this section is to approximately calculate under suitable hypotheses the solution $u: [0, T] \times D \rightarrow \mathbb{R}$ of the PDE in (1).

2.2 Reflection principle for the simulation of time discrete reflected processes

Framework 2.1 (Reflection principle for the simulation of time discrete reflected processes). *Let $d \in \mathbb{N}$, let $D \subseteq \mathbb{R}^d$ be a closed set with sufficiently smooth boundary ∂_D , let*

¹Throughout this article we denote by $\langle \cdot, \cdot \rangle: (\bigcup_{n \in \mathbb{N}} (\mathbb{R}^n \times \mathbb{R}^n)) \rightarrow \mathbb{R}$ and $\|\cdot\|: (\bigcup_{n \in \mathbb{N}} \mathbb{R}^n) \rightarrow \mathbb{R}$ the functions which satisfy for all $n \in \mathbb{N}$, $v = (v_1, \dots, v_n)$, $w = (w_1, \dots, w_n) \in \mathbb{R}^n$ that $\langle v, w \rangle = \sum_{i=1}^n v_i w_i$ and $\|v\| = \sqrt{\langle v, v \rangle} = [\sum_{i=1}^n |v_i|^2]^{1/2}$.

$\mathbf{n}: \partial_D \rightarrow \mathbb{R}^d$ be a suitable outer unit normal vector field associated to D , let $\mathbf{c}: (\mathbb{R}^d)^2 \rightarrow \mathbb{R}^d$ satisfy for every $a, b \in \mathbb{R}^d$ that

$$\mathbf{c}(a, b) = a + [\inf(\{r \in [0, 1]: a + r(b - a) \notin D\} \cup \{1\})](b - a), \quad (2)$$

let $\mathcal{R}: (\mathbb{R}^d)^2 \rightarrow (\mathbb{R}^d)^2$ satisfy for every $a, b \in \mathbb{R}^d$ that

$$\mathcal{R}(a, b) = \begin{cases} (a, b) & : \mathbf{c}(a, b) = a \\ (\mathbf{c}(a, b), b - 2\mathbf{n}(\mathbf{c}(a, b))\langle b - \mathbf{c}(a, b), \mathbf{n}(\mathbf{c}(a, b)) \rangle) & : \mathbf{c}(a, b) \notin \{a, b\} \\ (b, b) & : \mathbf{c}(a, b) = b, \end{cases} \quad (3)$$

let $P: (\mathbb{R}^d)^2 \rightarrow \mathbb{R}^d$ satisfy for every $a, b \in \mathbb{R}^d$ that $P(a, b) = b$, let $\mathcal{R}_n: (\mathbb{R}^d)^2 \rightarrow (\mathbb{R}^d)^2$, $n \in \mathbb{N}_0 = \{0\} \cup \mathbb{N}$, satisfy for every $n \in \mathbb{N}_0$, $x, y \in \mathbb{R}^d$ that $\mathcal{R}_0(x, y) = (x, y)$ and $\mathcal{R}_{n+1}(x, y) = \mathcal{R}(\mathcal{R}_n(x, y))$, and let $R: (\mathbb{R}^d)^2 \rightarrow \mathbb{R}^d$ satisfy for every $x, y \in \mathbb{R}^d$ that

$$R(x, y) = \lim_{n \rightarrow \infty} P(\mathcal{R}_n(x, y)). \quad (4)$$

2.3 Description of the proposed approximation method in a special case

Framework 2.2 (Special case of the machine learning-based approximation method). Assume Framework 2.1, let $T, \gamma \in (0, \infty)$, $N, M, K \in \mathbb{N}$, $g \in C^2(\mathbb{R}^d, \mathbb{R})$, $\mathfrak{d}, \mathfrak{h} \in \mathbb{N} \setminus \{1\}$, $t_0, t_1, \dots, t_N \in [0, T]$ satisfy $\mathfrak{d} = \mathfrak{h}(N + 1)d(d + 1)$ and

$$0 = t_0 < t_1 < \dots < t_N = T, \quad (5)$$

let $\tau_0, \tau_1, \dots, \tau_N \in [0, T]$ satisfy for every $n \in \{0, 1, \dots, N\}$ that $\tau_n = T - t_{N-n}$, let $f: \mathbb{R} \times \mathbb{R} \rightarrow \mathbb{R}$ be measurable, let $(\Omega, \mathcal{F}, \mathbb{P}, (\mathcal{F}_t)_{t \in [0, T]})$ be a filtered probability space, let $\xi^m: \Omega \rightarrow \mathbb{R}^d$, $m \in \mathbb{N}$, be i.i.d. $\mathcal{F}_0/\mathcal{B}(\mathbb{R}^d)$ -measurable random variables, let $W^m: [0, T] \times \Omega \rightarrow \mathbb{R}^d$, $m \in \mathbb{N}$, be i.i.d. standard $(\mathcal{F}_t)_{t \in [0, T]}$ -Brownian motions, for every $m \in \mathbb{N}$ let $\mathcal{Y}^m: \{0, 1, \dots, N\} \times \Omega \rightarrow \mathbb{R}^d$ be the stochastic process which satisfies for every $n \in \{0, 1, \dots, N - 1\}$ that $\mathcal{Y}_0^m = \xi^m$ and

$$\mathcal{Y}_{n+1}^m = R(\mathcal{Y}_n^m, \mathcal{Y}_n^m + \sqrt{2}(W_{\tau_{n+1}}^m - W_{\tau_n}^m)), \quad (6)$$

let $\mathcal{L}: \mathbb{R}^d \rightarrow \mathbb{R}^d$ satisfy for every $x = (x_1, \dots, x_d) \in \mathbb{R}^d$ that

$$\mathcal{L}(x) = \left(\frac{\exp(x_1)}{\exp(x_1) + 1}, \dots, \frac{\exp(x_d)}{\exp(x_d) + 1} \right), \quad (7)$$

for every $\theta = (\theta_1, \dots, \theta_{\mathfrak{d}}) \in \mathbb{R}^{\mathfrak{d}}$, $k, l, v \in \mathbb{N}$ with $v + l(k + 1) \leq \mathfrak{d}$ let $A_{k,l}^{\theta,v}: \mathbb{R}^k \rightarrow \mathbb{R}^l$ satisfy for every $x = (x_1, \dots, x_k) \in \mathbb{R}^k$ that

$$A_{k,l}^{\theta,v}(x) = \left(\theta_{v+kl+1} + \left[\sum_{i=1}^k x_i \theta_{v+i} \right], \dots, \theta_{v+kl+l} + \left[\sum_{i=1}^k x_i \theta_{v+(l-1)k+i} \right] \right), \quad (8)$$

let $\mathbb{V}_n: \mathbb{R}^{\mathfrak{d}} \times \mathbb{R}^d \rightarrow \mathbb{R}$, $n \in \{0, 1, \dots, N\}$, satisfy for every $n \in \{1, 2, \dots, N\}$, $\theta \in \mathbb{R}^{\mathfrak{d}}$, $x \in \mathbb{R}^d$ that $\mathbb{V}_0(\theta, x) = g(x)$ and

$$\mathbb{V}_n(\theta, x) = \left(A_{d,1}^{\theta, (\mathfrak{h}n + \mathfrak{h} - 1)d(d+1)} \circ \mathcal{L} \circ A_{d,d}^{\theta, (\mathfrak{h}n + \mathfrak{h} - 2)d(d+1)} \circ \dots \circ \mathcal{L} \circ A_{d,d}^{\theta, (\mathfrak{h}n + 1)d(d+1)} \circ \mathcal{L} \circ A_{d,d}^{\theta, \mathfrak{h}nd(d+1)} \right)(x), \quad (9)$$

let $\nu_x: \mathcal{B}(D) \rightarrow [0, 1]$, $x \in D$, be probability measures, for every $x \in D$ let $Z_{x,k}^{n,m}: \Omega \rightarrow D$, $k, n, m \in \mathbb{N}$, be i.i.d. random variables which satisfy for every $A \in \mathcal{B}(D)$ that $\mathbb{P}(Z_{x,1}^{1,1} \in A) = \nu_x(A)$, let $\Theta^n: \mathbb{N}_0 \times \Omega \rightarrow \mathbb{R}^{\mathfrak{d}}$, $n \in \{0, 1, \dots, N\}$, be stochastic processes, for every $n \in \{1, 2, \dots, N\}$, $m \in \mathbb{N}$ let $\phi^{n,m}: \mathbb{R}^{\mathfrak{d}} \times \Omega \rightarrow \mathbb{R}$ satisfy for every $\theta \in \mathbb{R}^{\mathfrak{d}}$, $\omega \in \Omega$ that

$$\begin{aligned} \phi^{n,m}(\theta, \omega) = & \left[\mathbb{V}_n(\theta, \mathcal{Y}_{N-n}^m(\omega)) - \mathbb{V}_{n-1}(\Theta_M^{n-1}(\omega), \mathcal{Y}_{N-n+1}^m(\omega)) \right. \\ & \left. - \frac{(t_n - t_{n-1})}{K} \left[\sum_{k=1}^K f(\mathbb{V}_{n-1}(\Theta_M^{n-1}(\omega), \mathcal{Y}_{N-n+1}^m(\omega)), \mathbb{V}_{n-1}(\Theta_M^{n-1}(\omega), Z_{\mathcal{Y}_{N-n+1}^m(\omega), k}^{n,m}(\omega))) \right] \right]^2, \quad (10) \end{aligned}$$

for every $n \in \{1, 2, \dots, N\}$, $m \in \mathbb{N}$ let $\Phi^{n,m}: \mathbb{R}^{\mathfrak{d}} \times \Omega \rightarrow \mathbb{R}^{\mathfrak{d}}$ satisfy for every $\theta \in \mathbb{R}^{\mathfrak{d}}$, $\omega \in \Omega$ that $\Phi^{n,m}(\theta, \omega) = (\nabla_{\theta} \phi^{n,m})(\theta, \omega)$, and assume for every $n \in \{1, 2, \dots, N\}$, $m \in \mathbb{N}$ that

$$\Theta_m^n = \Theta_{m-1}^n - \gamma \Phi^{n,m}(\Theta_{m-1}^n). \quad (11)$$

As indicated in Subsection 2.1 above, the algorithm described in Framework 2.2 computes an approximation for a solution of the PDE in (1), i.e., a function $u \in C^{1,2}([0, T] \times D, \mathbb{R})$ which has at most polynomially growing derivatives, which satisfies for every $t \in (0, T]$, $x \in \partial_D$ that $\langle \mathbf{n}(x), (\nabla_x u)(t, x) \rangle = 0$ and which satisfies for every $t \in [0, T]$, $x \in D$ that $u(0, x) = g(x)$, $\int_D |f(u(t, x), u(t, \mathbf{x}))| \nu_x(d\mathbf{x}) < \infty$, and

$$\left(\frac{\partial}{\partial t} u \right)(t, x) = (\Delta_x u)(t, x) + \int_D f(u(t, x), u(t, \mathbf{x})) \nu_x(d\mathbf{x}). \quad (12)$$

Let us now add some explanatory comments on the objects and notations employed in Framework 2.2 above. The algorithm in Framework 2.2 decomposes the time interval $[0, T]$ into N subintervals at the times $t_0, t_1, t_2, \dots, t_N \in [0, T]$ (cf. (5)). For every $n \in \{1, 2, \dots, N\}$ we aim to approximate the function $\mathbb{R}^d \ni x \mapsto u(t_n, x) \in \mathbb{R}$ by a suitable (realization function of a) fully-connected feedforward neural network. Each of these neural networks is an alternating composition of $\mathfrak{h} - 1$ affine linear functions from \mathbb{R}^d to \mathbb{R}^d (where we think of $\mathfrak{h} \in \mathbb{N} \setminus \{1\}$ as the *length* or *depth* of the neural network), $\mathfrak{h} - 1$ instances of a d -dimensional version of the standard logistic function and finally an affine linear function from \mathbb{R}^d to \mathbb{R} . Every such neural network can be specified by means of $(\mathfrak{h} - 1)(d^2 + d) + d + 1 \leq \mathfrak{h}d(d + 1)$ real parameters and so $N + 1$ of these neural networks can be specified by a parameter vector of length $\mathfrak{d} = \mathfrak{h}(N + 1)d(d + 1) \in \mathbb{N}$. Note that $\mathcal{L}: \mathbb{R}^d \rightarrow \mathbb{R}^d$ in Framework 2.2 above denotes the d -dimensional version of the standard logistic function

(cf. (7)) and for every $k, l, v \in \mathbb{N}$, $\theta \in \mathbb{R}^{\mathfrak{d}}$ with $v + kl + l \leq \mathfrak{d}$ the function $A_{k,l}^{\theta,v}: \mathbb{R}^k \rightarrow \mathbb{R}^l$ in Framework 2.2 denotes an affine linear function specified by means of the parameters $v + 1, v + 2, \dots, v + kl + l$ (cf. (8)). Furthermore, observe that for every $n \in \{1, 2, \dots, N\}$, $\theta \in \mathbb{R}^{\mathfrak{d}}$ the function

$$\mathbb{R}^d \ni x \mapsto \mathbb{V}_n(\theta, x) \in \mathbb{R} \quad (13)$$

denotes a neural network specified by means of the parameters $\mathfrak{h}nd(d+1) + 1, \mathfrak{h}nd(d+1) + 2, \dots, (\mathfrak{h}n + \mathfrak{h} - 1)d(d+1) + d + 1$.

The goal of the optimization algorithm in Framework 2.2 above is to find a suitable parameter vector $\theta \in \mathbb{R}^{\mathfrak{d}}$ such that for every $n \in \{1, 2, \dots, N\}$ the neural network $\mathbb{R}^d \ni x \mapsto \mathbb{V}_n(\theta, x) \in \mathbb{R}$ is a good approximation for the solution $\mathbb{R}^d \ni x \mapsto u(t_n, x) \in \mathbb{R}$ to the PDE in (12) at time t_n . This is done by performing successively for each $n \in \{1, 2, \dots, N\}$ a plain vanilla stochastic gradient descent (SGD) optimization on a suitable loss function (cf. (11)).

Observe that for every $n \in \{1, 2, \dots, N\}$ the stochastic process $\Theta^n: \mathbb{N}_0 \times \Omega \rightarrow \mathbb{R}^{\mathfrak{d}}$ describes the successive estimates computed by the SGD algorithm for the parameter vector that represents (via $\mathbb{V}_n: \mathbb{R}^{\mathfrak{d}} \times \mathbb{R}^d \rightarrow \mathbb{R}$) a suitable approximation to the solution $\mathbb{R}^d \ni x \mapsto u(t_n, x) \in \mathbb{R}$ of the PDE in (12) at time t_n . Next note that $M \in \mathbb{N}$ in Framework 2.2 above denotes the number of gradient descent steps taken for each $n \in \{1, 2, \dots, N\}$ and that $\gamma \in (0, \infty)$ denotes the learning rate employed in the SGD algorithm. Moreover, observe that for every $n \in \{1, 2, \dots, N\}$, $m \in \{1, 2, \dots, M\}$ the function $\phi^{n,m}: \mathbb{R}^{\mathfrak{d}} \times \Omega \rightarrow \mathbb{R}$ denotes the loss function employed in the m th gradient descent step during the approximation of the solution of the PDE in (12) at time t_n (cf. (10)). The loss functions employ a family of i.i.d. time-discrete stochastic processes $\mathcal{Y}^m: \{0, 1, \dots, N\} \times \Omega \rightarrow \mathbb{R}^d$, $m \in \mathbb{N}$, which we think of as discretizations of suitable reflected Brownian motions (cf. (6)). In addition, for every $n \in \{1, 2, \dots, N\}$, $m \in \{1, 2, \dots, M\}$, $x \in D$ the loss function $\phi^{n,m}: \mathbb{R}^{\mathfrak{d}} \times \Omega \rightarrow \mathbb{R}$ employs a family of i.i.d. random variables $Z_{x,k}^{n,m}: \Omega \rightarrow D$, $k \in \mathbb{N}$, which are used for the Monte Carlo approximation of the non-local term in the PDE in (12) whose solution we are trying to approximate. The number of samples used in these Monte Carlo approximations is denoted by $K \in \mathbb{N}$ in Framework 2.2 above.

Finally, for sufficiently large $N, M, K \in \mathbb{N}$ and sufficiently small $\gamma \in (0, \infty)$ the algorithm in Framework 2.2 above yields for every $n \in \{1, 2, \dots, N\}$ a (random) parameter vector $\Theta_M^n: \Omega \rightarrow \mathbb{R}^{\mathfrak{d}}$ which represents a function $\mathbb{R}^d \times \Omega \ni (x, \omega) \mapsto \mathbb{V}_n(\Theta_M^n(\omega), x) \in \mathbb{R}$ that we think of as providing for every $x \in D$ a suitable approximation

$$\mathbb{V}_n(\Theta_M^n, x) \approx u(t_n, x). \quad (14)$$

3 Machine learning-based approximation method in the general case

In this section we describe in Framework 3.1 in Subsection 3.2 below the full version of our deep learning-based method for approximating solutions of non-local nonlinear PDEs with Neumann boundary conditions (see Subsection 3.1 for a description of the class of PDEs our approximation method applies to), which generalizes the algorithm introduced in Framework 2.2 in Subsection 2.3 above and which we apply in Section 5 below to several examples of non-local nonlinear PDEs.

3.1 PDEs under consideration

Let $T \in (0, \infty)$, $d \in \mathbb{N}$, let $D \subseteq \mathbb{R}^d$ be a closed set with sufficiently smooth boundary ∂_D , let $\mathbf{n}: \partial_D \rightarrow \mathbb{R}^d$ be an outer unit normal vector field associated to D , let $g: D \rightarrow \mathbb{R}$, $\mu: D \rightarrow \mathbb{R}^d$, and $\sigma: D \rightarrow \mathbb{R}^{d \times d}$ be continuous, let $\nu_x: \mathcal{B}(D) \rightarrow [0, 1]$, $x \in D$, be probability measures, let $f: [0, T] \times D \times D \times \mathbb{R} \times \mathbb{R} \rightarrow \mathbb{R}$ be measurable, let $u = (u(t, x))_{(t,x) \in [0,T] \times D} \in C^{1,2}([0, T] \times D, \mathbb{R})$ have at most polynomially growing partial derivatives, assume for every $t \in [0, T]$, $x \in \partial_D$ that $\langle \mathbf{n}(x), (\nabla_x u)(t, x) \rangle = 0$, and assume for every $t \in [0, T]$, $x \in D$ that $u(0, x) = g(x)$, $\int_D |f(t, x, \mathbf{x}, u(t, x), u(t, \mathbf{x}))| \nu_x(d\mathbf{x}) < \infty$, and

$$\begin{aligned} \left(\frac{\partial}{\partial t} u\right)(t, x) &= \int_D f(t, x, \mathbf{x}, u(t, x), u(t, \mathbf{x})) \nu_x(d\mathbf{x}) \\ &+ \langle \mu(x), (\nabla_x u)(t, x) \rangle + \frac{1}{2} \text{Trace}(\sigma(x)[\sigma(x)]^*(\text{Hess}_x u)(t, x)). \end{aligned} \quad (15)$$

Our goal is to approximately calculate under suitable hypotheses the solution $u: [0, T] \times D \rightarrow \mathbb{R}$ of the PDE in (15).

3.2 Description of the proposed approximation method in the general case

Framework 3.1 (General case of the machine learning-based approximation method). Assume Framework 2.1, let $T \in (0, \infty)$, $N, \varrho, \mathfrak{d}, \varsigma \in \mathbb{N}$, $(M_n)_{n \in \mathbb{N}_0} \subseteq \mathbb{N}$, $(K_n)_{n \in \mathbb{N}} \subseteq \mathbb{N}$, $(J_m)_{m \in \mathbb{N}} \subseteq \mathbb{N}$, $t_0, t_1, \dots, t_N \in [0, T]$ satisfy

$$0 = t_0 < t_1 < \dots < t_N = T, \quad (16)$$

let $\tau_0, \tau_1, \dots, \tau_N \in [0, T]$ satisfy for every $n \in \{0, 1, \dots, N\}$ that $\tau_n = T - t_{N-n}$, let $\nu_x: \mathcal{B}(D) \rightarrow [0, 1]$, $x \in D$, be probability measures, for every $x \in D$ let $Z_{x,k}^{n,m,j}: \Omega \rightarrow D$, $k, n, m, j \in \mathbb{N}$, be i.i.d. random variables which satisfy for every $A \in \mathcal{B}(D)$ that $\mathbb{P}(Z_{x,1}^{1,1,1} \in A) = \nu_x(A)$, let $f: [0, T] \times D \times D \times \mathbb{R} \times \mathbb{R} \rightarrow \mathbb{R}$ be measurable, let $(\Omega, \mathcal{F}, \mathbb{P}, (\mathcal{F}_t)_{t \in [0, T]})$ be a filtered probability space, for every $n \in \{1, 2, \dots, N\}$ let $W^{n,m,j}: [0, T] \times \Omega \rightarrow \mathbb{R}^d$, $m, j \in \mathbb{N}$, be

i.i.d. standard $(\mathcal{F}_t)_{t \in [0, T]}$ -Brownian motions, for every $n \in \{1, 2, \dots, N\}$ let $\xi^{n, m, j}: \Omega \rightarrow \mathbb{R}^d$, $m, j \in \mathbb{N}$, be i.i.d. $\mathcal{F}_0/\mathcal{B}(\mathbb{R}^d)$ -measurable random variables, let $H: [0, T]^2 \times \mathbb{R}^d \times \mathbb{R}^d \rightarrow \mathbb{R}^d$ be a function, for every $j \in \mathbb{N}$, $\mathbf{s} \in \mathbb{R}^s$, $n \in \{0, 1, \dots, N\}$ let $\mathbb{V}_n^{j, \mathbf{s}}: \mathbb{R}^d \times \mathbb{R}^d \rightarrow \mathbb{R}$ be a function, for every $n \in \{1, 2, \dots, N\}$, $m, j \in \mathbb{N}$ let $\mathcal{Y}^{n, m, j}: \{0, 1, \dots, N\} \times \Omega \rightarrow \mathbb{R}^d$ be a stochastic process which satisfies for every $k \in \{0, 1, \dots, N-1\}$ that $\mathcal{Y}_0^{n, m, j} = \xi^{n, m, j}$ and

$$\mathcal{Y}_{k+1}^{n, m, j} = H(\tau_{k+1}, \tau_k, \mathcal{Y}_k^{n, m, j}, W_{\tau_{k+1}}^{n, m, j} - W_{\tau_k}^{n, m, j}), \quad (17)$$

let $\Theta^n: \mathbb{N}_0 \times \Omega \rightarrow \mathbb{R}^d$, $n \in \{0, 1, \dots, N\}$, be stochastic processes, for every $n \in \{1, 2, \dots, N\}$, $m \in \mathbb{N}$, $\mathbf{s} \in \mathbb{R}^s$ let $\phi^{n, m, \mathbf{s}}: \mathbb{R}^d \times \Omega \rightarrow \mathbb{R}$ satisfy for every $\theta \in \mathbb{R}^d$, $\omega \in \Omega$ that

$$\begin{aligned} \phi^{n, m, \mathbf{s}}(\theta, \omega) &= \frac{1}{J_m} \sum_{j=1}^{J_m} \left[\mathbb{V}_n^{j, \mathbf{s}}(\theta, \mathcal{Y}_{N-n}^{n, m, j}(\omega)) - \mathbb{V}_{n-1}^{j, \mathbf{s}}(\Theta_{M_{n-1}}^{n-1}(\omega), \mathcal{Y}_{N-n+1}^{n, m, j}(\omega)) \right. \\ &\quad \left. - \frac{(t_n - t_{n-1})}{K_n} \left[\sum_{k=1}^{K_n} f\left(t_{n-1}, \mathcal{Y}_{N-n+1}^{n, m, j}(\omega), Z_{\mathcal{Y}_{N-n+1}^{n, m, j}(\omega), k}^{n, m, j}(\omega), \right. \right. \right. \\ &\quad \left. \left. \left. \mathbb{V}_{n-1}^{j, \mathbf{s}}(\Theta_{M_{n-1}}^{n-1}(\omega), \mathcal{Y}_{N-n+1}^{n, m, j}(\omega)), \mathbb{V}_{n-1}^{j, \mathbf{s}}(\Theta_{M_{n-1}}^{n-1}(\omega), Z_{\mathcal{Y}_{N-n+1}^{n, m, j}(\omega), k}^{n, m, j}(\omega))\right) \right] \right]^2, \end{aligned} \quad (18)$$

for every $n \in \{1, 2, \dots, N\}$, $m \in \mathbb{N}$, $\mathbf{s} \in \mathbb{R}^s$ let $\Phi^{n, m, \mathbf{s}}: \mathbb{R}^d \times \Omega \rightarrow \mathbb{R}^d$ satisfy for every $\omega \in \Omega$, $\theta \in \{\vartheta \in \mathbb{R}^d: (\mathbb{R}^d \ni \eta \mapsto \phi^{n, m, \mathbf{s}}(\eta, \omega) \in \mathbb{R})$ is differentiable at $\vartheta\}$ that

$$\Phi^{n, m, \mathbf{s}}(\theta, \omega) = (\nabla_{\theta} \phi^{n, m, \mathbf{s}})(\theta, \omega), \quad (19)$$

let $\mathcal{S}^n: \mathbb{R}^s \times \mathbb{R}^d \times (\mathbb{R}^d)^{\{0, 1, \dots, N\} \times \mathbb{N}} \rightarrow \mathbb{R}^s$, $n \in \{1, 2, \dots, N\}$, be functions, for every $n \in \{1, 2, \dots, N\}$, $m \in \mathbb{N}$ let $\psi_m^n: \mathbb{R}^e \rightarrow \mathbb{R}^d$ and $\Psi_m^n: \mathbb{R}^e \times \mathbb{R}^d \rightarrow \mathbb{R}^e$ be functions, and for every $n \in \{1, 2, \dots, N\}$ let $\mathbb{S}^n: \mathbb{N}_0 \times \Omega \rightarrow \mathbb{R}^s$ and $\Xi^n: \mathbb{N}_0 \times \Omega \rightarrow \mathbb{R}^e$ be stochastic processes which satisfy for every $m \in \mathbb{N}$ that

$$\mathbb{S}_m^n = \mathcal{S}^n(\mathbb{S}_{m-1}^n, \Theta_{m-1}^n, (\mathcal{Y}_k^{n, m, i})_{(k, i) \in \{0, 1, \dots, N\} \times \mathbb{N}}), \quad (20)$$

$$\Xi_m^n = \Psi_m^n(\Xi_{m-1}^n, \Phi^{n, m, \mathbb{S}_m^n}(\Theta_{m-1}^n)), \quad \text{and} \quad \Theta_m^n = \Theta_{m-1}^n - \psi_m^n(\Xi_m^n). \quad (21)$$

In the setting of Framework 3.1 above we think under suitable hypotheses for sufficiently large $N \in \mathbb{N}$, sufficiently large $(M_n)_{n \in \mathbb{N}_0} \subseteq \mathbb{N}$, sufficiently large $(K_n)_{n \in \mathbb{N}} \subseteq \mathbb{N}$, every $n \in \{0, 1, \dots, N\}$, and every $x \in D$ of $\mathbb{V}_n^{1, \mathbb{S}_{M_n}^n}(\Theta_{M_n}^n, x): \Omega \rightarrow \mathbb{R}$ as a suitable approximation

$$\mathbb{V}_n^{1, \mathbb{S}_{M_n}^n}(\Theta_{M_n}^n, x) \approx u(t_n, x) \quad (22)$$

of $u(t_n, x)$ where $u = (u(t, x))_{(t, x) \in [0, T] \times \mathbb{R}^d} \in C^{1,2}([0, T] \times \mathbb{R}^d, \mathbb{R})$ is a function with at most polynomially growing derivatives which satisfies for every $t \in (0, T]$, $x \in \partial_D$ that

$\langle \mathbf{n}(x), (\nabla_x u)(t, x) \rangle = 0$ and which satisfies for every $t \in [0, T]$, $x \in D$ that $u(0, x) = g(x)$, $\int_D |f(t, x, \mathbf{x}, u(t, x), u(t, \mathbf{x}))| \nu_x(d\mathbf{x}) < \infty$, and

$$\begin{aligned} \left(\frac{\partial}{\partial t} u\right)(t, x) &= \int_D f(t, x, \mathbf{x}, u(t, x), u(t, \mathbf{x})) \nu_x(d\mathbf{x}) \\ &+ \langle \mu(x), (\nabla_x u)(t, x) \rangle + \frac{1}{2} \text{Trace}(\sigma(x)[\sigma(x)]^*(\text{Hess}_x u)(t, x)) \end{aligned} \quad (23)$$

(cf. (15)). Compared to the simplified algorithm in Framework 2.2 above, the major new elements introduced in Framework 3.1 are the following:

- (a) The numbers of gradient descent steps taken to compute approximations for the solution of the PDE at the times t_n , $n \in \{1, 2, \dots, N\}$, are allowed to vary with n , and so are specified by a sequence $(M_n)_{n \in \mathbb{N}_0} \subseteq \mathbb{N}$ in Framework 3.1 above.
- (b) The numbers of samples used for the Monte Carlo approximation of the non-local term in the approximation for the solution of the PDE at the times t_n , $n \in \{1, 2, \dots, N\}$, are allowed to vary with n , and so are specified by a sequence $(K_n)_{n \in \mathbb{N}_0} \subseteq \mathbb{N}$ in Framework 3.1 above.
- (c) The approximating functions $\mathbb{V}_n^{j, \mathbf{s}}$, $(j, \mathbf{s}, n) \in \mathbb{N} \times \mathbb{R}^s \times \{0, 1, \dots, N\}$, in Framework 3.1 above are not specified concretely in order to allow for a variety of neural network architectures. For the concrete choice of these functions employed in our numerical simulations, we refer the reader to Section 5.
- (d) For every $m \in \{1, 2, \dots, M\}$ the loss function used in the m th gradient descent step may be computed using a minibatch of samples instead of just one sample (cf. (18)). The sizes of these minibatches are specified by a sequence $(J_m)_{m \in \mathbb{N}} \subseteq \mathbb{N}$.
- (e) Compared to Framework 2.2 above, the more general form of the PDEs considered in this section (cf. (23)) requires more flexibility in the definition of the time-discrete stochastic processes $\mathcal{Y}^{n, m, j}: \{0, 1, \dots, N\} \times \Omega \rightarrow \mathbb{R}^d$, $(n, m, j) \in \{1, 2, \dots, N\} \times \mathbb{N} \times \mathbb{N}$, which are specified in Framework 3.1 above in terms of the Brownian motions $W^{n, m, j}: [0, T] \times \Omega \rightarrow \mathbb{R}^d$, $(n, m, j) \in \{1, 2, \dots, N\} \times \mathbb{N} \times \mathbb{N}$, via a function $H: [0, T]^2 \times \mathbb{R}^d \times \mathbb{R}^d \rightarrow \mathbb{R}^d$ (cf. (17)). We refer the reader to (44) in Subsection 5.1 below, (46) in Subsection 5.2 below, (48) in Subsection 5.3 below, (50) in Subsection 5.4 below, and (72) in Subsection 5.5 below for concrete choices of H in the approximation of various example PDEs.
- (f) For every $n \in \{1, 2, \dots, N\}$, $m \in \mathbb{N}$ the optimization step in (21) in Framework 3.1 above is specified generically in terms of the functions $\psi_m^n: \mathbb{R}^e \rightarrow \mathbb{R}^d$ and $\Psi_m^n: \mathbb{R}^e \times \mathbb{R}^d \rightarrow \mathbb{R}^e$ and the random variable $\Xi_m^n: \Omega \rightarrow \mathbb{R}^e$. This generic formulation covers a variety of SGD based optimization algorithms such as Adagrad [31], RMSprop, or Adam [64]. For example, in order to implement the Adam optimization algorithm,

for every $n \in \{1, 2, \dots, N\}$, $m \in \mathbb{N}$ the random variable Ξ_m^n can be used to hold suitable first and second moment estimates (see (42) and (43) in Section 5 below for the concrete specification of these functions implementing the Adam optimization algorithm).

- (g) The processes $\mathbb{S}^n: \mathbb{N}_0 \times \Omega \rightarrow \mathbb{R}^c$, $n \in \{1, 2, \dots, N\}$, and functions $\mathcal{S}^n: \mathbb{R}^c \times \mathbb{R}^d \times (\mathbb{R}^d)^{\{0,1,\dots,N\} \times \mathbb{N}} \rightarrow \mathbb{R}^c$, $n \in \{1, 2, \dots, N\}$, in Framework 3.1 above can be used to implement batch normalization; see [61] for details. Loosely speaking, for every $n \in \{1, 2, \dots, N\}$, $m \in \mathbb{N}$ the random variable $\mathbb{S}_m^n: \Omega \rightarrow \mathbb{R}^c$ then holds mean and variance estimates of the outputs of each layer of the approximating neural networks related to the minibatches that are used as inputs to the neural networks in computing the loss function at the corresponding gradient descent step.

4 Multilevel Picard approximation method for non-local PDEs

In this section we introduce in Framework 4.1 in Subsection 4.1 below our extension of the full history recursive multilevel Picard approximation method for approximating solutions of non-local nonlinear PDEs with Neumann boundary conditions. The MLP method was first introduced in E et al. [36] and Hutzenthaler et al. [60] and later extended in a number of directions; see E et al. [33] and Beck et al. [12] for recent surveys. We also refer the reader to Becker et al. [13] and E et al. [35] for numerical simulations illustrating the performance of MLP methods across a range of example PDE problems.

In Subsection 4.2 below, we will specify five concrete examples of (non-local) nonlinear PDEs and describe how Framework 4.1 can be specialized to compute approximate solutions to these example PDEs. These computations will be used in Section 5 to obtain reference values to compare the deep learning-based approximation method proposed in Section 3 above against.

4.1 Description of the proposed approximation method

Framework 4.1 (Multilevel Picard approximation method). *Assume Framework 2.1, let $c, T \in (0, \infty)$, $\mathfrak{I} = \bigcup_{n \in \mathbb{N}} \mathbb{Z}^n$, $f \in C([0, T] \times D \times D \times \mathbb{R} \times \mathbb{R}, \mathbb{R})$, $g \in C(D, \mathbb{R})$, $u \in C([0, T] \times D, \mathbb{R})$, assume $u|_{[0, T] \times D} \in C^{1,2}([0, T] \times D, \mathbb{R})$, let $\nu_x: \mathcal{B}(D) \rightarrow [0, 1]$, $x \in D$, be probability measures, for every $x \in D$ let $Z_x^i: \Omega \rightarrow D$, $i \in \mathfrak{I}$, be i.i.d. random variables, assume for every $A \in \mathcal{B}(D)$, $i \in \mathfrak{I}$ that $\mathbb{P}(Z_x^i \in A) = \nu_x(A)$, let $\phi_r: \mathbb{R} \rightarrow \mathbb{R}$, $r \in [0, \infty]$, satisfy for every $r \in [0, \infty]$, $y \in \mathbb{R}$ that*

$$\phi_r(y) = \min\{r, \max\{-r, y\}\}, \quad (24)$$

let $(\Omega, \mathcal{F}, \mathbb{P})$ be a probability space, let $\mathcal{V}^i: \Omega \rightarrow (0, 1)$, $i \in \mathfrak{I}$, be independent $\mathcal{U}_{(0,1)}$ -distributed random variables, let $V^i: [0, T] \times \Omega \rightarrow [0, T]$, $i \in \mathfrak{I}$, satisfy for every $t \in [0, T]$, $i \in \mathfrak{I}$ that

$$V_t^i = t + (T - t)\mathcal{V}^i, \quad (25)$$

let $W^i: [0, T] \times \Omega \rightarrow \mathbb{R}^d$, $i \in \mathfrak{I}$, be independent standard Brownian motions, assume that $(\mathcal{V}^i)_{i \in \mathfrak{I}}$ and $(W^i)_{i \in \mathfrak{I}}$ are independent, let $\mu: \mathbb{R}^d \rightarrow \mathbb{R}^d$ and $\sigma: \mathbb{R}^d \rightarrow \mathbb{R}^{d \times d}$ be globally Lipschitz continuous, for every $x \in \mathbb{R}^d$, $i \in \mathfrak{I}$, $t \in [0, T]$ let $X_t^{x,i} = (X_{t,s}^{x,i})_{s \in [t, T]}: [t, T] \times \Omega \rightarrow \mathbb{R}^d$ be a stochastic process with continuous sample paths, let $(K_{n,l,m})_{n,l,m \in \mathbb{N}_0} \subseteq \mathbb{N}$, for every $i \in \mathfrak{I}$, $n, M \in \mathbb{N}_0$, $r \in [0, \infty]$ let $U_{n,M,r}^i: [0, T] \times \mathbb{R}^d \times \Omega \rightarrow \mathbb{R}^k$ satisfy for every $t \in [0, T]$, $x \in \mathbb{R}^d$ that

$$\begin{aligned} U_{n,M,r}^i(t, x) = & \left[\sum_{l=0}^{n-1} \frac{(T-t)}{M^{n-l}} \sum_{m=1}^{M^{n-l}} \frac{1}{K_{n,l,m}} \sum_{k=1}^{K_{n,l,m}} \left[f \left(V_t^{(i,l,m)}, X_{t,V_t^{(i,l,m)}}^{x,(i,l,m)}, Z_{X_{t,V_t^{(i,l,m)}}^{x,(i,l,m)}, V_t^{(i,l,m)}}^{(i,l,m,k)} \right), \right. \right. \\ & \left. \left. \phi_r \left(U_{l,M,r}^{(i,l,m)} \left(V_t^{(i,l,m)}, X_{t,V_t^{(i,l,m)}}^{x,(i,l,m)} \right) \right), \phi_r \left(U_{l,M,r}^{(i,l,m)} \left(V_t^{(i,l,m)}, Z_{X_{t,V_t^{(i,l,m)}}^{x,(i,l,m)}, V_t^{(i,l,m)}}^{(i,l,m,k)} \right) \right) \right) \right. \\ & \left. - \mathbb{1}_{\mathbb{N}}(l) f \left(V_t^{(i,l,m)}, X_{t,V_t^{(i,l,m)}}^{x,(i,l,m)}, Z_{X_{t,V_t^{(i,l,m)}}^{x,(i,l,m)}, V_t^{(i,l,m)}}^{(i,l,m,k)} \right), \phi_r \left(U_{\max\{l-1,0\},M,r}^{(i,l,-m)} \left(V_t^{(i,l,m)}, X_{t,V_t^{(i,l,m)}}^{x,(i,l,m)} \right) \right) \right. \\ & \left. \left. \phi_r \left(U_{\max\{l-1,0\},M,r}^{(i,l,-m)} \left(V_t^{(i,l,m)}, Z_{X_{t,V_t^{(i,l,m)}}^{x,(i,l,m)}, V_t^{(i,l,m)}}^{(i,l,m,k)} \right) \right) \right) \right] + \frac{\mathbb{1}_{\mathbb{N}}(n)}{M^n} \left[\sum_{m=1}^{M^n} g \left(X_{t,T}^{x,(i,0,-m)} \right) \right], \quad (26) \end{aligned}$$

assume for every $t \in [0, T]$, $x \in \partial_D$ that $\langle \mathbf{n}(x), (\nabla_x u)(t, x) \rangle = 0$, and assume for every $t \in [0, T]$, $x \in D$ that $\|u(t, x)\| \leq c(1 + \|x\|^c)$, $u(T, x) = g(x)$, and

$$\begin{aligned} & \left(\frac{\partial}{\partial t} u \right)(t, x) + \frac{1}{2} \text{Trace}(\sigma(x)[\sigma(x)]^* (\text{Hess}_x u)(t, x)) + \langle \mu(x), (\nabla_x u)(t, x) \rangle \\ & + \int_D f(t, x, \mathbf{x}, u(t, x), u(t, \mathbf{x})) \nu_x(d\mathbf{x}) = 0. \quad (27) \end{aligned}$$

4.2 Examples for the approximation method

Example 4.2 (Fisher–KPP PDEs with Neumann boundary conditions). *In this example we specialize Framework 4.1 to the case of certain Fisher–KPP PDEs with Neumann boundary conditions (cf., e.g., Bian et al. [18] and Wang et al. [92]).*

Assume Framework 4.1, let $\epsilon \in (0, \infty)$ satisfy $\epsilon = \frac{1}{10}$, assume that $d \in \{1, 2, 5, 10\}$, $D = [-1/2, 1/2]^d$, and $T \in \{1/5, 1/2, 1\}$, assume for every $n, l, m \in \mathbb{N}$ that $K_{n,l,m} = 1$, assume for every $t \in [0, T]$, $x, \mathbf{x} \in D$, $y, \mathbf{y} \in \mathbb{R}$, $v \in \mathbb{R}^d$ that $g(x) = \exp(-\frac{1}{4}\|x\|^2)$, $\mu(x) = (0, \dots, 0)$, $\sigma(x)v = \epsilon v$, and $f(t, x, \mathbf{x}, y, \mathbf{y}) = y(1 - y)$, and assume that for every $x \in \mathbb{R}^d$, $i \in \mathfrak{I}$, $t \in [0, T]$, $s \in [t, T]$ it holds \mathbb{P} -a.s. that

$$X_{t,s}^{x,i} = R \left(x, x + \int_t^s \mu(X_{t,r}^{x,i}) dr + \int_t^s \sigma(X_{t,r}^{x,i}) dW_r^i \right) = R(x, x + \epsilon(W_s^i - W_t^i)). \quad (28)$$

The solution $u: [0, T] \times D \rightarrow \mathbb{R}$ of the PDE in (27) then satisfies that for every $t \in [0, T]$, $x \in \partial_D$ it holds that $\langle \mathbf{n}(x), (\nabla_x u)(t, x) \rangle = 0$ and that for every $t \in [0, T]$, $x \in D$ it holds that $u(T, x) = \exp(-\frac{1}{4}\|x\|^2)$ and

$$\left(\frac{\partial}{\partial t}u\right)(t, x) + \frac{\epsilon^2}{2}(\Delta_x u)(t, x) + u(t, x)(1 - u(t, x)) = 0. \quad (29)$$

Example 4.3 (Non-local competition PDEs). *In this example we specialize Framework 4.1 to the case of certain non-local competition PDEs (cf., e.g., Doebeli & Ispolatov [30], Berestycki et al. [17], Perthame & Génieys [82], and Génieys et al. [43]).*

Assume Framework 4.1, let $\mathfrak{s}, \epsilon \in (0, \infty)$ satisfy $\mathfrak{s} = \epsilon = \frac{1}{10}$, assume that $d \in \{1, 2, 5, 10\}$, $D = \mathbb{R}^d$, and $T \in \{1/5, 1/2, 1\}$, assume for every $n, l, m \in \mathbb{N}$ that $K_{n,l,m} = 10$, assume for every $x \in \mathbb{R}^d$, $A \in \mathcal{B}(\mathbb{R}^d)$ that $\nu_x(A) = \pi^{-d/2}\mathfrak{s}^{-d} \int_A \exp(-\mathfrak{s}^{-2}\|x - \mathbf{x}\|^2) d\mathbf{x}$, assume for every $t \in [0, T]$, $v, x, \mathbf{x} \in \mathbb{R}^d$, $y, \mathbf{y} \in \mathbb{R}$ that $g(x) = \exp(-\frac{1}{4}\|x\|^2)$, $\mu(x) = (0, \dots, 0)$, $\sigma(x)v = \epsilon v$, and $f(t, x, \mathbf{x}, y, \mathbf{y}) = y(1 - \mathbf{y}\pi^{d/2}\mathfrak{s}^d)$, and assume that for every $x \in \mathbb{R}^d$, $\mathbf{i} \in \mathfrak{I}$, $t \in [0, T]$, $s \in [t, T]$ it holds \mathbb{P} -a.s. that

$$X_{t,s}^{x,\mathbf{i}} = x + \int_t^s \mu(X_{t,r}^{x,\mathbf{i}}) dr + \int_t^s \sigma(X_{t,r}^{x,\mathbf{i}}) dW_r^{\mathbf{i}} = x + \epsilon(W_s^{\mathbf{i}} - W_t^{\mathbf{i}}). \quad (30)$$

The solution $u: [0, T] \times \mathbb{R}^d \rightarrow \mathbb{R}$ of the PDE in (27) then satisfies that for every $t \in [0, T]$, $x \in \mathbb{R}^d$ it holds that $u(T, x) = \exp(-\frac{1}{4}\|x\|^2)$ and

$$\left(\frac{\partial}{\partial t}u\right)(t, x) + \frac{\epsilon^2}{2}(\Delta_x u)(t, x) + u(t, x) \left(1 - \int_{\mathbb{R}^d} u(t, \mathbf{x}) \exp\left(-\frac{\|x - \mathbf{x}\|^2}{s^2}\right) d\mathbf{x}\right) = 0. \quad (31)$$

Example 4.4 (Non-local sine-Gordon PDEs). *In this example we specialize Framework 4.1 to the case of certain non-local sine-Gordon type PDEs (cf., e.g., Hairer & Shen [49], Barone et al. [7], and Coleman [25]).*

Assume Framework 4.1, let $\mathfrak{s}, \epsilon \in (0, \infty)$ satisfy $\mathfrak{s} = \epsilon = \frac{1}{10}$, assume that $d \in \{1, 2, 5, 10\}$, $D = \mathbb{R}^d$, and $T \in \{1/5, 1/2, 1\}$, assume for every $n, l, m \in \mathbb{N}$ that $K_{n,l,m} = 10$, assume for every $x \in \mathbb{R}^d$, $A \in \mathcal{B}(\mathbb{R}^d)$ that $\nu_x(A) = \pi^{-d/2}\mathfrak{s}^{-d} \int_A \exp(-\mathfrak{s}^{-2}\|x - \mathbf{x}\|^2) d\mathbf{x}$, assume for every $t \in [0, T]$, $v, x, \mathbf{x} \in \mathbb{R}^d$, $y, \mathbf{y} \in \mathbb{R}$ that $g(x) = \exp(-\frac{1}{4}\|x\|^2)$, $\mu(x) = (0, \dots, 0)$, $\sigma(x)v = \epsilon v$, and $f(t, x, \mathbf{x}, y, \mathbf{y}) = \sin(y) - \mathbf{y}\pi^{d/2}\mathfrak{s}^d$, and assume that for every $x \in \mathbb{R}^d$, $\mathbf{i} \in \mathfrak{I}$, $t \in [0, T]$, $s \in [t, T]$ it holds \mathbb{P} -a.s. that

$$X_{t,s}^{x,\mathbf{i}} = x + \int_t^s \mu(X_{t,r}^{x,\mathbf{i}}) dr + \int_t^s \sigma(X_{t,r}^{x,\mathbf{i}}) dW_r^{\mathbf{i}} = x + \epsilon(W_s^{\mathbf{i}} - W_t^{\mathbf{i}}). \quad (32)$$

The solution $u: [0, T] \times \mathbb{R}^d \rightarrow \mathbb{R}$ of the PDE in (27) then satisfies that for every $t \in [0, T]$, $x \in \mathbb{R}^d$ it holds that $u(T, x) = \exp(-\frac{1}{4}\|x\|^2)$ and

$$\left(\frac{\partial}{\partial t}u\right)(t, x) + \frac{\epsilon^2}{2}(\Delta_x u)(t, x) + \sin(u(t, x)) - \int_{\mathbb{R}^d} u(t, \mathbf{x}) \exp\left(-\frac{\|x - \mathbf{x}\|^2}{s^2}\right) d\mathbf{x} = 0. \quad (33)$$

Example 4.5 (Replicator-mutator PDEs). *In this example we specialize Framework 4.1 to the case of certain d -dimensional replicator-mutator PDEs (cf., e.g., Hamel et al. [50]).*

Assume Framework 4.1, let $\mathbf{m}_1, \mathbf{m}_2, \dots, \mathbf{m}_d, \mathfrak{s}_1, \mathfrak{s}_2, \dots, \mathfrak{s}_d, \mathbf{u}_1, \mathbf{u}_2, \dots, \mathbf{u}_d \in \mathbb{R}$ satisfy for every $k \in \{1, 2, \dots, d\}$ that $\mathbf{m}_k = \frac{1}{10}$, $\mathfrak{s}_k = \frac{1}{20}$, and $\mathbf{u}_k = 0$, assume that $d \in \{1, 2, 5, 10\}$, $D = \mathbb{R}^d$, and $T \in \{1/5, 1/2, 1\}$, assume for every $n, l, m \in \mathbb{N}$ that $K_{n,l,m} = 10$, let $a: \mathbb{R}^d \rightarrow \mathbb{R}$ satisfy for every $x \in \mathbb{R}^d$ that $a(x) = -\frac{1}{2}\|x\|^2$, assume for every $x \in \mathbb{R}^d$, $A \in \mathcal{B}(\mathbb{R}^d)$ that $\nu_x(A) = \int_{A \cap [-1/2, 1/2]^d} d\mathbf{x}$, assume for every $t \in [0, T]$, $v = (v_1, \dots, v_d)$, $x = (x_1, \dots, x_d) \in \mathbb{R}^d$, $\mathbf{x} \in \mathbb{R}^d$, $y, \mathbf{y} \in \mathbb{R}$ that $g(x) = (2\pi)^{-d/2} [\prod_{i=1}^d |\mathfrak{s}_i|^{-1/2}] \exp(-\sum_{i=1}^d \frac{(x_i - \mathbf{u}_i)^2}{2\mathfrak{s}_i})$, $\mu(x) = (0, \dots, 0)$, $\sigma(x)v = (\mathbf{m}_1 v_1, \dots, \mathbf{m}_d v_d)$, and

$$f(t, x, \mathbf{x}, y, \mathbf{y}) = y(a(x) - \mathbf{y}a(\mathbf{x})), \quad (34)$$

and assume that for every $x \in \mathbb{R}^d$, $\mathbf{i} \in \mathfrak{I}$, $t \in [0, T]$, $s \in [t, T]$ it holds \mathbb{P} -a.s. that

$$X_{t,s}^{x,\mathbf{i}} = x + \int_t^s \mu(X_{t,r}^{x,\mathbf{i}}) dr + \int_t^s \sigma(X_{t,r}^{x,\mathbf{i}}) dW_r^{\mathbf{i}} = x + \sigma(0)(W_s^{\mathbf{i}} - W_t^{\mathbf{i}}). \quad (35)$$

The solution $u: [0, T] \times \mathbb{R}^d \rightarrow \mathbb{R}$ of the PDE in (27) then satisfies that for every $t \in [0, T]$, $x = (x_1, \dots, x_d) \in \mathbb{R}^d$ it holds that $u(T, x) = (2\pi)^{-d/2} [\prod_{i=1}^d |\mathfrak{s}_i|^{-1/2}] \exp(-\sum_{i=1}^d \frac{(x_i - \mathbf{u}_i)^2}{2\mathfrak{s}_i})$ and

$$\left(\frac{\partial}{\partial t} u\right)(t, x) + u(t, x) \left(a(x) - \int_{[-1/2, 1/2]^d} u(t, \mathbf{x}) a(\mathbf{x}) d\mathbf{x} \right) + \sum_{i=1}^d \frac{1}{2} |\mathbf{m}_i|^2 \left(\frac{\partial^2}{\partial x_i^2} u\right)(t, x) = 0. \quad (36)$$

Example 4.6 (Allen–Cahn PDEs with conservation of mass). *In this example we specialize Framework 4.1 to the case of certain Allen–Cahn PDEs with cubic nonlinearity, conservation of mass, and no-flux boundary conditions (cf., e.g., Rubinstein & Sternberg [86]).*

Assume Framework 4.1, let $\epsilon \in (0, \infty)$ satisfy $\epsilon = \frac{1}{10}$, assume that $d \in \{1, 2, 5, 10\}$, $D = [-1/2, 1/2]^d$, and $T \in \{1/5, 1/2, 1\}$, assume for every $n, l, m \in \mathbb{N}$ that $K_{n,l,m} = 10$, assume for every $x \in D$, $A \in \mathcal{B}(D)$ that $\nu_x(A) = \int_A d\mathbf{x}$, assume for every $t \in [0, T]$, $x, \mathbf{x} \in D$, $y, \mathbf{y} \in \mathbb{R}$, $v \in \mathbb{R}^d$ that $g(x) = \exp(-\frac{1}{4}\|x\|^2)$, $\mu(x) = (0, \dots, 0)$, $\sigma(x)v = \epsilon v$, and $f(t, x, \mathbf{x}, y, \mathbf{y}) = y - y^3 - (\mathbf{y} - \mathbf{y}^3)$, and assume that for every $x \in \mathbb{R}^d$, $\mathbf{i} \in \mathfrak{I}$, $t \in [0, T]$, $s \in [t, T]$ it holds \mathbb{P} -a.s. that

$$X_{t,s}^{x,\mathbf{i}} = R \left(x, x + \int_t^s \mu(X_{t,r}^{x,\mathbf{i}}) dr + \int_t^s \sigma(X_{t,r}^{x,\mathbf{i}}) dW_r^{\mathbf{i}} \right) = R(x, x + \epsilon(W_s^{\mathbf{i}} - W_t^{\mathbf{i}})). \quad (37)$$

The solution $u: [0, T] \times D \rightarrow \mathbb{R}$ of the PDE in (27) then satisfies that for every $t \in [0, T]$, $x \in \partial_D$ it holds that $\langle \mathbf{n}(x), (\nabla_x u)(t, x) \rangle = 0$ and that for every $t \in [0, T]$, $x \in D$ it holds that $u(T, x) = \exp(-\frac{1}{4}\|x\|^2)$ and

$$\left(\frac{\partial}{\partial t} u\right)(t, x) + \frac{\epsilon^2}{2} (\Delta_x u)(t, x) + u(t, x) - [u(t, x)]^3 - \int_{[-1/2, 1/2]^d} u(t, \mathbf{x}) - [u(t, \mathbf{x})]^3 d\mathbf{x} = 0. \quad (38)$$

5 Numerical simulations

In this section we illustrate the performance of the machine learning-based approximation method proposed in Framework 3.1 in Subsection 3.2 above by means of numerical simulations for five concrete (non-local) nonlinear PDEs; see Subsections 5.1, 5.2, 5.3, 5.4, and 5.5 below. In each of these numerical simulations we employ the general machine learning-based approximation method proposed in Framework 3.1 with certain 4-layer neural networks and using the Adam optimizer (cf. (42) and (43) in Framework 5.1 below and Kingma & Ba [64]).

More precisely, in each of the numerical simulations in Subsections 5.1, 5.2, 5.3, 5.4, and 5.5 the functions $\mathbb{V}_n^{j,s}: \mathbb{R}^d \times \mathbb{R}^d \rightarrow \mathbb{R}$ with $n \in \{1, 2, \dots, N\}$, $j \in \{1, 2, \dots, 8000\}$, $s \in \mathbb{R}^c$ are implemented as N fully-connected feedforward neural networks. These neural networks consist of 4 layers (corresponding to 3 affine linear transformations in the neural networks) where the input layer is d -dimensional (with d neurons on the input layer), where the two hidden layers are both $(d+50)$ -dimensional (with $d+50$ neurons on each of the two hidden layers), and where the output layer is 1-dimensional (with 1 neuron on the output layer). We refer to Figure 1 for a graphical illustration of the neural network architecture used in the numerical simulations in Subsections 5.1, 5.2, 5.3, 5.4, and 5.5.

As activation functions just in front of the two hidden layers we employ, in Subsections 5.1, 5.2, 5.3, and 5.4 below, multidimensional versions of the hyperbolic tangent function

$$\mathbb{R} \ni x \mapsto (e^x + e^{-x})^{-1}(e^x - e^{-x}) \in \mathbb{R}, \quad (39)$$

and we employ, in Subsection 5.5 below, multidimensional versions of the ReLU function

$$\mathbb{R} \ni x \mapsto \max\{x, 0\} \in \mathbb{R}. \quad (40)$$

In addition, in Subsections 5.1, 5.2, and 5.4 we use the square function $\mathbb{R} \ni x \mapsto x^2 \in \mathbb{R}$ as activation function just in front of the output layer and in Subsections 5.3 and 5.5 we use the identity function $\mathbb{R} \ni x \mapsto x \in \mathbb{R}$ as activation function just in front of the output layer. Furthermore, we employ Xavier initialization to initialize all neural network parameters; see Glorot & Bengio [44] for details. We did not employ batch normalization in our simulations.

Each of the numerical experiments presented below was performed with the JULIA library HIGHIMPDE.JL on a NVIDIA TITAN RTX GPU with 1350 MHz core clock and 24 GB GDDR6 memory with 7000 MHz clock rate where the underlying system consisted of an AMD EPYC 7742 64-core CPU with 2TB memory running JULIA 1.7.2 on Ubuntu 20.04.3. We refer to Section 6 below for the employed JULIA source codes.

Framework 5.1. *Assume Framework 3.1, assume $\mathfrak{d} = (d+50)(d+1) + (d+50)(d+51) + (d+51)$, let $\varepsilon, \beta_1, \beta_2 \in \mathbb{R}$, $(\gamma_m)_{m \in \mathbb{N}} \subseteq (0, \infty)$ satisfy $\varepsilon = 10^{-8}$, $\beta_1 = \frac{9}{10}$, and $\beta_2 = \frac{999}{1000}$, let $g: D \rightarrow \mathbb{R}$, $\mu: D \rightarrow \mathbb{R}^d$, and $\sigma: D \rightarrow \mathbb{R}^{d \times d}$ be continuous, let $u = (u(t, x))_{(t,x) \in [0,T] \times D} \in$*

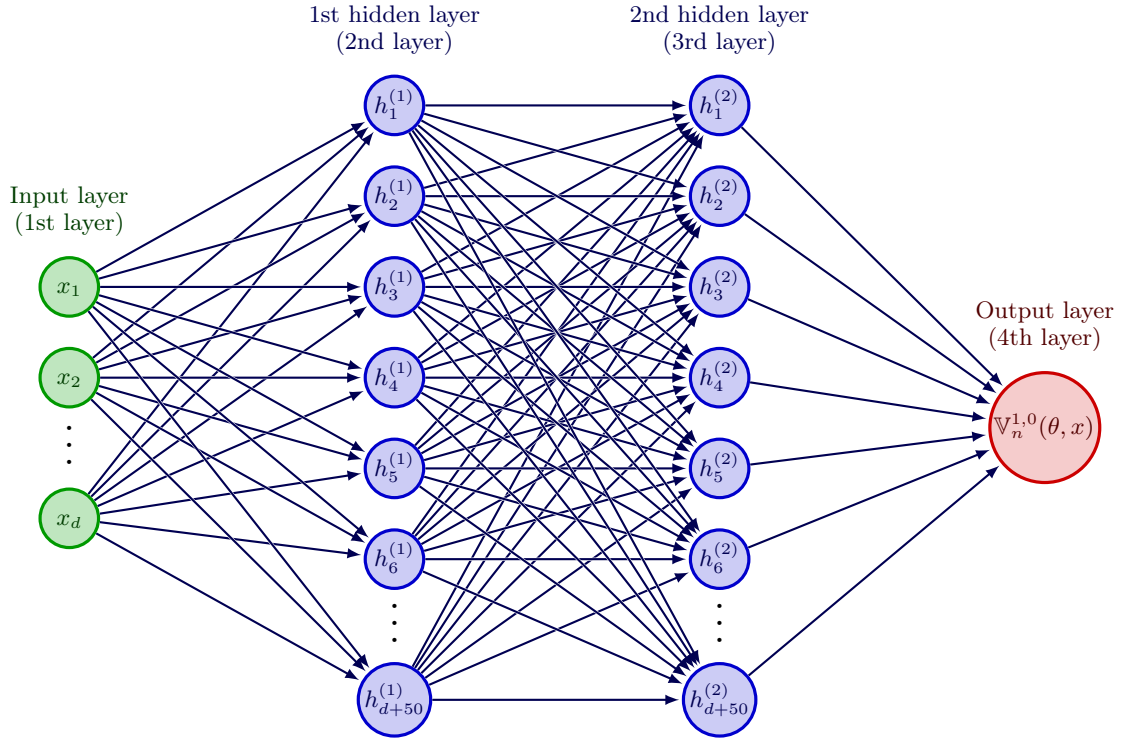


Figure 1: Graphical illustration of the neural network architecture used in the numerical simulations. In Subsections 5.1, 5.2, 5.3, 5.4, and 5.5 we employ neural networks with 4 layers (corresponding to 3 affine linear transformations in the neural networks) with d neurons on the input layer (corresponding to a d -dimensional input layer), with $d+50$ neurons on the 1st hidden layer (corresponding to a $(d+50)$ -dimensional 1st hidden layer), with $d+50$ neurons on the 2nd hidden layer (corresponding to a $(d+50)$ -dimensional 2nd hidden layer), and with 1 neuron on the output layer (corresponding to a 1-dimensional output layer) in the numerical simulations.

$C^{1,2}([0, T] \times D, \mathbb{R})$ have at most polynomially growing partial derivatives, assume for every $t \in (0, T]$, $x \in \partial_D$ that $\langle \mathbf{n}(x), (\nabla_x u)(t, x) \rangle = 0$, assume for every $t \in [0, T]$, $x \in D$, $j \in \mathbb{N}$, $\mathbf{s} \in \mathbb{R}^c$ that $u(0, x) = g(x) = \mathbb{V}_0^{j, \mathbf{s}}(\theta, x)$, $\int_D |f(t, x, \mathbf{x}, u(t, x), u(t, \mathbf{x}))| \nu_x(d\mathbf{x}) < \infty$, and

$$\begin{aligned} \left(\frac{\partial}{\partial t} u\right)(t, x) &= \frac{1}{2} \text{Trace}(\sigma(x)[\sigma(x)]^*(\text{Hess}_x u)(t, x)) + \langle \mu(x), (\nabla_x u)(t, x) \rangle \\ &+ \int_D f(t, x, \mathbf{x}, u(t, x), u(t, \mathbf{x})) \nu_x(d\mathbf{x}), \end{aligned} \quad (41)$$

assume for every $m \in \mathbb{N}$, $i \in \{0, 1, \dots, N\}$ that $J_m = 8000$, $t_i = \frac{iT}{N}$, and $\varrho = 2\mathfrak{d}$, and assume for every $n \in \{1, 2, \dots, N\}$, $m \in \mathbb{N}$, $x = (x_1, \dots, x_{\mathfrak{d}})$, $y = (y_1, \dots, y_{\mathfrak{d}})$, $\eta = (\eta_1, \dots, \eta_{\mathfrak{d}}) \in \mathbb{R}^{\mathfrak{d}}$ that

$$\Xi_0^n(x, y, \eta) = 0, \quad \Psi_m^n(x, y, \eta) = (\beta_1 x + (1 - \beta_1)\eta, \beta_2 y + (1 - \beta_2)((\eta_1)^2, \dots, (\eta_{\mathfrak{d}})^2)), \quad (42)$$

and

$$\psi_m^n(x, y) = \left(\left[\sqrt{\frac{|y_1|}{1 - (\beta_2)^m}} + \varepsilon \right]^{-1} \frac{\gamma_m x_1}{1 - (\beta_1)^m}, \dots, \left[\sqrt{\frac{|y_{\mathfrak{d}}|}{1 - (\beta_2)^m}} + \varepsilon \right]^{-1} \frac{\gamma_m x_{\mathfrak{d}}}{1 - (\beta_1)^m} \right). \quad (43)$$

5.1 Fisher–KPP PDEs with Neumann boundary conditions

In this subsection we use the machine learning-based approximation method in Framework 5.1 to approximately calculate the solutions of certain Fisher–KPP PDEs with Neumann boundary conditions (cf., e.g., Bian et al. [18] and Wang et al. [92]).

Assume Framework 5.1, let $\epsilon \in (0, \infty)$ satisfy $\epsilon = \frac{1}{10}$, assume that $d \in \{1, 2, 5, 10\}$, $D = [-1/2, 1/2]^d$, $T \in \{1/5, 1/2, 1\}$, $N = 10$, $K_1 = K_2 = \dots = K_N = 1$, and $M_1 = M_2 = \dots = M_N = 500$, assume for every $n, m, j \in \mathbb{N}$, $\omega \in \Omega$ that $\xi^{n, m, j}(\omega) = (0, \dots, 0)$, assume for every $m \in \mathbb{N}$ that $\gamma_m = 10^{-2}$, and assume for every $s, t \in [0, T]$, $x, \mathbf{x} \in D$, $y, \mathbf{y} \in \mathbb{R}$, $v \in \mathbb{R}^d$ that $g(x) = \exp(-\frac{1}{4}\|x\|^2)$, $\mu(x) = (0, \dots, 0)$, $\sigma(x)v = \epsilon v$, $f(t, x, \mathbf{x}, y, \mathbf{y}) = y(1 - y)$, and

$$H(t, s, x, v) = R(x, x + \mu(x)(t - s) + \sigma(x)v) = R(x, x + \epsilon v) \quad (44)$$

(cf. (6) and (17)). The solution $u: [0, T] \times D \rightarrow \mathbb{R}$ of the PDE in (41) then satisfies that for every $t \in (0, T]$, $x \in \partial_D$ it holds that $\langle \mathbf{n}(x), (\nabla_x u)(t, x) \rangle = 0$ and that for every $t \in [0, T]$, $x \in D$ it holds that $u(0, x) = \exp(-\frac{1}{4}\|x\|^2)$ and

$$\left(\frac{\partial}{\partial t} u\right)(t, x) = \frac{\epsilon^2}{2} (\Delta_x u)(t, x) + u(t, x)(1 - u(t, x)). \quad (45)$$

In (45) the function $u: [0, T] \times D \rightarrow \mathbb{R}$ models the proportion of a particular type of alleles in a biological population spatially structured over D . For every $t \in [0, T]$, $x \in \mathbb{R}^d$ the number $u(t, x) \in \mathbb{R}$ describes the proportion of individuals with a particular type of alleles located at position $x = (x_1, \dots, x_d) \in \mathbb{R}^d$ at time $t \in [0, T]$. In Table 1 we use the machine learning-based approximation method in Framework 5.1 to approximately calculate the mean of

d	T	N	Mean of the approx. method	Standard deviation of the approx. method	Reference value	Relative L^1 -approx. error	Standard deviation of the error	Average runtime in seconds
1	$1/5$	10	0.9995902	0.0000107	0.9996057	0.0000155	0.0000107	24.887
2	$1/5$	10	0.9991759	0.0000191	0.9991887	0.0000186	0.0000116	26.175
5	$1/5$	10	0.9979572	0.0000388	0.9979693	0.0000303	0.0000235	27.312
10	$1/5$	10	0.9959224	0.0000341	0.9959337	0.0000275	0.0000196	28.972
1	$1/2$	10	0.9992463	0.0000341	0.9992572	0.0000237	0.0000248	26.631
2	$1/2$	10	0.9984982	0.0000287	0.9985442	0.0000460	0.0000287	27.007
5	$1/2$	10	0.9962227	0.0000330	0.9962314	0.0000306	0.0000041	27.632
10	$1/2$	10	0.9925257	0.0001663	0.9921744	0.0003541	0.0001676	28.743
1	1	10	0.9991423	0.0000331	0.9989768	0.0001657	0.0000332	26.601
2	1	10	0.9982349	0.0000782	0.9982498	0.0000605	0.0000430	26.965
5	1	10	0.9956516	0.0000853	0.9957053	0.0000839	0.0000466	27.428
10	1	10	0.9912297	0.0001072	0.9904936	0.0007431	0.0001083	28.521

Table 1: Numerical simulations for the approximation method in Framework 3.1 in the case of the Fisher–KPP PDEs with Neumann boundary conditions in (45) in Subsection 5.1.

$\mathbb{V}_N^{1,0}(\Theta_{M_N}^N, (0, \dots, 0))$, the standard deviation of $\mathbb{V}_N^{1,0}(\Theta_{M_N}^N, (0, \dots, 0))$, the relative L^1 -approximation error associated to $\mathbb{V}_N^{1,0}(\Theta_{M_N}^N, (0, \dots, 0))$, the uncorrected sample standard deviation of the approximation error associated to $\mathbb{V}_N^{1,0}(\Theta_{M_N}^N, (0, \dots, 0))$, and the average runtime in seconds needed for calculating one realization of $\mathbb{V}_N^{1,0}(\Theta_{M_N}^N, (0, \dots, 0))$ based on 5 independent realizations (5 independent runs). The reference value, which is used as an approximation for the unknown value $u(T, (0, \dots, 0))$ of the exact solution of (45), has been calculated via the MLP approximation method for non-local nonlinear PDEs in Framework 4.1 (cf. Example 4.2 and Beck et al. [11, Remark 3.3]).

5.2 Non-local competition PDEs

In this subsection we use the machine learning-based approximation method in Framework 5.1 to approximately calculate the solutions of certain non-local competition PDEs (cf., e.g., Doebeli & Ispolatov [30], Berestycki et al. [17], Perthame & Génieys [82], and Génieys et al. [43]).

Assume Framework 5.1, let $\mathfrak{s}, \epsilon \in (0, \infty)$ satisfy $\mathfrak{s} = \epsilon = \frac{1}{10}$, assume that $d \in \{1, 2, 5, 10\}$, $D = \mathbb{R}^d$, $T \in \{1/5, 1/2, 1\}$, $N = 10$, $K_1 = K_2 = \dots = K_N = 5$, and $M_1 = M_2 = \dots = M_N = 500$, assume for every $n, m, j \in \mathbb{N}$, $\omega \in \Omega$ that $\xi^{n,m,j}(\omega) = (0, \dots, 0)$, assume for every $m \in \mathbb{N}$ that $\gamma_m = 10^{-2}$, and assume for every $s, t \in [0, T]$, $v, x, \mathbf{x} \in \mathbb{R}^d$, $y, \mathbf{y} \in \mathbb{R}$, $A \in \mathcal{B}(\mathbb{R}^d)$

that $\nu_x(A) = \pi^{-d/2} \mathfrak{s}^{-d} \int_A \exp(-\mathfrak{s}^{-2} \|x - \mathbf{x}\|^2) d\mathbf{x}$, $g(x) = \exp(-\frac{1}{4} \|x\|^2)$, $\mu(x) = (0, \dots, 0)$, $\sigma(x)v = \epsilon v$, $f(t, x, \mathbf{x}, y, \mathbf{y}) = y(1 - \mathbf{y} \mathfrak{s}^d \pi^{d/2})$, and

$$H(t, s, x, v) = x + \mu(x)(t - s) + \sigma(x)v = x + \epsilon v \quad (46)$$

(cf. (6) and (17)). The solution $u: [0, T] \times \mathbb{R}^d \rightarrow \mathbb{R}$ of the PDE in (41) then satisfies that for every $t \in [0, T]$, $x \in \mathbb{R}^d$ it holds that $u(0, x) = \exp(-\frac{1}{4} \|x\|^2)$ and

$$\left(\frac{\partial}{\partial t} u\right)(t, x) = \frac{\epsilon^2}{2} (\Delta_x u)(t, x) + u(t, x) \left(1 - \int_{\mathbb{R}^d} u(t, \mathbf{x}) \exp\left(-\frac{\|x - \mathbf{x}\|^2}{\mathfrak{s}^2}\right) d\mathbf{x}\right). \quad (47)$$

In (47) the function $u: [0, T] \times \mathbb{R}^d \rightarrow \mathbb{R}$ models the evolution of a population characterized by a set of d biological traits under the combined effects of selection, competition and mutation. For every $t \in [0, T]$, $x \in \mathbb{R}^d$ the number $u(t, x) \in \mathbb{R}$ describes the number of individuals with traits $x = (x_1, \dots, x_d) \in \mathbb{R}^d$ at time $t \in [0, T]$. In Table 2 we use the machine learning-based approximation method in Framework 5.1 to approximately calculate the mean of $\mathbb{V}_N^{1,0}(\Theta_{M_N}^N, (0, \dots, 0))$, the standard deviation of $\mathbb{V}_N^{1,0}(\Theta_{M_N}^N, (0, \dots, 0))$, the relative L^1 -approximation error associated to $\mathbb{V}_N^{1,0}(\Theta_{M_N}^N, (0, \dots, 0))$, the uncorrected sample standard deviation of the approximation error associated to $\mathbb{V}_N^{1,0}(\Theta_{M_N}^N, (0, \dots, 0))$, and the average runtime in seconds needed for calculating one realization of $\mathbb{V}_N^{1,0}(\Theta_{M_N}^N, (0, \dots, 0))$ based on 5 independent realizations (5 independent runs). The reference value, which is used as an approximation for the unknown value $u(T, (0, \dots, 0))$ of the exact solution of (47), has been calculated via the MLP approximation method for non-local nonlinear PDEs in Framework 4.1 (cf. Example 4.3 and Beck et al. [11, Remark 3.3]).

5.3 Non-local sine-Gordon type PDEs

In this subsection we use the machine learning-based approximation method in Framework 5.1 to approximately calculate the solutions of non-local sine-Gordon type PDEs (cf., e.g., Hairer & Shen [49], Barone et al. [7], and Coleman [25]).

Assume Framework 5.1, let $\mathfrak{s}, \epsilon \in (0, \infty)$ satisfy $\mathfrak{s} = \epsilon = \frac{1}{10}$, assume that $d \in \{1, 2, 5, 10\}$, $D = \mathbb{R}^d$, $T \in \{1/5, 1/2, 1\}$, $N = 10$, $K_1 = K_2 = \dots = K_N = 5$, and $M_1 = M_2 = \dots = M_N = 500$, assume for every $n, m, j \in \mathbb{N}$, $\omega \in \Omega$ that $\xi^{n,m,j}(\omega) = (0, \dots, 0)$, assume for every $m \in \mathbb{N}$ that $\gamma_m = 10^{-3}$, and assume for every $s, t \in [0, T]$, $v, x, \mathbf{x} \in \mathbb{R}^d$, $y, \mathbf{y} \in \mathbb{R}$, $A \in \mathcal{B}(\mathbb{R}^d)$ that $\nu_x(A) = \pi^{-d/2} \mathfrak{s}^{-d} \int_A \exp(-\mathfrak{s}^{-2} \|x - \mathbf{x}\|^2) d\mathbf{x}$, $g(x) = \exp(-\frac{1}{4} \|x\|^2)$, $\mu(x) = (0, \dots, 0)$, $\sigma(x)v = \epsilon v$, $f(t, x, \mathbf{x}, y, \mathbf{y}) = \sin(y) - \mathbf{y} \pi^{d/2} \mathfrak{s}^d$, and

$$H(t, s, x, v) = x + \mu(x)(t - s) + \sigma(x)v = x + \epsilon v \quad (48)$$

(cf. (6) and (17)). The solution $u: [0, T] \times \mathbb{R}^d \rightarrow \mathbb{R}$ of the PDE in (41) then satisfies that for every $t \in [0, T]$, $x \in \mathbb{R}^d$ it holds that $u(0, x) = \exp(-\frac{1}{4} \|x\|^2)$ and

$$\left(\frac{\partial}{\partial t} u\right)(t, x) = \frac{\epsilon^2}{2} (\Delta_x u)(t, x) + \sin(u(t, x)) - \int_{\mathbb{R}^d} u(t, \mathbf{x}) \exp\left(-\frac{\|x - \mathbf{x}\|^2}{\mathfrak{s}^2}\right) d\mathbf{x}. \quad (49)$$

d	T	N	Mean of the approx. method	Standard deviation of the approx. method	Reference value	Relative L^1 -approx. error	Standard deviation of the error	Average runtime in seconds
1	$1/5$	5	1.1748404	0.0006512	1.1735975	0.0010591	0.0005549	20.571
2	$1/5$	5	1.2114236	0.0008700	1.2096305	0.0014823	0.0007193	25.042
5	$1/5$	5	1.2186650	0.0007070	1.2159038	0.0022709	0.0005814	54.644
10	$1/5$	5	1.2153864	0.0007789	1.2128666	0.0020776	0.0006422	74.331
1	$1/2$	5	1.4755801	0.0032738	1.4694976	0.0041392	0.0022278	20.182
2	$1/2$	5	1.6112576	0.0110426	1.5948898	0.0103067	0.0068414	25.178
5	$1/2$	5	1.6433913	0.0067468	1.6186897	0.0152602	0.0041681	53.618
10	$1/2$	5	1.6323552	0.0053956	1.6090688	0.0144720	0.0033532	73.648
1	1	5	2.0795628	0.0223341	2.0493301	0.0147525	0.0108982	19.836
2	1	5	2.5651031	0.0513671	2.4683060	0.0392160	0.0208107	24.700
5	1	5	2.6977694	0.0381160	2.5606137	0.0535636	0.0148855	52.343
10	1	5	2.6490054	0.0155291	2.5299994	0.0470380	0.0061380	73.186

Table 2: Numerical simulations for the approximation method in Framework 3.1 in the case of the non-local competition PDEs in (47) in Subsection 5.2.

In Table 3 we use the machine learning-based approximation method in Framework 5.1 to approximately calculate the mean of $\mathbb{V}_N^{1,0}(\Theta_{M_N}^N, (0, \dots, 0))$, the standard deviation of $\mathbb{V}_N^{1,0}(\Theta_{M_N}^N, (0, \dots, 0))$, the relative L^1 -approximation error associated to $\mathbb{V}_N^{1,0}(\Theta_{M_N}^N, (0, \dots, 0))$, the uncorrected sample standard deviation of the approximation error associated to $\mathbb{V}_N^{1,0}(\Theta_{M_N}^N, (0, \dots, 0))$, and the average runtime in seconds needed for calculating one realization of $\mathbb{V}_N^{1,0}(\Theta_{M_N}^N, (0, \dots, 0))$ based on 5 independent realizations (5 independent runs). The reference value, which is used as an approximation for the unknown value $u(T, (0, \dots, 0))$ of the exact solution of (49), has been calculated via the MLP approximation method for non-local nonlinear PDEs in Framework 4.1 (cf. Example 4.4 and Beck et al. [11, Remark 3.3]).

5.4 Replicator-mutator PDEs

In this subsection we use the machine learning-based approximation method in Framework 5.1 to approximately calculate the solutions of certain replicator-mutator PDEs describing the dynamics of a phenotype distribution under the combined effects of selection and mutation (cf., e.g., Hamel et al. [50]).

Assume Framework 5.1, let $\mathcal{D} \subseteq \mathbb{R}^d$, $\mathbf{m}_1, \mathbf{m}_2, \dots, \mathbf{m}_d, \mathbf{s}_1, \mathbf{s}_2, \dots, \mathbf{s}_d, \mathbf{u}_1, \mathbf{u}_2, \dots, \mathbf{u}_d, \mathbf{t} \in \mathbb{R}$ satisfy for every $k \in \{1, 2, \dots, d\}$ that $\mathbf{m}_k = \frac{1}{10}$, $\mathbf{s}_k = \frac{1}{20}$, $\mathbf{u}_k = 0$, and $\mathbf{t} = \frac{1}{50}$, assume

d	T	N	Mean of the approx. method	Standard deviation of the approx. method	Reference value	Relative L^1 -approx. error	Standard deviation of the error	Average runtime in seconds
1	$1/5$	10	1.1363013	0.0000101	1.1366512	0.0003079	0.0000089	23.635
2	$1/5$	10	1.1678476	0.0000118	1.1685004	0.0005586	0.0000101	24.788
5	$1/5$	10	1.1731812	0.0000087	1.1740671	0.0007546	0.0000074	24.233
10	$1/5$	10	1.1704700	0.0000063	1.1715686	0.0009377	0.0000054	24.767
1	$1/2$	10	1.3514235	0.0000152	1.3529022	0.0010930	0.0000112	22.622
2	$1/2$	10	1.4393708	0.0000245	1.4423641	0.0020753	0.0000170	23.419
5	$1/2$	10	1.4546282	0.0000816	1.4598476	0.0035754	0.0000559	23.739
10	$1/2$	10	1.4473282	0.0000739	1.4503958	0.0021150	0.0000510	24.222
1	1	10	1.7114614	0.0000309	1.7136091	0.0012533	0.0000180	22.067
2	1	10	1.9019763	0.0000288	1.9062322	0.0022326	0.0000151	22.707
5	1	10	1.9364921	0.0000602	1.9411610	0.0024052	0.0000310	22.899
10	1	10	1.9223347	0.0001494	1.9272222	0.0025360	0.0000775	23.719

Table 3: Numerical simulations for the approximation method in Framework 3.1 in the case of the non-local sine-Gordon PDEs in (49) in Subsection 5.3.

that $d \in \{1, 2, 5, 10\}$, $D = \mathbb{R}^d$, $T \in \{1/10, 1/5, 1/2\}$, $N = 10$, $K_1 = K_2 = \dots = K_N = 5$, let $a \in C(\mathbb{R}^d, \mathbb{R})$, $\delta \in C(\mathbb{R}^d, (0, \infty))$ satisfy for every $x \in \mathbb{R}^d$ that $a(x) = -\frac{1}{2}\|x\|^2$, and assume for every $s, t \in [0, T]$, $v = (v_1, \dots, v_d)$, $x = (x_1, \dots, x_d) \in \mathbb{R}^d$, $\mathbf{x} \in \mathbb{R}^d$, $y, \mathbf{y} \in \mathbb{R}$, $A \in \mathcal{B}(\mathbb{R}^d)$ that $\nu_x(A) = \int_{A \cap \mathcal{D}} \delta(\mathbf{x}) \, d\mathbf{x}$, $g(x) = (2\pi)^{-d/2} \left[\prod_{i=1}^d |\mathfrak{s}_i|^{-1/2} \right] \exp\left(-\sum_{i=1}^d \frac{(x_i - u_i)^2}{2\mathfrak{s}_i}\right)$, $\mu(x) = (0, \dots, 0)$, $\sigma(x)v = (\mathbf{m}_1 v_1, \dots, \mathbf{m}_d v_d)$, $f(t, x, \mathbf{x}, y, \mathbf{y}) = y(a(x) - \mathbf{y}a(\mathbf{x})[\delta(\mathbf{x})]^{-1})$, and

$$H(t, s, x, v) = x + \mu(x)(t - s) + \sigma(x)v = x + (\mathbf{m}_1 v_1, \dots, \mathbf{m}_d v_d) \quad (50)$$

(cf. (6) and (17)). The solution $u: [0, T] \times \mathbb{R}^d \rightarrow \mathbb{R}$ of the PDE in (41) then satisfies that for every $t \in [0, T]$, $x = (x_1, \dots, x_d) \in \mathbb{R}^d$ it holds that

$$u(0, x) = (2\pi)^{-d/2} \left[\prod_{i=1}^d |\mathfrak{s}_i|^{-1/2} \right] \exp\left(-\sum_{i=1}^d \frac{(x_i - u_i)^2}{2\mathfrak{s}_i}\right) \quad (51)$$

and

$$\left(\frac{\partial}{\partial t} u\right)(t, x) = u(t, x) \left(a(x) - \int_{\mathcal{D}} u(t, \mathbf{x}) a(\mathbf{x}) \, d\mathbf{x} \right) + \sum_{i=1}^d \frac{1}{2} |\mathbf{m}_i|^2 \left(\frac{\partial^2}{\partial x_i^2} u \right)(t, x). \quad (52)$$

In (52) the function $u: [0, T] \times \mathbb{R}^d \rightarrow \mathbb{R}$ models the evolution of the phenotype distribution of a population composed of a set of d biological traits under the combined effects of selection and mutation. For every $t \in [0, T]$, $x \in \mathbb{R}^d$ the number $u(t, x) \in \mathbb{R}$ describes the

number of individuals with traits $x = (x_1, \dots, x_d) \in \mathbb{R}^d$ at time $t \in [0, T]$. The function a models a quadratic Malthusian fitness function.

In Table 4 we use the machine learning-based method in Framework 5.1 to approximately solve the PDE in (52) above in the case $\mathcal{D} = \mathbb{R}^d$. More precisely, we assume for every $n, m, j \in \mathbb{N}$ that $\xi^{n,m,j} = 0$, $\gamma_m = 1/100$, $M_n = 1000$ and we assume for every $\mathbf{x} \in \mathbb{R}^d$ that $\delta(\mathbf{x}) = (2\pi)^{-d/2} t^{-d} \exp(-\frac{\|\mathbf{x}\|^2}{2t^2})$ to approximately calculate the mean of $\mathbb{V}_N^{1,0}(\Theta_{M_N}^N, (0, \dots, 0))$, the standard deviation of $\mathbb{V}_N^{1,0}(\Theta_{M_N}^N, (0, \dots, 0))$, the relative L^1 -approximation error associated to $\mathbb{V}_N^{1,0}(\Theta_{M_N}^N, (0, \dots, 0))$, the uncorrected sample standard deviation of the approximation error associated to $\mathbb{V}_N^{1,0}(\Theta_{M_N}^N, (0, \dots, 0))$, and the average runtime in seconds needed for calculating one realization of $\mathbb{V}_N^{1,0}(\Theta_{M_N}^N, (0, \dots, 0))$ based on 5 independent realizations (5 independent runs). The value $u(T, (0, \dots, 0))$ of the exact solution of (52) has been calculated by means of Lemma 5.2 below.

In Figure 2 we use the machine learning-based method in Framework 5.1 to approximate the solution $u: [0, T] \times \mathbb{R}^d \rightarrow \mathbb{R}$ of the PDE in (52) above with $d = 5$, $T = 1/2$, and $\mathcal{D} = \mathbb{R}^d$. The right-hand side of Figure 2 shows a plot of $[-1/4, 1/4] \ni x \mapsto u(t, (x, 0, \dots, 0)) \in \mathbb{R}$ for $t \in \{0, 0.05, 0.1, 0.15\}$ where u is the exact solution of the PDE in (52) with $d = 5$, $T = 1/2$, and $\mathcal{D} = \mathbb{R}^d$ computed via (54) in Lemma 5.2 below. The left-hand side of Figure 2 shows a plot of $[-1/4, 1/4] \ni x \mapsto \mathbb{V}_n^{1,0}(\Theta_{M_n}^n(\omega), (x, 0, \dots, 0)) \in \mathbb{R}$ for $n \in \{0, 1, 2, 3\}$ and one realization $\omega \in \Omega$ where the functions $\mathbb{R}^d \ni x \mapsto \mathbb{V}_n^{1,0}(\Theta_{M_n}^n(\omega), x) \in \mathbb{R}$ for $n \in \{0, 1, 2, 3\}$, $\omega \in \Omega$ were computed via Framework 5.1 as an approximation of the solution of the PDE in (52) with $d = 5$, $T = 1/2$, and $\mathcal{D} = [-1/2, 1/2]^d$. For the approximation, we take $M_1 = M_2 = \dots = M_N = 2000$, $\gamma_1 = \gamma_2 = \dots = \gamma_{2000} = 1/200$, and $\delta = \mathbb{1}_{\mathbb{R}^d}$ and we take $\xi^{n,m,j}: \Omega \rightarrow \mathbb{R}^d$, $n, m, j \in \mathbb{N}$, to be independent $\mathcal{U}_{[-1/2, 1/2]^d}$ -distributed random variables. Note that the solution of the PDE in (52) in the case $\mathcal{D} = [-R, R]^d$ with $R \in (0, \infty)$ sufficiently large is a good approximation of the solution $u: [0, T] \times \mathbb{R}^d \rightarrow \mathbb{R}$ of the PDE in (52) in the case $\mathcal{D} = \mathbb{R}^d$ since we have that for all $t \in [0, T]$ the value $u(t, x)$ of the solution u of the PDE in (52) in the case $\mathcal{D} = \mathbb{R}^d$ quickly tends to 0 as $\|x\|$ tends to ∞ .

Lemma 5.2. *Let $d \in \mathbb{N}$, $\mathbf{u}_1, \mathbf{u}_2, \dots, \mathbf{u}_d \in \mathbb{R}$, $\mathbf{m}_1, \mathbf{m}_2, \dots, \mathbf{m}_d, \mathfrak{s}_1, \mathfrak{s}_2, \dots, \mathfrak{s}_d \in (0, \infty)$, let $a: \mathbb{R}^d \rightarrow \mathbb{R}$ satisfy for every $x \in \mathbb{R}^d$ that $a(x) = -\frac{1}{2}\|x\|^2$, for every $i \in \{1, 2, \dots, d\}$ let $\mathfrak{G}_i: [0, \infty) \rightarrow (0, \infty)$ and $\mathfrak{U}_i: [0, \infty) \rightarrow \mathbb{R}$ satisfy for every $t \in [0, \infty)$ that*

$$\mathfrak{G}_i(t) = \mathbf{m}_i \left[\frac{\mathbf{m}_i \sinh(\mathbf{m}_i t) + \mathfrak{s}_i \cosh(\mathbf{m}_i t)}{\mathbf{m}_i \cosh(\mathbf{m}_i t) + \mathfrak{s}_i \sinh(\mathbf{m}_i t)} \right] \quad \text{and} \quad \mathfrak{U}_i(t) = \frac{\mathbf{m}_i \mathbf{u}_i}{\mathbf{m}_i \cosh(\mathbf{m}_i t) + \mathfrak{s}_i \sinh(\mathbf{m}_i t)}, \quad (53)$$

and let $u: [0, \infty) \times \mathbb{R}^d \rightarrow \mathbb{R}$ satisfy for every $t \in [0, \infty)$, $x = (x_1, \dots, x_d) \in \mathbb{R}^d$ that

$$u(t, x) = (2\pi)^{-d/2} \left[\prod_{i=1}^d |\mathfrak{G}_i(t)|^{-1/2} \right] \exp\left(-\sum_{i=1}^d \frac{(x_i - \mathfrak{U}_i(t))^2}{2\mathfrak{G}_i(t)}\right). \quad (54)$$

Then

d	T	N	Mean of the approx. method	Standard deviation of the approx. method	Reference value	Relative L^1 -approx. error	Standard deviation of the error	Average runtime in seconds
1	$1/10$	10	1.7650547	0.0048907	1.7709574	0.0033330	0.0027616	43.949
2	$1/10$	10	3.1210874	0.0015513	3.1362901	0.0048474	0.0004946	45.002
5	$1/10$	10	17.1948978	0.0160821	17.4196954	0.0129048	0.0009232	45.934
10	$1/10$	10	295.8776489	0.0572639	303.4457874	0.0249407	0.0001887	47.750
1	$1/5$	10	1.7499938	0.0005580	1.7582066	0.0046711	0.0003174	43.129
2	$1/5$	10	3.0621917	0.0027811	3.0912904	0.0094131	0.0008996	44.443
5	$1/5$	10	16.3846066	0.0139748	16.8015567	0.0248162	0.0008318	45.019
10	$1/5$	10	268.2944397	0.0623432	282.2923073	0.0495864	0.0002208	45.612
1	$1/2$	10	1.7018557	0.0060157	1.7222757	0.0118564	0.0034929	42.092
2	$1/2$	10	2.8911286	0.0027431	2.9662336	0.0253200	0.0009248	42.657
5	$1/2$	10	14.2520916	0.1356645	15.1535149	0.0594861	0.0089527	43.338
10	$1/2$	10	201.6446228	0.3009756	229.6290127	0.1218678	0.0013107	44.190

Table 4: Numerical simulations for the approximation method in Framework 3.1 in the case of the replicator-mutator PDEs in (52) in Subsection 5.4 where we assume for every $n, m, j \in \mathbb{N}$ that $\mathcal{D} = \mathbb{R}^d$, $\xi^{n,m,j} = 0$, $\gamma_m = 1/100$, and $M_n = 1000$ and where we assume for every $\mathbf{x} \in \mathbb{R}^d$ that $\delta(\mathbf{x}) = (2\pi)^{-d/2} \mathbf{t}^{-d} \exp(-\frac{\|\mathbf{x}\|^2}{2\mathbf{t}^2})$.

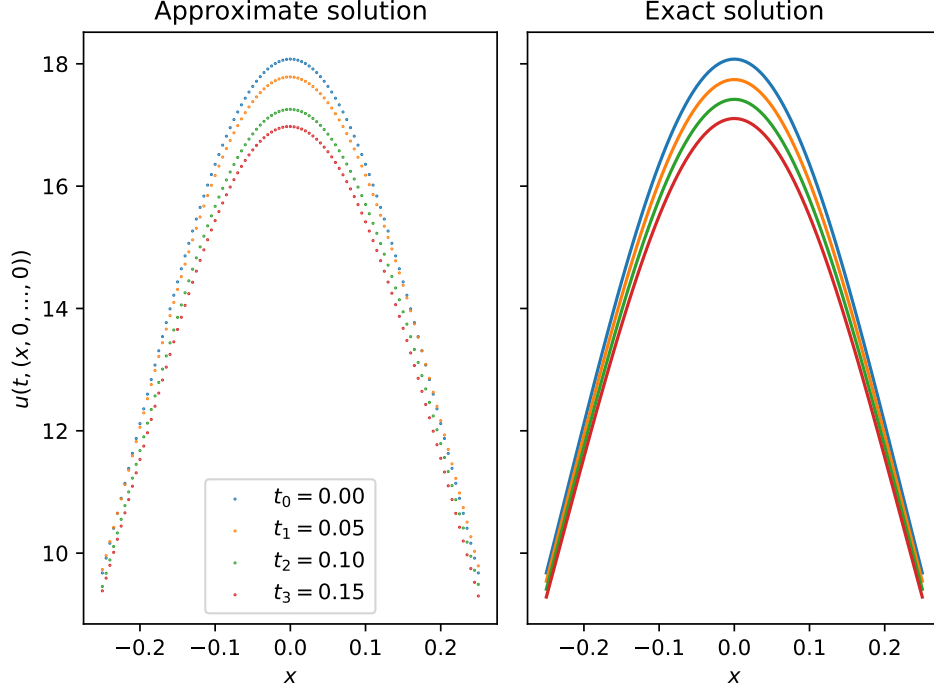


Figure 2: Plot of a machine learning-based approximation of the solution of the replicator-mutator PDE in (52) in the case $d = 5$, $T = 1/2$, and $\mathcal{D} = \mathbb{R}^d$. The left-hand side shows a plot of $[-1/4, 1/4] \ni x \mapsto \mathbb{V}_n^{1,0}(\Theta_{M_n}^n(\omega), (x, 0, \dots, 0)) \in \mathbb{R}$ for $n \in \{0, 1, 2, 3\}$ and one realization $\omega \in \Omega$ where the functions $\mathbb{R}^d \ni x \mapsto \mathbb{V}_n^{1,0}(\Theta_{M_n}^n(\omega), x) \in \mathbb{R}$ for $n \in \{0, 1, 2, 3\}$, $\omega \in \Omega$ were computed via Framework 5.1 as an approximation of the solution of the PDE in (52) with $d = 5$, $T = 1/2$, and $\mathcal{D} = [-1/2, 1/2]^d$ where we take $M_1 = M_2 = \dots = M_N = 2000$, $\gamma_1 = \gamma_2 = \dots = \gamma_{2000} = 1/200$, and $\delta = \mathbb{1}_{\mathbb{R}^d}$ and where we take $\xi^{n,m,j}: \Omega \rightarrow \mathbb{R}^d$, $n, m, j \in \mathbb{N}$, to be independent $\mathcal{U}_{[-1/2, 1/2]^d}$ -distributed random variables. The right-hand side of Figure 2 shows a plot of $[-1/4, 1/4] \ni x \mapsto u(t, (x, 0, \dots, 0)) \in \mathbb{R}$ for $t \in \{0, 0.05, 0.1, 0.15\}$ where u is the exact solution of the PDE in (52) with $d = 5$, $T = 1/2$, and $\mathcal{D} = \mathbb{R}^d$.

(i) it holds that $u \in C^{1,2}([0, \infty) \times \mathbb{R}^d, \mathbb{R})$,

(ii) it holds for every $x = (x_1, \dots, x_d) \in \mathbb{R}^d$ that

$$u(0, x) = (2\pi)^{-d/2} \left[\prod_{i=1}^d |\mathfrak{s}_i|^{-1/2} \right] \exp\left(-\sum_{i=1}^d \frac{(x_i - \mathbf{u}_i)^2}{2\mathfrak{s}_i}\right), \quad (55)$$

and

(iii) it holds for every $t \in [0, \infty)$, $x = (x_1, \dots, x_d) \in \mathbb{R}^d$ that

$$\left(\frac{\partial}{\partial t} u\right)(t, x) = u(t, x) \left(a(x) - \int_{\mathbb{R}^d} u(t, \mathbf{x}) a(\mathbf{x}) d\mathbf{x} \right) + \sum_{i=1}^d \frac{1}{2} |\mathbf{m}_i|^2 \left(\frac{\partial^2}{\partial x_i^2} u\right)(t, x). \quad (56)$$

Proof of Lemma 5.2. First, note that the fact that for every $i \in \{1, 2, \dots, d\}$ it holds that $\mathfrak{S}_i \in C^\infty([0, \infty), (0, \infty))$, the fact that for every $i \in \{1, 2, \dots, d\}$ it holds that $\mathfrak{U}_i \in C^\infty([0, \infty), \mathbb{R})$, and (54) establish item (i). Moreover, observe that the fact that for every $i \in \{1, 2, \dots, d\}$ it holds that $\mathfrak{S}_i(0) = \mathfrak{s}_i$, the fact that for every $i \in \{1, 2, \dots, d\}$ it holds that $\mathfrak{U}_i(0) = \mathbf{u}_i$, and (53) prove item (ii). Next note that (54) ensures that for every $t \in [0, \infty)$, $x = (x_1, \dots, x_d) \in \mathbb{R}^d$ it holds that

$$u(t, x) = \prod_{i=1}^d \left[(2\pi \mathfrak{S}_i(t))^{-1/2} \exp\left(-\frac{(x_i - \mathfrak{U}_i(t))^2}{2\mathfrak{S}_i(t)}\right) \right]. \quad (57)$$

The product rule hence implies that for every $t \in [0, \infty)$, $x = (x_1, \dots, x_d) \in \mathbb{R}^d$ it holds that

$$\begin{aligned} & \left(\frac{\partial}{\partial t} u\right)(t, x) \\ &= \frac{\partial}{\partial t} \left(\prod_{i=1}^d \left[(2\pi \mathfrak{S}_i(t))^{-1/2} \exp\left(-\frac{(x_i - \mathfrak{U}_i(t))^2}{2\mathfrak{S}_i(t)}\right) \right] \right) \\ &= \sum_{i=1}^d \left[\left[\prod_{j \in \{1, \dots, d\} \setminus \{i\}} \left((2\pi \mathfrak{S}_j(t))^{-1/2} \exp\left(-\frac{(x_j - \mathfrak{U}_j(t))^2}{2\mathfrak{S}_j(t)}\right) \right) \right] \right. \\ & \quad \cdot \left. \left[\frac{\partial}{\partial t} \left((2\pi \mathfrak{S}_i(t))^{-1/2} \exp\left(-\frac{(x_i - \mathfrak{U}_i(t))^2}{2\mathfrak{S}_i(t)}\right) \right) \right] \right]. \end{aligned} \quad (58)$$

The chain rule, the product rule, and (57) therefore show that for every $t \in [0, \infty)$, $x =$

$(x_1, \dots, x_d) \in \mathbb{R}^d$ it holds that

$$\begin{aligned}
& \left(\frac{\partial}{\partial t} u\right)(t, x) \\
&= \sum_{i=1}^d \left[\left[\prod_{j \in \{1, \dots, d\} \setminus \{i\}} \left((2\pi \mathfrak{S}_j(t))^{-1/2} \exp\left(-\frac{(x_j - \mathfrak{U}_j(t))^2}{2\mathfrak{S}_j(t)}\right) \right) \right] \right. \\
&\quad \cdot \left[\left(\frac{\partial}{\partial t} \left((2\pi \mathfrak{S}_i(t))^{-1/2} \right) \right) \exp\left(-\frac{(x_i - \mathfrak{U}_i(t))^2}{2\mathfrak{S}_i(t)}\right) \right. \\
&\quad \left. \left. + (2\pi \mathfrak{S}_i(t))^{-1/2} \left(\frac{\partial}{\partial t} \left(-\frac{(x_i - \mathfrak{U}_i(t))^2}{2\mathfrak{S}_i(t)} \right) \right) \exp\left(-\frac{(x_i - \mathfrak{U}_i(t))^2}{2\mathfrak{S}_i(t)}\right) \right] \right] \\
&= \sum_{i=1}^d \left[\left[\prod_{j \in \{1, \dots, d\} \setminus \{i\}} \left((2\pi \mathfrak{S}_j(t))^{-1/2} \exp\left(-\frac{(x_j - \mathfrak{U}_j(t))^2}{2\mathfrak{S}_j(t)}\right) \right) \right] \right. \\
&\quad \cdot \left[- (2\pi \mathfrak{S}_i(t))^{-1/2} \left[\frac{\left(\frac{\partial}{\partial t} \mathfrak{S}_i\right)(t)}{2\mathfrak{S}_i(t)} \right] \exp\left(-\frac{(x_i - \mathfrak{U}_i(t))^2}{2\mathfrak{S}_i(t)}\right) \right. \\
&\quad \left. + (2\pi \mathfrak{S}_i(t))^{-1/2} \left(\frac{2\left(\frac{\partial}{\partial t} \mathfrak{U}_i\right)(t)(x_i - \mathfrak{U}_i(t))}{2\mathfrak{S}_i(t)} \right. \right. \\
&\quad \left. \left. + \frac{(x_i - \mathfrak{U}_i(t))^2 \left(\frac{\partial}{\partial t} \mathfrak{S}_i\right)(t)}{2|\mathfrak{S}_i(t)|^2} \right) \exp\left(-\frac{(x_i - \mathfrak{U}_i(t))^2}{2\mathfrak{S}_i(t)}\right) \right] \right] \\
&= u(t, x) \left[\sum_{i=1}^d \left(\frac{-\left(\frac{\partial}{\partial t} \mathfrak{S}_i\right)(t)}{2\mathfrak{S}_i(t)} + \frac{2\mathfrak{S}_i(t) \left(\frac{\partial}{\partial t} \mathfrak{U}_i\right)(t)(x_i - \mathfrak{U}_i(t)) + (x_i - \mathfrak{U}_i(t))^2 \left(\frac{\partial}{\partial t} \mathfrak{S}_i\right)(t)}{2|\mathfrak{S}_i(t)|^2} \right) \right].
\end{aligned} \tag{59}$$

Moreover, observe that (53), the chain rule, and the product rule ensure that for every $i \in \{1, \dots, d\}$, $t \in [0, \infty)$ it holds that

$$\begin{aligned}
\left(\frac{\partial}{\partial t} \mathfrak{U}_i\right)(t) &= \frac{\partial}{\partial t} \left(\frac{\mathfrak{m}_i \mathfrak{u}_i}{\mathfrak{m}_i \cosh(\mathfrak{m}_i t) + \mathfrak{s}_i \sinh(\mathfrak{m}_i t)} \right) \\
&= -|\mathfrak{m}_i|^2 \mathfrak{u}_i \left[\frac{\mathfrak{m}_i \sinh(\mathfrak{m}_i t) + \mathfrak{s}_i \cosh(\mathfrak{m}_i t)}{[\mathfrak{m}_i \cosh(\mathfrak{m}_i t) + \mathfrak{s}_i \sinh(\mathfrak{m}_i t)]^2} \right] \\
&= -\mathfrak{S}_i(t) \mathfrak{U}_i(t)
\end{aligned} \tag{60}$$

and

$$\begin{aligned}
& \left(\frac{\partial}{\partial t} \mathfrak{S}_i\right)(t) \\
&= \frac{\partial}{\partial t} \left(\mathfrak{m}_i \left[\frac{\mathfrak{m}_i \sinh(\mathfrak{m}_i t) + \mathfrak{s}_i \cosh(\mathfrak{m}_i t)}{\mathfrak{m}_i \cosh(\mathfrak{m}_i t) + \mathfrak{s}_i \sinh(\mathfrak{m}_i t)} \right] \right) \\
&= |\mathfrak{m}_i|^2 \left[\frac{\mathfrak{m}_i \cosh(\mathfrak{m}_i t) + \mathfrak{s}_i \sinh(\mathfrak{m}_i t)}{\mathfrak{m}_i \cosh(\mathfrak{m}_i t) + \mathfrak{s}_i \sinh(\mathfrak{m}_i t)} \right] - |\mathfrak{m}_i|^2 \left[\frac{\mathfrak{m}_i \sinh(\mathfrak{m}_i t) + \mathfrak{s}_i \cosh(\mathfrak{m}_i t)}{\mathfrak{m}_i \cosh(\mathfrak{m}_i t) + \mathfrak{s}_i \sinh(\mathfrak{m}_i t)} \right]^2 \\
&= |\mathfrak{m}_i|^2 - |\mathfrak{S}_i(t)|^2.
\end{aligned} \tag{61}$$

Combining this with (59) implies that for every $i \in \{1, 2, \dots, d\}$, $t \in [0, \infty)$ it holds that

$$\begin{aligned}
\left(\frac{\partial}{\partial t}u\right)(t, x) &= \frac{u(t, x)}{2} \sum_{i=1}^d \left[\frac{-[|\mathbf{m}_i|^2 - |\mathfrak{S}_i(t)|^2]}{\mathfrak{S}_i(t)} \right. \\
&\quad \left. + \frac{2|\mathfrak{S}_i(t)|^2 \mathfrak{U}_i(t)(\mathfrak{U}_i(t) - x_i) + (x_i - \mathfrak{U}_i(t))^2 (|\mathbf{m}_i|^2 - |\mathfrak{S}_i(t)|^2)}{|\mathfrak{S}_i(t)|^2} \right] \\
&= \frac{u(t, x)}{2} \sum_{i=1}^d \left[|\mathbf{m}_i|^2 \left(\left(\frac{x_i - \mathfrak{U}_i(t)}{\mathfrak{S}_i(t)} \right)^2 - \frac{1}{\mathfrak{S}_i(t)} \right) \right. \\
&\quad \left. + \mathfrak{S}_i(t) + 2(|\mathfrak{U}_i(t)|^2 - \mathfrak{U}_i(t) x_i) - (|x_i|^2 - 2\mathfrak{U}_i(t) x_i + |\mathfrak{U}_i(t)|^2) \right] \\
&= \frac{u(t, x)}{2} \sum_{i=1}^d \left[|\mathbf{m}_i|^2 \left(\left(\frac{x_i - \mathfrak{U}_i(t)}{\mathfrak{S}_i(t)} \right)^2 - \frac{1}{\mathfrak{S}_i(t)} \right) + \mathfrak{S}_i(t) + |\mathfrak{U}_i(t)|^2 - |x_i|^2 \right].
\end{aligned} \tag{62}$$

Furthermore, note that (57) and the product rule show that for every $i \in \{1, 2, \dots, d\}$, $t \in [0, \infty)$, $x = (x_1, \dots, x_d) \in \mathbb{R}^d$ it holds that

$$\begin{aligned}
\left(\frac{\partial}{\partial x_i}u\right)(t, x) &= \frac{\partial}{\partial x_i} \left[\prod_{j=1}^d \left[(2\pi \mathfrak{S}_j(t))^{-1/2} \exp\left(-\frac{(x_j - \mathfrak{U}_j(t))^2}{2\mathfrak{S}_j(t)}\right) \right] \right] \\
&= \left[\frac{\partial}{\partial x_i} \left[(2\pi \mathfrak{S}_i(t))^{-1/2} \exp\left(-\frac{(x_i - \mathfrak{U}_i(t))^2}{2\mathfrak{S}_i(t)}\right) \right] \right] \\
&\quad \cdot \prod_{j \in \{1, 2, \dots, d\} \setminus \{i\}} \left[(2\pi \mathfrak{S}_j(t))^{-1/2} \exp\left(-\frac{(x_j - \mathfrak{U}_j(t))^2}{2\mathfrak{S}_j(t)}\right) \right] \\
&= -u(t, x) \left(\frac{x_i - \mathfrak{U}_i(t)}{\mathfrak{S}_i(t)} \right) = u(t, x) \left(\frac{\mathfrak{U}_i(t) - x_i}{\mathfrak{S}_i(t)} \right).
\end{aligned} \tag{63}$$

The product rule therefore assures that for every $i \in \{1, 2, \dots, d\}$, $t \in [0, \infty)$, $x = (x_1, \dots, x_d) \in \mathbb{R}^d$ it holds that

$$\begin{aligned}
\left(\frac{\partial^2}{\partial x_i^2}u\right)(t, x) &= \frac{\partial}{\partial x_i} \left(u(t, x) \left(\frac{\mathfrak{U}_i(t) - x_i}{\mathfrak{S}_i(t)} \right) \right) \\
&= \left(\frac{\partial}{\partial x_i}u\right)(t, x) \left(\frac{\mathfrak{U}_i(t) - x_i}{\mathfrak{S}_i(t)} \right) - \frac{u(t, x)}{\mathfrak{S}_i(t)} = u(t, x) \left[\left(\frac{x_i - \mathfrak{U}_i(t)}{\mathfrak{S}_i(t)} \right)^2 - \frac{1}{\mathfrak{S}_i(t)} \right].
\end{aligned} \tag{64}$$

Hence, we obtain that for every $t \in [0, \infty)$, $x = (x_1, \dots, x_d) \in \mathbb{R}^d$ it holds that

$$\sum_{i=1}^d \left[\frac{1}{2} |\mathbf{m}_i|^2 \left(\frac{\partial^2}{\partial x_i^2}u\right)(t, x) \right] = \frac{u(t, x)}{2} \sum_{i=1}^d \left[|\mathbf{m}_i|^2 \left(\left(\frac{x_i - \mathfrak{U}_i(t)}{\mathfrak{S}_i(t)} \right)^2 - \frac{1}{\mathfrak{S}_i(t)} \right) \right]. \tag{65}$$

Next observe that (57) and Fubini's theorem ensure that for every $t \in [0, \infty)$, $x = (x_1, \dots, x_d) \in \mathbb{R}^d$ it holds that

$$\begin{aligned}
& u(t, x) \left(a(x) - \int_{\mathbb{R}^d} u(t, \mathbf{x}) a(\mathbf{x}) \, d\mathbf{x} \right) \\
&= u(t, x) \left(-\frac{1}{2} \left[\sum_{i=1}^d |x_i|^2 \right] - \int_{\mathbb{R}^d} -\frac{1}{2} \left[\sum_{i=1}^d |\mathbf{x}_i|^2 \right] u(t, \mathbf{x}) \, d\mathbf{x} \right) \\
&= \frac{u(t, x)}{2} \left(- \left[\sum_{i=1}^d |x_i|^2 \right] \right. \\
&\quad + \sum_{i=1}^d \left[\int_{\mathbb{R}} |\mathbf{x}_i|^2 (2\pi \mathfrak{S}_i(t))^{-1/2} \exp\left(-\frac{(\mathbf{x}_i - \mathfrak{U}_i(t))^2}{2\mathfrak{S}_i(t)}\right) \, d\mathbf{x}_i \right. \\
&\quad \left. \left. \cdot \left(\prod_{j \in \{1, 2, \dots, d\} \setminus \{i\}} \int_{\mathbb{R}} (2\pi \mathfrak{S}_j(t))^{-1/2} \exp\left(-\frac{(\mathbf{x}_j - \mathfrak{U}_j(t))^2}{2\mathfrak{S}_j(t)}\right) \, d\mathbf{x}_j \right) \right] \right).
\end{aligned} \tag{66}$$

This and the fact that for every $i \in \{1, 2, \dots, d\}$, $t \in [0, \infty)$ it holds that

$$\int_{\mathbb{R}} (2\pi \mathfrak{S}_i(t))^{-1/2} \exp\left(-\frac{(x - \mathfrak{U}_i(t))^2}{2\mathfrak{S}_i(t)}\right) \, dx = 1 \tag{67}$$

imply that for every $t \in [0, \infty)$, $x = (x_1, \dots, x_d) \in \mathbb{R}^d$ it holds that

$$\begin{aligned}
& u(t, x) \left(a(x) - \int_{\mathbb{R}^d} u(t, \mathbf{x}) a(\mathbf{x}) \, d\mathbf{x} \right) \\
&= \frac{u(t, x)}{2} \sum_{i=1}^d \left[-|x_i|^2 + \int_{\mathbb{R}} |\mathbf{x}_i|^2 (2\pi \mathfrak{S}_i(t))^{-1/2} \exp\left(-\frac{(\mathbf{x}_i - \mathfrak{U}_i(t))^2}{2\mathfrak{S}_i(t)}\right) \, d\mathbf{x}_i \right].
\end{aligned} \tag{68}$$

Next observe that the integral transformation theorem demonstrates that for every $i \in \{1, 2, \dots, d\}$, $t \in [0, \infty)$ it holds that

$$\begin{aligned}
& \int_{\mathbb{R}} x^2 \left[(2\pi \mathfrak{S}_i(t))^{-1/2} \exp\left(-\frac{(x - \mathfrak{U}_i(t))^2}{2\mathfrak{S}_i(t)}\right) \right] \, dx \\
&= \int_{\mathbb{R}} (x + \mathfrak{U}_i(t))^2 \left[(2\pi \mathfrak{S}_i(t))^{-1/2} \exp\left(-\frac{x^2}{2\mathfrak{S}_i(t)}\right) \right] \, dx \\
&= \int_{\mathbb{R}} x^2 \left[(2\pi \mathfrak{S}_i(t))^{-1/2} \exp\left(-\frac{x^2}{2\mathfrak{S}_i(t)}\right) \right] \, dx \\
&\quad + \int_{\mathbb{R}} |\mathfrak{U}_i(t)|^2 \left[(2\pi \mathfrak{S}_i(t))^{-1/2} \exp\left(-\frac{x^2}{2\mathfrak{S}_i(t)}\right) \right] \, dx \\
&= \mathfrak{S}_i(t) + |\mathfrak{U}_i(t)|^2.
\end{aligned} \tag{69}$$

Combining this with (68) ensures that for every $t \in [0, \infty)$, $x = (x_1, \dots, x_d) \in \mathbb{R}^d$ it holds that

$$u(t, x) \left(a(x) - \int_{\mathbb{R}^d} u(t, \mathbf{x}) a(\mathbf{x}) \, d\mathbf{x} \right) = \frac{u(t, x)}{2} \sum_{i=1}^d (\mathfrak{S}_i(t) + |\mathfrak{U}_i(t)|^2 - |x_i|^2). \quad (70)$$

This and (65) demonstrate that for every $t \in [0, \infty)$, $x = (x_1, \dots, x_d) \in \mathbb{R}^d$ it holds that

$$\begin{aligned} & u(t, x) \left(a(x) - \int_D u(t, \mathbf{x}) a(\mathbf{x}) \, d\mathbf{x} \right) + \sum_{i=1}^d \frac{1}{2} |\mathbf{m}_i|^2 \left(\frac{\partial^2}{\partial x_i^2} u \right)(t, x) \\ &= \frac{u(t, x)}{2} \sum_{i=1}^d \left[|\mathbf{m}_i|^2 \left(\left(\frac{x_i - \mathfrak{U}_i(t)}{\mathfrak{S}_i(t)} \right)^2 - \frac{1}{\mathfrak{S}_i(t)} \right) + \mathfrak{S}_i(t) + |\mathfrak{U}_i(t)|^2 - |x_i|^2 \right]. \end{aligned} \quad (71)$$

Combining this with (62) proves item (iii). The proof of Lemma 5.2 is thus complete. \square

5.5 Allen–Cahn PDEs with conservation of mass

In this subsection we use the machine learning-based approximation method in Framework 5.1 to approximately calculate the solutions of certain Allen–Cahn PDEs with cubic nonlinearity, conservation of mass and no-flux boundary conditions (cf., e.g., Rubinstein & Sternberg [86]).

Assume Framework 5.1, let $\epsilon \in (0, \infty)$ satisfy $\epsilon = \frac{1}{10}$, assume that $d \in \{1, 2, 5, 10\}$, $D = [-1/2, 1/2]^d$, $T \in \{1/5, 1/2, 1\}$, $N = 10$, $K_1 = K_2 = \dots = K_N = 5$, and $M_1 = M_2 = \dots = M_N = 500$, assume that $\xi^{n,m,j}$, $n, m, j \in \mathbb{N}$, are independent \mathcal{U}_D -distributed random variables, assume for every $m \in \mathbb{N}$ that $\gamma_m = 10^{-2}$, and assume for every $s, t \in [0, T]$, $x, \mathbf{x} \in D$, $y, \mathbf{y} \in \mathbb{R}$, $v \in \mathbb{R}^d$, $A \in \mathcal{B}(D)$ that $\nu_x(A) = \int_A d\mathbf{x}$, $g(x) = \exp(-\frac{1}{4}\|x\|^2)$, $\mu(x) = (0, \dots, 0)$, $\sigma(x)v = \epsilon v$, $f(t, x, \mathbf{x}, y, \mathbf{y}) = y - y^3 - (\mathbf{y} - \mathbf{y}^3)$, and

$$H(t, s, x, v) = R(x, x + \mu(x)(t - s) + \sigma(x)v) = R(x, x + \epsilon v) \quad (72)$$

(cf. (6) and (17)). The solution $u: [0, T] \times D \rightarrow \mathbb{R}$ of the PDE in (41) then satisfies that for every $t \in (0, T]$, $x \in \partial_D$ it holds that $\langle \mathbf{n}(x), (\nabla_x u)(t, x) \rangle = 0$ and that for every $t \in [0, T]$, $x \in D$ it holds that $u(0, x) = \exp(-\frac{1}{4}\|x\|^2)$ and

$$\left(\frac{\partial}{\partial t} u \right)(t, x) = \frac{\epsilon^2}{2} (\Delta_x u)(t, x) + u(t, x) - [u(t, x)]^3 - \int_{[-1/2, 1/2]^d} u(t, \mathbf{x}) - [u(t, \mathbf{x})]^3 \, d\mathbf{x}. \quad (73)$$

In Table 5 we use the machine learning-based approximation method in Framework 5.1 to approximately calculate the mean of $\mathbb{V}_N^{1,0}(\Theta_{M_N}^N, (0, \dots, 0))$, the standard deviation of $\mathbb{V}_N^{1,0}(\Theta_{M_N}^N, (0, \dots, 0))$, the relative L^1 -approximation error associated to $\mathbb{V}_N^{1,0}(\Theta_{M_N}^N, (0, \dots, 0))$, the uncorrected sample standard deviation of the approximation error associated to

d	T	N	Mean of the approx. method	Standard deviation of the approx. method	Reference value	Relative L^1 -approx. error	Standard deviation of the error	Average runtime in seconds
1	$1/5$	10	0.9947184	0.0021832	0.9932255	0.0015709	0.0021380	31.417
2	$1/5$	10	0.9908873	0.0027061	0.9868883	0.0040521	0.0027421	35.069
5	$1/5$	10	0.9942151	0.0052064	0.9710707	0.0238340	0.0053615	38.363
10	$1/5$	10	0.9792556	0.0203935	0.9514115	0.0292661	0.0214350	42.782
1	$1/2$	10	0.9870476	0.0014673	0.9880013	0.0014996	0.0007477	30.297
2	$1/2$	10	0.9763564	0.0030895	0.9750274	0.0024841	0.0021561	34.922
5	$1/2$	10	0.9518845	0.0051304	0.9431354	0.0092766	0.0054398	37.963
10	$1/2$	10	0.9249420	0.0052786	0.9063239	0.0205424	0.0058242	43.139
1	1	10	0.9823494	0.0003647	0.9780817	0.0043633	0.0003729	29.250
2	1	10	0.9659823	0.0004128	0.9658025	0.0003195	0.0003137	34.485
5	1	10	0.9209547	0.0019223	0.9158821	0.0055385	0.0020988	39.318
10	1	10	0.8693402	0.0029947	0.8683143	0.0030165	0.0015052	44.258

Table 5: Numerical simulations for the approximation method in Framework 3.1 in the case of the Allen–Cahn PDEs with conservation of mass in (73) in Subsection 5.5.

$\mathbb{V}_N^{1,0}(\Theta_{M_N}^N, (0, \dots, 0))$, and the average runtime in seconds needed for calculating one realization of $\mathbb{V}_N^{1,0}(\Theta_{M_N}^N, (0, \dots, 0))$ based on 5 independent realizations (5 independent runs). The reference value, which is used as an approximation for the unknown value $u(T, (0, \dots, 0))$ of the exact solution of (73), has been calculated via the MLP approximation method for non-local nonlinear PDEs in Framework 4.1 (cf. Example 4.6 and Beck et al. [11, Remark 3.3]).

6 JULIA source codes

6.1 General package for high-dimensional PDE approximations

```

1 module HighDimPDE
2     using Reexport
3     @reexport using DiffEqBase
4     using Statistics
5     using Flux, Zygote, LinearAlgebra
6     using Functors
7     # using ProgressMeter: @showprogress
8     using CUDA
9     using Random
10    using SparseArrays
11
12    abstract type HighDimPDEAlgorithm <: DiffEqBase.AbstractODEAlgorithm end
13

```

```

14 """
15     PIDEProblem(g, f, μ, σ, x, tspan, p = nothing, x0_sample=nothing, neumann_bc=nothing)
16
17 Defines a Partial Integro Differential Problem, of the form
18  $\dot{u}/dt = 1/2 \text{Tr}(\sigma \sigma^T) \Delta u(t,x) + \mu \nabla u(t,x) + \int f(x, y, u(x, t), u(y, t), p, t) dy$ ,
19 where f is a nonlinear Lipschitz function
20
21 # Arguments
22 * `g` : The initial condition g(x, p, t).
23 * `f` : The function f(x, y, u(x, t), u(y, t), p, t)
24 * `μ` : The drift function of X from Ito's Lemma μ(x, p, t)
25 * `σ` : The noise function of X from Ito's Lemma σ(x, p, t)
26 * `x` : the point where `u(x,t)` is approximated. Is required even in the case where `x0_sample`
27 is provided.
28 * `tspan` : The timespan of the problem.
29 * `p` : the parameter
30 * `x0_sample` : sampling method for x0.
31 Can be `UniformSampling(a,b)`, `NormalSampling(σ_sampling, shifted)`, or `NoSampling` (by default).
32 If `NoSampling`, `x` is used.
33 * `neumann_bc` : if provided, neumann boundary conditions on the hypercube
34 `neumann_bc[1] × neumann_bc[2]`.
35 """
36 struct PIDEProblem{uType,
37     G,
38     F,
39     Mu,
40     Sigma,
41     xType,
42     tType,
43     P,
44     UD,
45     NBC,
46     K} <: DiffEqBase.AbstractODEProblem{uType,tType,false}
47
48     u0::uType
49     g::G # initial condition
50     f::F # nonlinear part
51     μ::Mu
52     σ::Sigma
53     x::xType
54     tspan::Tuple{tType,tType}
55     p::P
56     x0_sample::UD # for DeepSplitting only
57     neumann_bc::NBC # neumann boundary conditions
58     kwargs::K
59 end
60
61 function PIDEProblem(g, f, μ, σ, x::Vector{X}, tspan;
62     p=nothing,
63     x0_sample=NoSampling(),
64     neumann_bc::NBC=nothing,
65     kwargs...) where {X <: AbstractFloat,
66     NBC <: Union{Nothing, AbstractVector}}
67
68 @assert eltype(tspan) <: AbstractFloat "`tspan` should be a tuple of Float"
69
70 isnothing(neumann_bc) ? nothing : @assert eltype(eltype(neumann_bc)) <: eltype(x)
71 @assert eltype(g(x)) == eltype(x) "Type of `g(x)` must match type of x"
72 @assert(eltype(f(x, x, g(x), g(x), p, tspan[1])) == eltype(x),
73     "Type of non linear function `f(x)` must type of x")
74
75 PIDEProblem(typeof(g(x)),
76     typeof(g),
77     typeof(f),
78     typeof(μ),
79     typeof(σ),
80     typeof(x),
81     eltype(tspan),
82     typeof(p),
83     typeof(x0_sample),
84     typeof(neumann_bc),
85     typeof(kwargs)){
86     g(x), g, f, μ, σ, x, tspan, p, x0_sample, neumann_bc, kwargs}
87
88 end
89
90 Base.summary(prob::PIDEProblem) = string(nameof(typeof(prob)))
91
92 function Base.show(io::IO, A::PIDEProblem)
93     println(io, summary(A))
94     print(io, "timespan: ")
95     show(io, A.tspan)
96 end
97
98 struct PIDESolution{X0, Ts, L, Us, NNs}

```

```

97     x0::X0
98     ts::Ts
99     losses::L
100    us::Us # array of solution evaluated at x0, ts[i]
101    ufuncs::NNs # array of parametric functions
102    end
103
104    Base.summary(prob::PIDESolution) = string(nameof(typeof(prob)))
105
106    function Base.show(io::IO, A::PIDESolution)
107        println(io, summary(A))
108        print(io, "timespan: ")
109        show(io, A.tspan)
110        print(io, "u(x,t): ")
111        show(io, A.us)
112    end
113
114    include("MCSample.jl")
115    include("reflect.jl")
116    include("DeepSplitting.jl")
117    include("MLP.jl")
118
119    export PIDEProblem, PIDESolution, DeepSplitting, MLP
120
121    export NormalSampling, UniformSampling, NoSampling, solve
122 end

```

```

1  # ""
2  #     MCSampling
3
4  # Sampling method for the Monte Carlo integration.
5  # ""
6  abstract type MCSampling{T} end
7  Base.eltypes(::MCSampling{T}) where T = eltypes(T)
8
9  ""
10     UniformSampling(a, b)
11
12     Uniform sampling for the Monte Carlo integration, in the hypercube `[a, b]^2`.
13     ""
14     struct UniformSampling{A} <: MCSampling{A}
15         a::A
16         b::A
17     end
18     @functor UniformSampling
19
20
21     function (mc_sample::UniformSampling{T})(x_mc, kwargs...) where T
22         Tel = eltype(T)
23         rand!(x_mc)
24         m = (mc_sample.b + mc_sample.a) ./ convert(Tel,2)
25         x_mc .= (x_mc .- convert(Tel,0.5)) .* (mc_sample.b - mc_sample.a) .+ m
26     end
27
28
29     ""
30     NormalSampling( $\sigma$ )
31     NormalSampling( $\sigma$ , shifted)
32
33     Normal sampling method for the Monte Carlo integration.
34
35     # Arguments
36     * ` $\sigma$ `: the standard deviation of the sampling
37     * `shifted`: if true, the integration is shifted by `x`. Defaults to false.
38     ""
39     struct NormalSampling{T} <: MCSampling{T}
40          $\sigma$ ::T
41         shifted::Bool # if true, we shift integration by x when invoking mc_sample::MCSampling(x)
42     end
43     @functor NormalSampling
44
45     NormalSampling( $\sigma$ ) = NormalSampling( $\sigma$ , false)
46
47     function (mc_sample::NormalSampling)(x_mc)
48         randn!(x_mc)
49         x_mc .*= mc_sample. $\sigma$ 
50     end
51
52     function (mc_sample::NormalSampling)(x_mc, x)

```

```

53     mc_sample(x_mc)
54     mc_sample.shifted ? x_mc .+= x : nothing
55 end
56
57
58
59 struct NoSampling <: MCSampling{Nothing} end
60
61 (mc_sample::NoSampling)(x...) = nothing
62
63 function _integrate(::MCS) where {MCS <: MCSampling}
64     if MCS <: NoSampling
65         return false
66     else
67         return true
68     end
69 end

```

```

1     """
2     _reflect(a,b,s,e)
3
4     reflection of the Brownian motion `B` where `B_{t-1} = a` and `B_t = b`
5     on the hypercube `[s,e]^d` where `d = size(a,1)`.
6     """
7     # Used by `MLP` algorithm.
8     function _reflect(a::T, b::T, s::T, e::T) where T <: Vector
9         r = 2; n = zeros(size(a))
10        # first checking if b is in the hypercube
11        all((a .>= s) .& (a .<= e)) ? nothing : error("a = $a not in hypercube")
12        size(a) == size(b) ? nothing : error("a not same dim as b")
13        for i in 1:length(a)
14            if b[i] < s[i]
15                rtemp = (a[i] - s[i]) / (a[i] - b[i])
16                if rtemp < r
17                    r = rtemp
18                    n .= 0
19                    n[i] = -1
20                end
21            elseif b[i] > e[i]
22                rtemp = (e[i] - a[i]) / (b[i] - a[i])
23                if rtemp < r
24                    r = rtemp
25                    n .= 0
26                    n[i] = 1
27                end
28            end
29        end
30        while r < 1
31            c = a + r * (b - a)
32            a = c
33            b = b - 2 * n * (dot(b-c,n))
34            r = 2;
35            for i in 1:length(a)
36                if b[i] < s[i]
37                    rtemp = (a[i] - s[i]) / (a[i] - b[i])
38                    if rtemp < r
39                        r = rtemp
40                        n .= 0
41                        n[i] = -1
42                    end
43                elseif b[i] > e[i]
44                    rtemp = (e[i] - a[i]) / (b[i] - a[i])
45                    if rtemp < r
46                        r = rtemp
47                        n .= 0
48                        n[i] = 1
49                    end
50                end
51            end
52        end
53        return b
54    end
55
56    # Used by `DeepSplitting` algorithm.
57    function _reflect(a::T, b::T, s, e) where T <: CuArray
58        @assert all((a .>= s) .& (a .<= e)) "a = $a not in hypercube"
59        @assert size(a) == size(b) "a not same dim as b"
60        out1 = b .< s
61        out2 = b .> e

```

```

62 out = out1 .| out2
63 n = similar(a)
64 n .= 0
65 # Allocating
66 while any(out)
67     rtemp1 = @. (s - a) #left
68     rtemp2 = @. (e - a) #right
69     div = @. (out * (b-a) + !out)
70     rtemp = (rtemp1 .* out1 .+ rtemp2 .* out2) ./ div .+ (.(out1 .| out2))
71     rmin = minimum(rtemp,dims=1)
72     n .= rtemp .== minimum(rtemp;dims=1)
73     c = @. (a + (b-a) * rmin)
74     b = @. (b - 2 * n * (b-c) )
75     a = c
76     @. out1 = b < s
77     @. out2 = b > e
78     @. out = out1 | out2
79 end
80 return b
81 end

```

6.2 Implementation of the machine learning-based approximation method

```

1 Base.copy(t::Tuple) = t # required for below
2 function Base.copy(opt::O) where O<:Flux.Optimise.AbstractOptimiser
3     return O([copy(getfield(opt,f)) for f in fieldnames(typeof(opt))])...
4 end
5
6 """
7     DeepSplitting(nn, K=1, opt = ADAM(0.01), λs = nothing, mc_sample = NoSampling())
8
9     Deep splitting algorithm.
10
11     # Arguments
12     * `nn`: a [Flux.Chain](https://fluxml.ai/Flux.jl/stable/models/layers/#Flux.Chain),
13     or more generally a [functor](https://github.com/FluxML/Functors.jl).
14     * `K`: the number of Monte Carlo integrations.
15     * `opt`: optimiser to be use. By default, `Flux.ADAM(0.01)`.
16     * `λs`: the learning rates, used sequentially. Defaults to a single value taken from `opt`.
17     * `mc_sample::MCSampling` : sampling method for Monte Carlo integrations of the non local term.
18     Can be `UniformSampling(a,b)`, `NormalSampling(σ_sampling, shifted)`, or `NoSampling` (by default).
19
20     # Example
21     ```julia
22     hls = d + 50 # hidden layer size
23     d = 10 # size of the sample
24
25     # Neural network used by the scheme
26     nn = Flux.Chain(Dense(d, hls, tanh),
27                     Dense(hls, hls, tanh),
28                     Dense(hls, 1, x->x^2))
29
30     alg = DeepSplitting(nn, K=10, opt = ADAM(), λs = [5e-3,1e-3],
31                       mc_sample = UniformSampling(zeros(d), ones(d)) )
32     ...
33     """
34 struct DeepSplitting{NN,F,O,L,MCS} <: HighDimPDEAlgorithm
35     nn::NN
36     K::F
37     opt::O
38     λs::L
39     mc_sample!::MCS # Monte Carlo sample
40 end
41
42 function DeepSplitting(nn;
43                       K=1,
44                       opt::O = ADAM(0.01),
45                       λs::L = nothing,
46                       mc_sample::MCSampling = NoSampling()) where
47     {O <: Flux.Optimise.AbstractOptimiser,
48     L <: Union{Nothing,Vector{N}} where N <: Number}
49     isnnothing(λs) ? λs = [opt.eta] : nothing

```

```

50     DeepSplitting(nn, K, opt, λs, mc_sample)
51 end
52
53 """
54 solve(prob::PIDEProblem,
55       alg::DeepSplitting,
56       dt;
57       batch_size = 1,
58       abstol = 1f-6,
59       verbose = false,
60       maxiters = 300,
61       use_cuda = false,
62       cuda_device = nothing,
63       verbose_rate = 100)
64
65 Returns a `PIDESolution` object.
66
67 # Arguments
68 - `maxiters`: number of iterations per time step. Can be a tuple,
69 where `maxiters[1]` is used for the training of the neural network used in
70 the first time step (which can be long) and `maxiters[2]` is used for the rest of the time steps.
71 - `batch_size` : the batch size.
72 - `abstol` : threshold for the objective function under which the training is stopped.
73 - `verbose` : print training information.
74 - `verbose_rate` : rate for printing training information (every `verbose_rate` iterations).
75 - `use_cuda` : set to "true" to use CUDA.
76 - `cuda_device` : integer, to set the CUDA device used in the training, if `use_cuda == true`.
77 """
78 function solve(
79     prob::PIDEProblem,
80     alg::DeepSplitting,
81     dt;
82     batch_size = 1,
83     abstol = 1f-6,
84     verbose = false,
85     maxiters = 300,
86     use_cuda = false,
87     cuda_device = nothing,
88     verbose_rate = 100
89 )
90     if use_cuda
91         if CUDA.functional()
92             @info "Training on CUDA GPU"
93             CUDA.allowscalar(false)
94             !isnothing(cuda_device) ? CUDA.device!(cuda_device) : nothing
95             _device = Flux.gpu
96         else
97             error("CUDA not functional, deactivate `use_cuda` and retry")
98         end
99     else
100         @info "Training on CPU"
101         _device = Flux.cpu
102     end
103
104     ## unbin stuff
105     neumann_bc = prob.neumann_bc |> _device
106     x0 = prob.x |> _device
107     mc_sample! = alg.mc_sample! |> _device
108     x0_sample! = prob.x0_sample |> _device
109
110     d = size(x0,1)
111     K = alg.K
112     opt = alg.opt
113     λs = alg.λs
114     g, f, μ, σ, p = prob.g, prob.f, prob.μ, prob.σ, prob.p
115     T = eltype(x0)
116
117     # neural network model
118     nn = alg.nn |> _device
119     vi = g
120     # fix for deepcopy
121     vj = Flux.fmap(nn) do x
122         x isa AbstractArray && return copy(x)
123     end
124     ps = Flux.params(vj)
125
126     dt = convert(T, dt)
127     ts = prob.tspan[1]:dt-eps(T):prob.tspan[2]
128     N = length(ts) - 1
129
130     usol = [g(x0 |>cpu) []]
131     nns = Any[g]

```

```

133 losses = [Vector{eltype(prob.x)}() for net in 1:N+1]
134
135 # allocating
136 x0_batch = repeat(x0, 1, batch_size)
137 y1 = similar(x0_batch)
138 y0 = similar(y1)
139 z = similar(x0, d, batch_size, K) # for MC non local integration
140
141 # checking element types
142 eltype(mc_sample!) == T || !_integrate(mc_sample!) ? nothing : error(
143     "Element type of `mc_sample` not the same as element type of `x`")
144
145 function splitting_model(y0, y1, z, t)
146     _int = reshape(sum(f(y1, z, vi(y1), vi(z), p, t), dims = 3), 1, :)
147     return vj(y0) - (vi(y1) + dt * _int / K)
148 end
149
150 function loss(y0, y1, z, t)
151     u = splitting_model(y0, y1, z, t)
152     return sum(u.^2) / batch_size
153 end
154
155 # calculating SDE trajectories
156 function sde_loop!(y0, y1, dWall)
157     randn!(dWall) # points normally distributed for brownian motion
158     x0_sample!(y1) # points for initial conditions
159     for i in 1:size(dWall,3)
160         t = ts[N + 1 - i]
161         dW = @view dWall[:, :, i]
162         y0 .= y1
163         y1 .= y0 .+  $\mu$ (y0,p,t) .* dt .+  $\sigma$ (y0,p,t) .* sqrt(dt) .* dW
164         if !isnothing(neumann_bc)
165             y1 .= _reflect(y0, y1, neumann_bc[1], neumann_bc[2])
166         end
167     end
168 end
169
170 for net in 1:N
171     # preallocate dWall
172     dWall = similar(x0, d, batch_size, N + 1 - net) # for SDE
173
174     verbose && println("Step $(net) / $(N) ")
175     t = ts[net]
176     # first of maxiters used for first nn, second used for the other nn
177     _maxiters = length(maxiters) > 1 ? maxiters[min(net,2)] : maxiters[]
178
179     for  $\lambda$  in  $\lambda$ s
180         opt_net = copy(opt) # starting with a new optimiser state at each time step
181         opt_net.eta =  $\lambda$ 
182         verbose && println("Training started with ", typeof(opt_net), " and  $\lambda$  :", opt_net.eta)
183         for epoch in 1:_maxiters
184             y1 .= x0_batch
185             # generating sdes
186             sde_loop!(y0, y1, dWall)
187
188             if !_integrate(mc_sample!)
189                 # generating z for MC non local integration
190                 mc_sample!(z, y1)
191             end
192
193             # training
194             gs = Flux.gradient(ps) do
195                 loss(y0, y1, z, t)
196             end
197             Flux.Optimise.update!(opt_net, ps, gs) # update parameters
198
199             # report on training
200             if epoch % verbose_rate == 1
201                 l = loss(y0, y1, z, t) # explicitly computing loss every verbose_rate
202                 verbose && println("Current loss is: $l")
203                 push!(losses[net], l)
204                 if l < abstol
205                     break
206                 end
207             end
208             if epoch == maxiters
209                 l = loss(y0, y1, z, t)
210                 push!(losses[net+1], l)
211                 verbose && println("Final loss for step $(net) / $(N) is: $l")
212             end
213         end
214     end
215     # saving

```

```

216     # fix for deepcopy
217     vi = Flux.fmap(vj) do x
218         x isa AbstractArray && return copy(x)
219         x
220     end
221     # vj = deepcopy(nn)
222     # ps = Flux.params(vj)
223     push!(usol, cpu(vi(reshape(x0, d, 1))))[]
224     push!(nns, vi |> cpu)
225 end
226
227 # return
228 sol = PIDEsolution(x0, ts, losses, usol, nns)
229 return sol
230 end

```

6.3 Implementation of the multilevel Picard approximation method

```

1  """
2  MLP( M=4, L=4, K=10, mc_sample = NoSampling())
3
4  Multi level Picard algorithm.
5
6  # Arguments
7  * `L`: number of Picard iterations (Level),
8  * `M`: number of Monte Carlo integrations (at each level `l`, `M^(L-l)` integrations),
9  * `K`: number of Monte Carlo integrations for the non local term
10 * `mc_sample::MCSampling`: sampling method for Monte Carlo integrations of the non local term.
11 Can be `UniformSampling(a,b)`, `NormalSampling(σ_sampling)`, or `NoSampling` (by default).
12 """
13 struct MLP{T, MCS} <: HighDimPDEAlgorithm where {T <: Int, MCS <: MCSampling}
14     M::T # nb of MC integrations
15     L::T # nb of levels
16     K::T # nb MC integration non local term
17     mc_sample!::MCS
18 end
19
20 #Note: mc_sample mutates its first argument but for the user interface we hide this technicality
21 MLP(; M=4, L=4, K=10, mc_sample = NoSampling()) = MLP(M, L, K, mc_sample)
22
23 """
24 solve(prob::PIDEProblem,
25     alg::MLP;
26     multithreading=true,
27     verbose=false)
28
29 Returns a `PIDEsolution` object.
30
31 # Arguments
32 * multithreading : if `true`, distributes the job over all the threads
33 available.
34 * verbose: print information over the iterations.
35 """
36 function solve(
37     prob::PIDEProblem,
38     alg::MLP;
39     multithreading=true,
40     verbose=false,
41 )
42
43     # unbin stuff
44     x = prob.x
45     neumann_bc = prob.neumann_bc
46     K = alg.K
47     M = alg.M
48     L = alg.L
49     mc_sample! = alg.mc_sample!
50     g, f = prob.g, prob.f
51
52     # errors
53     typeof(prob.x0_sample) <: NoSampling ? nothing : error(
54         "`MLP` algorithm can only be used with `x0_sample=NoSampling()`.")

```



```

55
56   if multithreading
57       usol = _ml_picard_mlt(M, L, K, x, prob.tspan[1], prob.tspan[2],
58                           mc_sample!, g, f, verbose, prob, neumann_bc)
59   else
60       usol = _ml_picard(M, L, K, x, prob.tspan[1], prob.tspan[2],
61                           mc_sample!, g, f, verbose, prob, neumann_bc)
62   end
63   return PIDEsolution(x, [prob.tspan...], nothing, [g(x), usol], nothing)
64 end
65
66 function _ml_picard(M, # monte carlo integration
67                   L, # level
68                   K, # non local term monte carlo
69                   x::xType, # initial point
70                   s, # time
71                   t::tType, # time
72                   mc_sample!,
73                   g,
74                   f,
75                   verbose,
76                   prob,
77                   neumann_bc
78                   ) where {xType, tType}
79
80   elxType = eltype(xType)
81   if L == 0
82       return zero(elxType)
83   end
84
85   x2 = similar(x)
86   _integrate(mc_sample!) ? x3 = similar(x) : x3 = nothing
87   p = prob.p
88
89   a = zero(elxType)
90   for l in 0:(min(L-1, 1))
91       verbose && println("loop l")
92       b = zero(elxType)
93       num = M^(L-1)
94       for k in 1:num
95           verbose && println("loop k")
96           r = s + (t - s) * rand(tType)
97           _mlt_sde_loop!(x2, x, s, r, prob, neumann_bc)
98           b2 = _ml_picard(M, l, K, x2, r, t, mc_sample!, g, f, verbose, prob, neumann_bc)
99           b3 = zero(elxType)
100          # non local integration
101          for h in 1:K
102              verbose && println("loop h")
103              mc_sample!(x3, x2)
104              b3 += f(x2, x3, b2, _ml_picard(M, l, K, x3, r, t, mc_sample!, g, f, verbose,
105              prob, neumann_bc), p, t)
106          end
107          b += b3 / K
108      end
109      a += (t - s) * b / num
110  end
111
112  for l in 2:(L-1)
113      b = zero(elxType)
114      num = M^(L-1)
115      for k in 1:num
116          r = s + (t - s) * rand(tType)
117          _mlt_sde_loop!(x2, x, s, r, prob, neumann_bc)
118          b2 = _ml_picard(M, l, K, x2, r, t, mc_sample!, g, f, verbose, prob, neumann_bc)
119          b4 = _ml_picard(M, l-1, K, x2, r, t, mc_sample!, g, f, verbose, prob, neumann_bc)
120          b3 = zero(elxType)
121          # non local integration
122          for h in 1:K
123              mc_sample!(x3, x2)
124              b3 += f(x2, x3, b2, _ml_picard(M, l, K, x3, r, t, mc_sample!, g, f, verbose,
125              prob, neumann_bc), p, t) -
126              f(x2, x3, b4, _ml_picard(M, l-1, K, x3, r,
127              t, mc_sample!, g, f, verbose, prob, neumann_bc), p, t)
128          end
129          b += b3 / K
130      end
131      a += (t - s) * b / num
132  end
133
134  num = M^L
135  a2 = zero(elxType)
136  for k in 1:num
137      verbose && println("loop k3")

```

```

138     _mlt_sde_loop!(x2, x, s, t, prob, neumann_bc)
139     a2 += g(x2)
140 end
141 a2 /= num
142
143 return a + a2
144 end
145
146 _ml_picard(M::Int, L::Int, K::Int, x::Nothing, s::Real, t::Real, mc_sample!, g, f, verbose::Bool,
147 prob, neumann_bc) = nothing
148
149 function _ml_picard_mlt(M, # monte carlo integration
150     L, # level
151     K, # non local term monte carlo
152     x::xType, # initial point
153     s, # time
154     t, # time
155     mc_sample!,
156     g,
157     f,
158     verbose,
159     prob,
160     neumann_bc) where {xType}
161
162     elxType = eltype(xType)
163
164     # distributing tasks
165     NUM_THREADS = Threads.nthreads()
166     tasks = [Threads.@spawn(_ml_picard_call(M, L, K, x, s, t, mc_sample!, g, f, verbose,
167         NUM_THREADS, thread_id, prob, neumann_bc)) for thread_id in 1:NUM_THREADS]
168
169     # first level
170     num = M^L
171     x2 = similar(x)
172     a2 = zero(elxType)
173     for k in 1:num
174         verbose && println("loop k3")
175         _mlt_sde_loop!(x2, x, s, t, prob, neumann_bc)
176         a2 += g(x2)
177     end
178     a2 /= num
179
180     # fetching tasks
181     a = sum([fetch(t) for t in tasks])
182
183     return a + a2
184 end
185
186
187 function _ml_picard_call(M, # monte carlo integration
188     L, # level
189     K, # non local term monte carlo
190     x::xType, # initial point
191     s, # time
192     t::tType, # time
193     mc_sample!,
194     g,
195     f,
196     verbose,
197     NUM_THREADS,
198     thread_id,
199     prob,
200     neumann_bc
201     ) where {xType, tType}
202
203     x2 = similar(x)
204     _integrate(mc_sample!) ? x3 = similar(x) : x3 = nothing
205     p = prob.p
206     elxType = eltype(xType)
207
208     a = zero(elxType)
209     for l in 0:(min(L - 1, 1))
210         b = zero(elxType)
211         num = M^(L - l)
212         loop_num = _get_loop_num(M, num, thread_id, NUM_THREADS)
213         for k in 1:loop_num
214             verbose && println("loop k")
215             r = s + (t - s) * rand(tType)
216             _mlt_sde_loop!(x2, x, s, r, prob, neumann_bc)
217             b2 = _ml_picard(M, l, K, x2, r, t, mc_sample!, g, f, verbose, prob, neumann_bc)
218             b3 = zero(elxType)
219             for h in 1:K # non local integration
220                 verbose && println("loop h")

```

```

221         mc_sample!(x3, x2)
222         b3 += f(x2, x3, b2, _ml_picard(M, l, K, x3, r, t, mc_sample!, g, f, verbose,
223             prob, neumann_bc), p, t)
224     end
225     b += b3 / K
226 end
227 a += (t - s) * b / num
228 end
229
230 for l in 2:(L-1)
231     b = zero(elxType)
232     num = M^(L - 1)
233     loop_num = _get_loop_num(M, num, thread_id, NUM_THREADS)
234     for k in 1:loop_num
235         r = s + (t - s) * rand(tType)
236         _mlt_sde_loop!(x2, x, s, r, prob, neumann_bc)
237         b2 = _ml_picard(M, l, K, x2, r, t, mc_sample!, g, f, verbose, prob, neumann_bc)
238         b4 = _ml_picard(M, l - 1, K, x2, r, t, mc_sample!, g, f, verbose, prob, neumann_bc)
239         b3 = zero(elxType)
240         # non local integration
241         for h in 1:K
242             mc_sample!(x3, x2)
243             b3 += f(x2, x3, b2, _ml_picard(M, l, K, x3, r, t,
244                 mc_sample!, g, f, verbose, prob, neumann_bc), p, t) -
245                 f(x2, x3, b4, _ml_picard(M, l - 1, K, x3, r, t,
246                     mc_sample!, g, f, verbose, prob, neumann_bc), p, t)
247         end
248         b += b3 / K
249     end
250     a += (t - s) * b / num
251 end
252
253 return a
254
255 end
256
257 #decides how many iteration given thread id and num
258 function _get_loop_num(M, num, thread_id, NUM_THREADS)
259     if num < NUM_THREADS
260         # each thread only goes once through the loop
261         loop_num = thread_id > num ? 0 : 1
262     else
263         remainder = M % num
264         if (remainder > 0) && (thread_id <= remainder) # remainder > 0 iff num == M or num == 1
265             # each thread goes num / NUM_THREADS + the remainder
266             loop_num = num / NUM_THREADS + 1
267         else
268             loop_num = num / NUM_THREADS
269         end
270     end
271 end
272
273 function _mlt_sde_loop!(x2,
274     x,
275     s,
276     t,
277     prob,
278     neumann_bc)
279     #randn! allows to save one allocation
280     dt = t - s
281     randn!(x2)
282     x2 .= x + (prob.μ(x, prob.p, t) .* dt .+ prob.σ(x, prob.p, t) .* sqrt(dt) .* x2)
283     if !isnothing(neumann_bc)
284         x2 .= _reflect(x, x2, neumann_bc...)
285     end
286 end

```

6.4 JULIA source codes associated to Subsection 5.1

```

1 using HighDimPDE
2 using Random
3 using Test
4 using Flux
5 using Revise
6

```

```

7 function DeepSplitting_fisher_kpp_neumann(d, T, dt, cuda_device)
8     #####
9     ##### ML params #####
10    #####
11    maxiters = 500
12    batch_size = 8000
13    K = 1
14
15    hls = d + 50 #hidden layer size
16
17    # Neural network used by the scheme
18    nn = Flux.Chain(Dense(d,hls,tanh),
19                   Dense(hls,hls,tanh),
20                   Dense(hls, 1, x->x^2))
21
22    opt = Flux.ADAM(1e-2) #optimiser
23
24    #####
25    ##### PDE Problem #####
26    #####
27    tspan = (0f0,T)
28    neumann_bc = [fill(-5f-1, d), fill(5f-1, d)]
29    x0 = fill(0f0,d) # point where u(x,t) is approximated
30     $\mu(X,p,t) = 0f0$  # advection coefficients
31     $\sigma(X,p,t) = 1f-1$  # diffusion coefficients
32    g(x) = exp.(-0.25f0 * sum(x.^2, dims = 1)) # initial condition
33    f(y, z, v_y, v_z, p, t) = v_y .* ( 1f0 .- v_y )
34
35    # defining the problem
36    alg = DeepSplitting(nn, K=K, opt = opt)
37    prob = PIDEProblem(g, f,  $\mu$ ,  $\sigma$ , x0, tspan, neumann_bc = neumann_bc)
38
39    # solving
40    sol = solve(prob,
41               alg,
42               dt,
43               verbose = true,
44               abstol=1f-99,
45               maxiters = maxiters,
46               batch_size = batch_size,
47               use_cuda = true,
48               cuda_device = cuda_device
49               )
50    lossmax = maximum([loss[end] for loss in sol.losses[2:end]])
51    return sol.us[end], lossmax, missing
52 end
53
54 if false
55     d = 10
56     dt = 1f-1
57     T = 2f-1
58     @show DeepSplitting_fisher_kpp_neumann(d, T, dt, 1)
59 end

```

```

1 using HighDimPDE
2 using Random
3 using Test
4 using Flux
5 using Revise
6
7 function MLP_fisher_kpp_neumann(d, T, L)
8     tspan = (0e0,T)
9     #####
10    ##### PDE Problem #####
11    #####
12     $\partial = 5e-1$ 
13    neumann_bc = [fill(- $\partial$ , d), fill( $\partial$ , d)]
14    x0 = fill(0e0,d) # initial point
15     $\mu(X,p,t) = 0e0$  # advection coefficients
16     $\sigma(X,p,t) = 1e-1$  # diffusion coefficients
17    g(x) = exp.(-0.25e0 * sum(x.^2)) # initial condition
18    f(y, z, v_y, v_z, p, t) = max.(0e0, v_y) .*
19        ( 1e0 .- max.(0e0,v_y) )
20
21    # defining the problem
22    alg = MLP(M = L, K = 1, L = L)
23    prob = PIDEProblem(g, f,  $\mu$ ,  $\sigma$ , x0, tspan, neumann_bc = neumann_bc)
24
25    # solving

```

```

26     sol = solve(prob,
27         alg,
28         multithreading=true)
29     return sol.us[end]
30 end
31
32 if false
33     d = 5
34     T = 2f0
35     L = 5
36     @show MLP_fisher_kpp_neumann(d, T, L)
37 end

```

6.5 JULIA source codes associated to Subsection 5.2

```

1 using HighDimPDE
2 using Random
3 using Test
4 using Flux
5 using Revise
6
7 function DeepSplitting_nonlocal_comp(d, T, dt, cuda_device)
8     #####
9     ##### ML params #####
10    #####
11    maxiters = 500
12    batch_size = 8000
13    K = 5
14
15    hls = d + 50 #hidden layer size
16
17    # Neural network used by the scheme
18    nn = Flux.Chain(Dense(d, hls, tanh),
19                  Dense(hls, hls, tanh),
20                  Dense(hls, 1, x->x^2))
21
22    opt = Flux.ADAM(1e-2) #optimiser
23
24    #####
25    ##### PDE Problem #####
26    #####
27    tspan = (0f0, T)
28     $\sigma_{\text{sampling}} = 1f-1 / \text{sqrt}(2f0)$ 
29    x0 = fill(0f0, d) # initial point
30     $\mu(X, p, t) = 0f0$  # advection coefficients
31     $\sigma(X, p, t) = 1f-1$  # diffusion coefficients
32    g(x) = exp(-0.25f0 * sum(x.^2, dims = 1)) # initial condition
33    _scale = Float32((2 *  $\pi$ )^(d/2) *  $\sigma_{\text{sampling}}^d$ )
34    f(y, z, v_y, v_z, p, t) = v_y .* (1f0 .- v_z * _scale)
35
36    # defining the problem
37    alg = DeepSplitting(nn, K=K, opt = opt,
38                      mc_sample = NormalSampling( $\sigma_{\text{sampling}}$ , true))
39    prob = PIDEProblem(g, f,  $\mu$ ,  $\sigma$ , x0, tspan)
40    # solving
41    sol = solve(prob,
42              alg,
43              dt,
44              verbose = true,
45              abstol=1f-99,
46              maxiters = maxiters,
47              batch_size = batch_size,
48              use_cuda = true,
49              cuda_device = cuda_device
50              )
51    lossmax = maximum([loss[end] for loss in sol.losses[2:end]])
52    return sol.us[end], lossmax, missing
53 end
54
55 if false
56     d = 10
57     dt = 1f-1
58     T = 2f-1
59     @show DeepSplitting_nonlocal_comp(d, T, dt, 1)
60 end

```

```

1 using HighDimPDE
2 using Random
3 using Test
4 using Flux
5 using Revise
6
7 function MLP_nonlocal_comp(d, T, L)
8     tspan = (0f0,T)
9     #####
10    ##### PDE Problem #####
11    #####
12     $\sigma_{\text{sampling}} = 1e-1 / \text{sqrt}(2)$ 
13    x0 = fill(0e0,d) # initial point
14    g_mlp(X) = exp.(-0.25e0 * sum(X.^2)) # initial condition
15    f_mlp(y, z, v_y, v_z, p, t) = max.(0e0, v_y) .*
16        (1e0 .- max.(0e0, v_z) * Float64((2 *  $\pi$ )^(d/2) *  $\sigma_{\text{sampling}}^d$ ))
17     $\mu_{\text{mlp}}(X,p,t) = 0.0e0$  # advection coefficients
18     $\sigma_{\text{mlp}}(X,p,t) = 1e-1$  # diffusion coefficients
19    mc_sample = NormalSampling( $\sigma_{\text{sampling}}$ , true) # uniform distrib in x0_sample
20    # defining the problem
21    prob = PIDEProblem(g_mlp, f_mlp,  $\mu_{\text{mlp}}$ ,  $\sigma_{\text{mlp}}$ , x0, tspan)
22    alg = MLP(M = L, K = 10, L = L, mc_sample = mc_sample)
23    # solving
24    sol = solve(prob, alg, multithreading=true)
25    return sol.us[end]
26 end
27
28 if false
29     d = 5
30     T = 3f-1
31     L = 4
32     @show MLP_nonlocal_comp(d, T, L)
33 end

```

6.6 JULIA source codes associated to Subsection 5.3

```

1 using HighDimPDE
2 using Random
3 using Test
4 using Flux
5 using Revise
6
7 function DeepSplitting_nonlocal_sinegordon(d, T, dt, cuda_device)
8     #####
9     ##### ML params #####
10    #####
11    maxiters = 500
12    batch_size = 8000
13    K = 5
14
15    hls = d + 50 #hidden layer size
16
17    # Neural network used by the scheme
18    nn = Flux.Chain(Dense(d,hls,tanh),
19                    Dense(hls,hls,tanh),
20                    Dense(hls, 1))
21
22    opt = Flux.ADAM(1e-3) #optimiser
23
24    #####
25    ##### PDE Problem #####
26    #####
27    tspan = (0f0,T)
28
29     $\sigma_{\text{sampling}} = 1f-1 / \text{sqrt}(2f0)$ 
30    x0 = fill(0f0,d) # initial point
31     $\mu(X,p,t) = 0f0$  # advection coefficients
32     $\sigma(X,p,t) = 1f-1$  # diffusion coefficients
33    g(x) = exp.(-0.25f0 * sum(x.^2, dims = 1)) #initial condition
34    _scale = Float32((2 *  $\pi$ )^(d/2) *  $\sigma_{\text{sampling}}^d$ )
35    f(y, z, v_y, v_z, p, t) = sin.(v_y) .- v_z * _scale
36
37    # defining the problem
38    alg = DeepSplitting(nn, K=K, opt = opt,

```

```

39         mc_sample = NormalSampling( $\sigma$ _sampling, true)
40     prob = PIDEProblem(g, f,  $\mu$ ,  $\sigma$ , x0, tspan)
41
42     # solving
43     sol = solve(prob,
44               alg,
45               dt,
46               verbose = true,
47               abstol=1f-99,
48               maxiters = maxiters,
49               batch_size = batch_size,
50               use_cuda = true,
51               cuda_device = cuda_device
52             )
53     lossmax = maximum([loss[end] for loss in sol.losses[2:end]])
54     return sol.us[end], lossmax, missing
55 end
56
57 if false
58     d = 10
59     dt = 1f-1
60     T = 3f-1
61     @show DeepSplitting_nonlocal_sinegordon(d, T, dt, 1)
62 end

```

```

1  using HighDimPDE
2  using Random
3  using Test
4  using Flux
5  using Revise
6
7  function MLP_nonlocal_sinegordon(d, T, L)
8      tspan = (0e0,T)
9      #####
10     ##### PDE Problem #####
11     #####
12      $\sigma$ _sampling = 1e-1 / sqrt(2e0)
13     x0 = fill(0e0,d) # initial point
14      $\mu$ (X,p,t) = 0e0 # advection coefficients
15      $\sigma$ (X,p,t) = 1e-1 # diffusion coefficients
16     g(x) = exp(-0.25e0 * sum(x.^2)) # initial condition
17     f(y, z, v_y, v_z, p, t) = sin.(v_y) .- v_z * (2 *  $\pi$ )^(d/2) *  $\sigma$ _sampling^d
18
19     # defining the problem
20     mc_sample = NormalSampling( $\sigma$ _sampling,true)
21     alg = MLP(M = L, K = 10, L = L, mc_sample = mc_sample )
22     prob = PIDEProblem(g, f,  $\mu$ ,  $\sigma$ , x0, tspan)
23
24     # solving
25     sol = solve(prob, alg, multithreading=true)
26     return sol.us[end]
27 end
28
29 if false
30     d = 10
31     T = 3f-1
32     L = 4
33     @show MLP_nonlocal_sinegordon(d, T, L)
34 end

```

6.7 JULIA source codes associated to Subsection 5.4

```

1  using HighDimPDE
2  using Random
3  using Test
4  using Flux
5  using Revise
6
7  function DeepSplitting_rep_mut(d, T, dt, cuda_device)
8      #####

```

```

9      ##### ML params #####
10     #####
11     maxiters = 1000
12     batch_size = 8000
13     K = 5
14
15     hls = d + 50 #hidden layer size
16
17     # Neural network used by the scheme
18     nn = Flux.Chain(Dense(d, hls, tanh),
19                    Dense(hls, hls, tanh),
20                    Dense(hls, 1, x->x^2))
21
22     opt = Flux.ADAM(1e-3) #optimiser
23
24     #####
25     ##### PDE Problem #####
26     #####
27     tspan = (0f0, T)
28      $\sigma_{\text{sampling}} = 2f-2$ 
29     x0 = fill(0f0, d) # initial point
30     ss0 = 5f-2#std g0
31
32      $\mu(X, p, t) = 0f0$  # advection coefficients
33      $\sigma(X, p, t) = 1f-1$  # diffusion coefficients
34     g(x) = Float32((2f0* $\pi$ )^(-d/2f0)) * ss0^(- Float32(d) * 5f-1) *
35           exp.(-5f-1 * sum(x.^2 / ss0, dims = 1)) # initial condition
36     m(x) = - 5f-1 * sum(x.^2, dims=1)
37     _scale = Float32((2 *  $\pi$ )^(d/2) *  $\sigma_{\text{sampling}}^d$ )
38     f(y, z, v_y, v_z, p, t) = v_y .* (m(y) ./ _scale *
39           exp.(5f-1 * sum(z.^2, dims = 1) /  $\sigma_{\text{sampling}}^2$ )) .* v_z .* m(z)
40
41     # reference solution
42     function _SS(x, t, p)
43         d = length(x)
44         MM =  $\sigma(x, p, t) * \text{ones}(d)$ 
45         SSt = MM .* ((MM .* sinh.(MM * t) .+ ss0 .*
46                   cosh.(MM * t)) ./ (MM .* cosh.(MM * t) .+ ss0 .* sinh.(MM * t)))
47         return SSt
48     end
49
50     function rep_mut_anal(x, t, p)
51         d = length(x)
52         return (2* $\pi$ )^(-d/2) * prod(_SS(x, t, p) .^(-1/2)) *
53               exp(-0.5 * sum(x.^2 ./ _SS(x, t, p)))
54     end
55
56     # defining the problem
57     alg = DeepSplitting(nn, K=K, opt = opt,
58                       mc_sample = NormalSampling( $\sigma_{\text{sampling}}$ , false))
59     prob = PIDEProblem(g, f,  $\mu$ ,  $\sigma$ , x0, tspan,
60                      x0_sample = NoSampling())
61
62     # solving
63     sol = solve(prob,
64               alg,
65               dt,
66               verbose = true,
67               abstol=1f-99,
68               maxiters = maxiters,
69               batch_size = batch_size,
70               use_cuda = true,
71               cuda_device = cuda_device
72             )
73     lossmax = maximum(maximum(sol.losses[2:end]))
74     return sol.us[end], lossmax, rep_mut_anal(zeros(d), T, Dict())
75 end
76
77 if false
78     d = 10
79     dt = 5f-2
80     T = 5f-1
81     @time sol, lossmax, truesol = DeepSplitting_rep_mut(d, T, dt, 7)
82     println("True solution: $truesol, Deep splitting approximation = $(sol)")
83 end

```

```

1 using CUDA
2 CUDA.device!(6)
3 using HighDimPDE
4 using Random

```



```

5 using Test
6 using Flux
7 using Revise
8
9 function MLP_rep_mut(d, T, L)
10     tspan = (0e0,T)
11     #####
12     ##### PDE Problem #####
13     #####
14     ss0 = 5e-2#std g0
15     U = 5e-1
16     mc_sample_θ = (fill(-U, d), fill(U, d))
17     x0 = fill(0e0,d) # initial point
18     μ(X,p,t) = 0e0 # advection coefficients
19     σ(X,p,t) = 1e-1 # diffusion coefficients
20     g(x) = (2*π)^(-d/2) * ss0^(- d * 5e-1) *
21         exp.(-5e-1 *sum(x.^2e0 / ss0)) # initial condition
22     m(x) = - 5e-1 * sum(x.^2)
23     vol = prod(mc_sample_θ[2] - mc_sample_θ[1])
24     f(y, z, v_y, v_z, p, t) = max(0.0, v_y) *
25         (m(y) - vol * max(0.0, v_z) * m(z))
26
27     # defining the problem
28     alg = MLP(M = L, K = 10, L = L, mc_sample = UniformSampling(mc_sample_θ...))
29     prob = PIDEProblem(g, f, μ, σ, x0, tspan)
30
31     # solving
32     sol = solve(prob, alg, multithreading=true )
33     return sol.us[end]
34 end
35
36 if false
37     d = 5
38     T = 5e-1
39     L = 4
40     @show MLP_rep_mut(d, T, L)
41
42     # Analytic sol
43     ss0 = 5e-2#std g0
44     μ(X,p,t) = 0e0 # advection coefficients
45     σ(X,p,t) = 1e-1 # diffusion coefficients
46     function _SS(x, t, p)
47         d = length(x)
48         MM = σ(x, p, t) * ones(d)
49         SSt = MM .* ((MM .* sinh.(MM *t) .+ ss0 .*
50             cosh.( MM * t)) ./ (MM .* cosh.(MM * t) .+ ss0 .* sinh.(MM * t)))
51         return SSt
52     end
53
54     function uanal(x, t, p)
55         d = length(x)
56         return (2*π)^(-d/2) * prod(_SS(x, t, p) .^(-1/2)) *
57             exp(-0.5 *sum(x.^2 ./ _SS(x, t, p)) )
58     end
59     @show uanal(zeros(d), T, nothing)
60 end
61

```

6.8 JULIA source codes associated to Subsection 5.5

```

1 using HighDimPDE
2 using Random
3 using Test
4 using Flux
5 using Revise
6
7 function DeepSplitting_allencahn_neumann(d, T, dt, cuda_device)
8     #####
9     ##### ML params #####
10    #####
11    maxiters = 500
12    batch_size = 8000
13    K = 5
14
15    hls = d + 50 #hidden layer size

```

```

16
17 # Neural network used by the scheme
18 nn = Flux.Chain(Dense(d,hls,relu),
19                 Dense(hls,hls,relu),
20                 Dense(hls, 1))
21
22 opt = Flux.ADAM(1e-2) #optimiser
23
24 #####
25 ##### PDE Problem #####
26 #####
27 tspan = (0f0,T)
28  $\partial$  = fill(5f-1, d)
29 x0_sample = UniformSampling(- $\partial$ ,  $\partial$ )
30 x0 = fill(0f0,d) # point where u(x,t) is approximated
31
32  $\mu$ (X,p,t) = 0f0 # advection coefficients
33  $\sigma$ (X,p,t) = 1f-1 # diffusion coefficients
34 g(x) = exp.(-0.25f0 * sum(x.^2, dims = 1)) # initial condition
35 a(u) = u - u^3
36 f(y, z, v_y, v_z, p, t) = a.(v_y) .- a.(v_z)
37
38 # defining the problem
39 alg = DeepSplitting(nn, K=K, opt = opt, mc_sample = x0_sample)
40 prob = PIDEProblem(g, f,  $\mu$ ,  $\sigma$ , x0, tspan, neumann_bc = [- $\partial$ ,  $\partial$ ], x0_sample = x0_sample)
41
42 # solving
43 sol = solve(prob,
44             alg,
45             dt,
46             verbose = true,
47             abstol=1f-99,
48             maxiters = maxiters,
49             batch_size = batch_size,
50             use_cuda = true,
51             cuda_device = cuda_device
52             )
53 lossmax = maximum([loss[end] for loss in sol.losses[2:end]])
54 return sol.us[end], lossmax, missing
55 end
56
57 if false
58     d = 1
59     dt = 1f-1
60     T = 2f-1
61     @show DeepSplitting_allencahn_neumann(d, T, dt, 6)
62 end

```

```

1 using HighDimPDE
2 using Random
3 using Test
4 using Flux
5 using Revise
6
7 function MLP_allencahn_neumann(d, T, L)
8     tspan = (0f0,T)
9     #####
10    ##### PDE Problem #####
11    #####
12    neumann_bc = [fill(-5e-1, d), fill(5e-1, d)]
13    x0 = fill(0e0,d) # initial point
14    g_mlp(X) = exp.(-0.25e0 * sum(X.^2)) # initial condition
15    a(u) = u - u^3
16    f_mlp(y, z, v_y, v_z, p, t) = a.(max.(0f0, v_y)) .- a.(max.(0f0, v_z))
17     $\mu$ _mlp(X,p,t) = 0.0e0 # advection coefficients
18     $\sigma$ _mlp(X,p,t) = 1e-1 # diffusion coefficients
19    mc_sample = UniformSampling(neumann_bc...) # uniform distrib in x0_sample
20    # defining the problem
21    prob = PIDEProblem(g_mlp, f_mlp,  $\mu$ _mlp,  $\sigma$ _mlp, x0, tspan,
22                      neumann_bc = neumann_bc)
23    alg = MLP(M = L, K = 10, L = L, mc_sample = mc_sample )
24    # solving
25    sol = solve(prob, alg, multithreading=true)
26    return sol.us[end]
27 end
28
29 if false
30     d = 1
31     T = 3f-1

```

```
32     L = 4
33     @show MLP_allencahn_neumann(d, T, L)
34 end
```

Acknowledgments

This project has been funded by the Deutsche Forschungsgemeinschaft (DFG, German Research Foundation) under Germany's Excellence Strategy EXC 2044-390685587, Mathematics Münster: Dynamics-Geometry-Structure. This project has been partially supported by the startup fund project of Shenzhen Research Institute of Big Data under grant No. T00120220001.

References

- [1] ABERGEL, F., AND TACHET, R. A nonlinear partial integro-differential equation from mathematical finance. *Discrete Contin. Dyn. Syst.* 27, 3 (2010), 907–917.
- [2] AL-ARADI, A., CORREIA, A., NAIFF, D. D. F., JARDIM, G., AND SAPORITO, Y. Extensions of the deep Galerkin method. *arXiv:1912.01455* (2019), 27 pp.
- [3] ALFARO, M., AND CARLES, R. Replicator-mutator equations with quadratic fitness. *Proc. Amer. Math. Soc.* 145, 12 (2017), 5315–5327.
- [4] ALFARO, M., AND VERUETE, M. Evolutionary branching via replicator-mutator equations. *J. Dynam. Differential Equations* 31, 4 (2019), 2029–2052.
- [5] AMADORI, A. L. Nonlinear integro-differential evolution problems arising in option pricing: a viscosity solutions approach. *Differential Integral Equations* 16, 7 (2003), 787–811.
- [6] BANERJEE, M., PETROVSKII, S. V., AND VOLPERT, V. Nonlocal reaction-diffusion models of heterogeneous wealth distribution. *Mathematics* 9, 4 (2021), Article No. 351, 18 pp.
- [7] BARONE, A., ESPOSITO, F., MAGEE, C. J., AND SCOTT, A. C. Theory and applications of the sine-Gordon equation. *La Rivista del Nuovo Cimento* 1, 2 (1971), 227–267.
- [8] BAUER, W. F. The Monte Carlo method. *J. Soc. Ind. Appl. Math.* 6, 4 (1958), 438–451.

- [9] BECK, C., BECKER, S., CHERIDITO, P., JENTZEN, A., AND NEUFELD, A. Deep splitting method for parabolic PDEs. *SIAM J. Sci. Comput.* 43, 5 (2021), A3135–A3154.
- [10] BECK, C., BECKER, S., GROHS, P., JAAFARI, N., AND JENTZEN, A. Solving the Kolmogorov PDE by means of deep learning. *J. Sci. Comput.* 88 (2021), Article No. 73, 28 pp.
- [11] BECK, C., E, W., AND JENTZEN, A. Machine learning approximation algorithms for high-dimensional fully nonlinear partial differential equations and second-order backward stochastic differential equations. *J. Nonlinear Sci.* 29, 4 (2019), 1563–1619.
- [12] BECK, C., HUTZENTHALER, M., JENTZEN, A., AND KUCKUCK, B. An overview on deep learning-based approximation methods for partial differential equations. *Revision requested from Discrete Contin. Dyn. Syst., arXiv:2012.12348* (2020), 22 pp.
- [13] BECKER, S., BRAUNWARTH, R., HUTZENTHALER, M., JENTZEN, A., AND VON WURSTEMBERGER, P. Numerical simulations for full history recursive multilevel Picard approximations for systems of high-dimensional partial differential equations. *Commun. Comput. Phys.* 28, 5 (2020), 2109–2138.
- [14] BELLMAN, R. *Dynamic Programming*. Princeton Landmarks in Mathematics. Princeton University Press, Princeton, NJ, 2010. Reprint of the 1957 edition.
- [15] BENTH, F. E., KARLSEN, K. H., AND REIKVAM, K. Optimal portfolio selection with consumption and nonlinear integro-differential equations with gradient constraint: a viscosity solution approach. *Finance Stoch.* 5, 3 (2001), 275–303.
- [16] BERESTYCKI, H., JIN, T., AND SILVESTRE, L. Propagation in a non local reaction diffusion equation with spatial and genetic trait structure. *Nonlinearity* 29, 4 (2016), 1434–1466.
- [17] BERESTYCKI, H., NADIN, G., PERTHAME, B., AND RYZHIK, L. The non-local Fisher-KPP equation: travelling waves and steady states. *Nonlinearity* 22, 12 (2009), 2813–2844.
- [18] BIAN, S., CHEN, L., AND LATOS, E. A. Global existence and asymptotic behavior of solutions to a nonlocal Fisher-KPP type problem. *Nonlinear Anal.* 149 (2017), 165–176.
- [19] BURGER, R., AND HOFBAUER, J. Mutation load and mutation-selection-balance in quantitative genetic traits. *J. Math. Biol.* 32, 3 (1994), 193–218.

- [20] CAGLIOTI, E., LIONS, P.-L., MARCHIORO, C., AND PULVIRENTI, M. A special class of stationary flows for two-dimensional Euler equations: a statistical mechanics description. II. *Comm. Math. Phys.* 174, 2 (1995), 229–260.
- [21] CASTRO, J. Deep learning schemes for parabolic nonlocal integro-differential equations. *arXiv:2103.15008* (2021), 28 pp.
- [22] CHAN, T. Pricing contingent claims on stocks driven by Lévy processes. *Ann. Appl. Probab.* 9, 2 (1999), 504–528.
- [23] CHEN, J., DU, R., AND WU, K. A comparison study of deep Galerkin method and deep Ritz method for elliptic problems with different boundary conditions. *Comm. Math. Res.* 36, 3 (2020), 354–376.
- [24] CHEN, L., PAINTER, K., SURULESCU, C., AND ZHIGUN, A. Mathematical models for cell migration: a non-local perspective. *Philos. Trans. Roy. Soc. B* 375, 1807 (2020), Article No. 20190379, 9 pp.
- [25] COLEMAN, S. Quantum sine-Gordon equation as the massive Thirring model. In *Bosonization*, vol. 1. World Scientific, 1994, pp. 128–137.
- [26] CONT, R., AND TANKOV, P. *Financial modelling with jump processes*. Chapman & Hall/CRC Financial Mathematics Series. Chapman & Hall/CRC, Boca Raton, FL, 2004.
- [27] COX, S., AND VAN NEERVEN, J. Pathwise Hölder convergence of the implicit-linear Euler scheme for semi-linear SPDEs with multiplicative noise. *Numer. Math.* 125, 2 (2013), 259–345.
- [28] CRUZ, J. M. T. S., AND ŠEVČOVIČ, D. On solutions of a partial integro-differential equation in Bessel potential spaces with applications in option pricing models. *Jpn. J. Ind. Appl. Math.* 37, 3 (2020), 697–721.
- [29] D’ELIA, M., DU, Q., GLUSA, C., GUNZBURGER, M., TIAN, X., AND ZHOU, Z. Numerical methods for nonlocal and fractional models. *Acta Numerica* 29 (2020), 1–124.
- [30] DOEBELI, M., AND ISPOLATOV, I. Complexity and diversity. *Science* 328, 5977 (2010), 494–497.
- [31] DUCHI, J., HAZAN, E., AND SINGER, Y. Adaptive subgradient methods for online learning and stochastic optimization. *J. Mach. Learn. Res.* 12, 61 (2011), 2121–2159.

- [32] E, W., HAN, J., AND JENTZEN, A. Deep learning-based numerical methods for high-dimensional parabolic partial differential equations and backward stochastic differential equations. *Commun. Math. Stat.* 5, 4 (2017), 349–380.
- [33] E, W., HAN, J., AND JENTZEN, A. Algorithms for Solving High Dimensional PDEs: From Nonlinear Monte Carlo to Machine Learning. *Nonlinearity* 35, 1 (2021), 278–310.
- [34] E, W., HUTZENTHALER, M., JENTZEN, A., AND KRUSE, T. On multilevel Picard numerical approximations for high-dimensional nonlinear parabolic partial differential equations and high-dimensional nonlinear backward stochastic differential equations. *J. Sci. Comput.* 79, 3 (2019), 1534–1571.
- [35] E, W., HUTZENTHALER, M., JENTZEN, A., AND KRUSE, T. On multilevel Picard numerical approximations for high-dimensional nonlinear parabolic partial differential equations and high-dimensional nonlinear backward stochastic differential equations. *J. Sci. Comput.* 79, 3 (2019), 1534–1571.
- [36] E, W., HUTZENTHALER, M., JENTZEN, A., AND KRUSE, T. Multilevel Picard iterations for solving smooth semilinear parabolic heat equations. *Partial Differ. Equ. Appl.* 2, 6 (2021), Article No. 80, 31 pp.
- [37] E, W., AND YU, B. The Deep Ritz method: A deep learning-based numerical algorithm for solving variational problems. *Commun. Math. Stat.* 6, 1 (2018), 1–12.
- [38] FISHER, R. A. The wave of advance of advantageous genes. *Annals of Eugenics* 7, 4 (1937), 355–369.
- [39] FREY, R., AND KÖCK, V. Deep neural network algorithms for parabolic PIDEs and applications in insurance mathematics. *arXiv:2109.11403* (2021), 24 pp.
- [40] FREY, R., AND KÖCK, V. Deep neural network algorithms for parabolic PIDEs and applications in insurance mathematics. In *Mathematical and Statistical Methods for Actuarial Sciences and Finance* (Cham, 2022), M. Corazza, C. Perna, C. Pizzi, and M. Sibillo, Eds., Springer International Publishing, pp. 272–277.
- [41] GAJEWSKI, H., AND ZACHARIAS, K. On a nonlocal phase separation model. *J. Math. Anal. Appl.* 286, 1 (2003), 11–31.
- [42] GAN, X., YANG, Y., AND ZHANG, K. A robust numerical method for pricing American options under Kou’s jump-diffusion models based on penalty method. *J. Appl. Math. Comput.* 62, 1–2 (2020), 1–21.
- [43] GÉNEIEYS, S., VOLPERT, V., AND AUGER, P. Pattern and waves for a model in population dynamics with nonlocal consumption of resources. *Math. Model. Nat. Phenom.* 1, 1 (2006), 65–82.

- [44] GLOT, X., AND BENGIO, Y. Understanding the difficulty of training deep feed-forward neural networks. In *Proceedings of the Thirteenth International Conference on Artificial Intelligence and Statistics* (Chia Laguna Resort, Sardinia, Italy, 13–15 May 2010), Y. W. Teh and M. Titterton, Eds., vol. 9 of *Proceedings of Machine Learning Research*, PMLR, pp. 249–256.
- [45] GONON, L., AND SCHWAB, C. Deep ReLU neural networks overcome the curse of dimensionality for partial integrodifferential equations. *arXiv:2102.11707* (2021), 35 pp.
- [46] GROHS, P., AND VOIGTLAENDER, F. Proof of the theory-to-practice gap in deep learning via sampling complexity bounds for neural network approximation spaces. *arXiv:2104.02746* (2021), 42 pp.
- [47] GUO, L., WU, H., YU, X., AND ZHOU, T. Monte Carlo PINNs: deep learning approach for forward and inverse problems involving high dimensional fractional partial differential equations. *arXiv:2203.08501* (2022), 18 pp.
- [48] GYÖNGY, I., AND KRYLOV, N. On the splitting-up method and stochastic partial differential equations. *Ann. Probab.* 31, 2 (2003), 564–591.
- [49] HAIRER, M., AND SHEN, H. The dynamical sine-Gordon model. *Comm. Math. Phys.* 341, 3 (2016), 933–989.
- [50] HAMEL, F., LAVIGNE, F., MARTIN, G., AND ROQUES, L. Dynamics of adaptation in an anisotropic phenotype-fitness landscape. *Nonlinear Anal. Real World Appl.* 54 (2020), Article No. 103107, 33 pp.
- [51] HAMEL, F., AND NADIRASHVILI, N. Travelling fronts and entire solutions of the Fisher-KPP equation in \mathbb{R}^N . *Arch. Ration. Mech. Anal.* 157, 2 (2001), 91–163.
- [52] HAN, J., JENTZEN, A., AND E, W. Solving high-dimensional partial differential equations using deep learning. *Proc. Natl. Acad. Sci. USA* 115, 34 (2018), 8505–8510.
- [53] HEINRICH, S. Monte Carlo complexity of global solution of integral equations. *J. Complex.* 14, 2 (1998), 151–175.
- [54] HEINRICH, S., AND SINDAMBIWE, E. Monte Carlo complexity of parametric integration. *J. Complex.* 15, 3 (1999), 317–341.
- [55] HENRY-LABORDÈRE, P. Counterparty Risk Valuation: A Marked Branching Diffusion Approach. *arXiv:1203.2369* (2012), 17 pp.
- [56] HOCHBRUCK, M., AND OSTERMANN, A. Explicit exponential Runge–Kutta methods for semilinear parabolic problems. *SIAM J. Numer. Anal.* 43, 3 (2005), 1069–1090.

- [57] HOUCHEMANDZADEH, B., AND VALLADE, M. Fisher waves: An individual-based stochastic model. *Phys. Rev. E* 96, 1 (2017), Article No. 012414, 13 pp.
- [58] HUANG, J., CEN, Z., AND LE, A. A finite difference scheme for pricing American put options under Kou's jump-diffusion model. *J. Funct. Spaces Appl.* (2013), Article No. 651573, 11 pp.
- [59] HURÉ, C., PHAM, H., AND WARIN, X. Deep backward schemes for high-dimensional nonlinear PDEs. *Math. Comp.* 89 (2020), 1547–1579.
- [60] HUTZENTHALER, M., JENTZEN, A., KRUSE, T., NGUYEN, T. A., AND VON WURSTEMBERGER, P. Overcoming the curse of dimensionality in the numerical approximation of semilinear parabolic partial differential equations. *Proc. A.* 476, 2244 (2020), Article No. 20190630, 25 pp.
- [61] IOFFE, S., AND SZEGEDY, C. Batch normalization: Accelerating deep network training by reducing internal covariate shift. In *Proceedings of the 32nd International Conference on Machine Learning* (Lille, France, 07–09 Jul 2015), F. Bach and D. Blei, Eds., vol. 37 of *Proceedings of Machine Learning Research*, PMLR, pp. 448–456.
- [62] KAVALLARIS, N. I., LANKEIT, J., AND WINKLER, M. On a degenerate nonlocal parabolic problem describing infinite dimensional replicator dynamics. *SIAM J. Math. Anal.* 49, 2 (2017), 954–983.
- [63] KAVALLARIS, N. I., AND SUZUKI, T. *Non-local partial differential equations for engineering and biology*, vol. 31 of *Mathematics for Industry (Tokyo)*. Springer, Cham, 2018.
- [64] KINGMA, D. P., AND BA, J. Adam: A Method for Stochastic Optimization. *arXiv:1412.6980* (2014), 15 pp.
- [65] KOU, S. G. A Jump-Diffusion Model for Option Pricing. *Manag. Sci.* 48, 8 (2002), 1086–1101.
- [66] LACEY, A. A. Thermal runaway in a non-local problem modelling Ohmic heating. I. Model derivation and some special cases. *European J. Appl. Math.* 6, 2 (1995), 127–144.
- [67] LAGARIS, I., LIKAS, A., AND PAPAGEORGIOU, D. Neural-network methods for boundary value problems with irregular boundaries. *IEEE Trans. Neural Netw.* 11, 5 (2000), 1041–1049.
- [68] LAGARIS, I. E., LIKAS, A., AND FOTIADIS, D. I. Artificial neural networks for solving ordinary and partial differential equations. *IEEE Trans. Neural Netw.* 9, 5 (1998), 987–1000.

- [69] LECUN, Y., BENGIO, Y., AND HINTON, G. Deep learning. *Nature* 521, 7553 (2015), 436–444.
- [70] LIAO, Y., AND MING, P. Deep Nitsche method: Deep Ritz method with essential boundary conditions. *Comm. Comput. Phys.* 29, 5 (2021), 1365–1384.
- [71] LORZ, A., LORENZI, T., HOCHBERG, M. E., CLAIRAMBAULT, J., AND PERTHAME, B. Populational adaptive evolution, chemotherapeutic resistance and multiple anti-cancer therapies. *ESAIM Math. Model. Numer. Anal.* 47, 2 (2013), 377–399.
- [72] LU, L., MENG, X., MAO, Z., AND KARNIADAKIS, G. E. DeepXDE: A deep learning library for solving differential equations. *SIAM Review* 63, 1 (2021), 208–228.
- [73] MCFALL, K. S., AND MAHAN, J. R. Artificial neural network method for solution of boundary value problems with exact satisfaction of arbitrary boundary conditions. *IEEE Trans. Neural Netw.* 20, 8 (2009), 1221–1233.
- [74] MERTON, R. C. Option pricing when underlying stock returns are discontinuous. *J. Financ. Econ.* 3, 1–2 (1976), 125–144.
- [75] METROPOLIS, N., AND ULAM, S. The Monte Carlo method. *J. Amer. Statist. Assoc.* 44, 247 (1949), 335–341.
- [76] NORDBOTTEN, J. M., BOKMA, F., HERMANSEN, J. S., AND STENSETH, N. C. The dynamics of trait variance in multi-species communities. *R. Soc. Open Sci.* 7, 8 (2020), Article No. 200321, 20 pp.
- [77] NORDBOTTEN, J. M., LEVIN, S. A., SZATHMÁRY, E., AND STENSETH, N. C. Ecological and evolutionary dynamics of interconnectedness and modularity. *Proc. Natl. Acad. Sci. USA* 115, 4 (2018), 750–755.
- [78] NORDBOTTEN, J. M., AND STENSETH, N. C. Asymmetric ecological conditions favor Red-Queen type of continued evolution over stasis. *Proc. Natl. Acad. Sci. USA* 113, 7 (2016), 1847–1852.
- [79] OECHSSLER, J., AND RIEDEL, F. Evolutionary dynamics on infinite strategy spaces. *Econom. Theory* 17, 1 (2001), 141–162.
- [80] PÁJARO, M., ALONSO, A. A., OTERO-MURAS, I., AND VÁZQUEZ, C. Stochastic modeling and numerical simulation of gene regulatory networks with protein bursting. *J. Theoret. Biol.* 421 (2017), 51–70.
- [81] PANG, G., LU, L., AND KARNIADAKIS, G. E. fPINNs: Fractional physics-informed neural networks. *SIAM Journal on Scientific Computing* 41, 4 (2019), A2603–A2626.

- [82] PERTHAME, B., AND GÉNIEYS, S. Concentration in the nonlocal Fisher equation: the Hamilton-Jacobi limit. *Math. Model. Nat. Phenom.* 2, 4 (2007), 135–151.
- [83] PHAM, H. *Continuous-time stochastic control and optimization with financial applications*, vol. 61 of *Stochastic Modelling and Applied Probability*. Springer-Verlag, Berlin, 2009.
- [84] RAISSI, M., PERDIKARIS, P., AND KARNIADAKIS, G. E. Physics-informed neural networks: A deep learning framework for solving forward and inverse problems involving nonlinear partial differential equations. *J. Comput. Phys.* 378 (2019), 686–707.
- [85] ROQUES, L., AND BONNEFON, O. Modelling Population Dynamics in Realistic Landscapes with Linear Elements: A Mechanistic-Statistical Reaction-Diffusion Approach. *PLoS ONE* 11, 3 (2016), Article No. e0151217, 20 pp.
- [86] RUBINSTEIN, J., AND STERNBERG, P. Nonlocal reaction-diffusion equations and nucleation. *IMA J. Appl. Math.* 48, 3 (1992), 249–264.
- [87] SIRIGNANO, J., AND SPILIOPOULOS, K. DGM: A deep learning algorithm for solving partial differential equations. *J. Comput. Phys.* 375 (2018), 1339–1364.
- [88] STOLERIU, I. Non-local models for solid-solid phase transitions. *ROMAI J.* 7, 1 (2011), 157–170.
- [89] SUKUMAR, N., AND SRIVASTAVA, A. Exact imposition of boundary conditions with distance functions in physics-informed deep neural networks. *Comput. Methods Appl. Mech. Engrg.* 389 (2022), Article No. 114333.
- [90] SUNDERASAN, S. Financial Modeling. In *Long-Term Investments*. Routledge India, 2020, pp. 33–51.
- [91] VILLA, C., CHAPLAIN, M. A. J., AND LORENZI, T. Evolutionary dynamics in vascularised tumours under chemotherapy: mathematical modelling, asymptotic analysis and numerical simulations. *Vietnam J. Math.* 49, 1 (2021), 143–167.
- [92] WANG, F., XUE, L., ZHAO, K., AND ZHENG, X. Global stabilization and boundary control of generalized Fisher/KPP equation and application to diffusive SIS model. *J. Differential Equations* 275 (2021), 391–417.
- [93] WANG, S., AND PERDIKARIS, P. Deep learning of free boundary and Stefan problems. *J. Comput. Phys.* (2020), Article No. 109914, 27 pp.
- [94] YUAN, L., NI, Y.-Q., DENG, X.-Y., AND HAO, S. A-PINN: Auxiliary physics informed neural networks for forward and inverse problems of nonlinear integro-differential equations. *J. Comput. Phys.* (2022), Article No. 111260. Early access version available online.

- [95] ZANG, Y., BAO, G., YE, X., AND ZHOU, H. Weak adversarial networks for high-dimensional partial differential equations. *Journal of Computational Physics* 411 (2020), Article No. 109409.